Aus dem Institut für Arbeits-, Sozial-, und Umweltmedizin

der Heinrich-Heine-Universität Düsseldorf

Direktor: Prof. Dr. med. Peter Angerer

Ultra-fine particle exposure and short-term mortality:

a time series study in the context of diesel-powered traffic interventions

Dissertation

zur Erlangung des Grades eines Doktors der Public Health
der Medizinischen Fakultät der Heinrich-Heine-Universität Düsseldorf

vorgelegt von

Arnt Diener

2022

Als Inauguraldissertation gedruckt mit Genehmigung der Medizinischen Fakultät der Heinrich-Heine-Universität Düsseldorf

Gez.:

Dekan: Prof. Dr. med. Nikolaj Klöcker
Erstgutachterin: Prof. Dr. med. Barbara Hoffmann
Zweitgutachter: Prof. Dr. Oliver Kuß

Zusammenfassung

Eine wachsende Zahl epidemiologischer Studien bringt Perioden hoher Konzentrationen von Ultrafeinstaub (UFP, Partikeldurchmesser <100 nm) in der Außenluft mit erhöhten, kurzfristigen Mortalitätsraten in Verbindung. Dieselabgaspartikel (DEPs) werden dabei als besonders toxisch eingestuft und diesel-betriebene Straßenfahrzeuge (DPVs) in vielen Ländern gesetzlich reguliert - insbesondere über Abgasfiltration. Es ist unklar, wie Dieselabgasfiltration sich auf das kurzfristige Mortalitätsrisiko von UFPs auswirkt. Die vorliegende Zeitreihenstudie für 2009-2018 untersuchte die Entwicklung größenspezifischer Partikelanzahlkonzentrationen (PNC) in der Außenluft, deren Assoziation mit kurzfristiger Mortalität und eine mögliche Effektmodifikation durch europäische Dieselabgasregulierung.

Die Analyse basierte auf täglichen, mittleren Messwerten für größenspezifische PNC (elektronischer Mobilitätsdurchmesser von 13.8-500 nm), Feinstaub (PM_{10}, aerodynamischer Durchmesser ≤ 10 µm) und Stickstoffdioxid (NO_2) einer zentralen, urbanen Hintergrundmessstation in Mülheim-Styrum (Deutschland) sowie täglichen natürlichen (NCM), kardiovaskulären (CVM) und respiratorischen (RM) Todesfällen für die umliegenden Gemeinden Mülheim an der Ruhr, Essen und Oberhausen über insgesamt 2965 Tage. Mit Poisson-Regressionen wurde das relative Mortalitätsrisiko (RR) (95% Konfidenzintervall (CI)) nach unmittelbarer (lag0-1, lag1-2; 0-2 Tage nach Exposition), mittelfristiger (lag2-3, lag3-4) und verzögerter (lag4-5, lag5-6, lag6-7) Exposition pro Interquartilsabstand berechnet. Die Modelle wurden für Wetter- und Zeitvariablen sowie zur Sensitivitätsanalyse für PM_{10} und NO_2 adjustiert. Die Größenfraktion von 30-120 nm ($PNC_{30\text{-}120}$) wurde evidenzbasiert zur Repräsentation ungefilterter Dieselabgaspartikel gewählt. Zur Abschätzung einer Effektmodifikation durch die europäische „Euro-4“ Abgasnorm und die damit zusammenhängende Installation von Diesel-partikelfiltern (DPFs) in DPVs wurden multiplikativen Interaktionstermen verwendet: einen Dichotomen für die Einführung eines Fahrverbot für nicht-Euro-4-konforme DPVs in städtischen Umweltzonen (UEZs), und einen Ordinalen für die jährlich erhöhte Prävalenz von DPF unter DPV.

Median-Werte (IQR) für mittlere, tägliche $PNC_{30\text{-}120}$, und Gesamt-PNC lagen bei 4970 (3189) und 11000 (5630) PNC/cm^3. Die linearen Regressionsschätzer für den täglichen Zeittrend ***(β)*** (95% (CI)) lagen bei -0.63 (-0.73; -0.56) bzw. -0.86 (-1.01; -0.71). Die größenspezifischen PNC waren mit NCM, CVM und RM assoziiert: unmittelbar (lag0-1) und verzögert (lag4-5, lag5-6, lag6-7) mit NCM bis zu einem RR von 1.0121 (1.0023; 1.022), verzögert (lag4-5, lag5-6, lag6-7) mit CVM bis zu 1.0199 (1.005; 1.0351) und unmittelbar (lag0-1, lag1-2) und verzögert (lag5-6, lag6-7) mit RM bis zu 1.0333 (0.9971; 1.0707). Das Modell mit dem dichotomen Interaktionsterm zum UEZ-Fahrverbot ab 01.07.2014 indizierte eine Effektmodifikation mit einer Senkung des RR für NCM, CVM, RM für PNCs bis zu einer Partikelgröße von 100 nm (inklusive $PNC_{30\text{-}120}$), 30 nm bzw. 50 nm, während für größere Partikel eher einen RR-Anstieg zu beobachten war. Das Modell mit ordinalem Interaktionsterm im Kontext erhöhter DPF Anteile (von 49 auf 88%) unter den DPVs zeigte keine graduelle Änderung, auch nicht für $PNC_{30\text{-}120}$. Insgesamt unterschieden sich die RR deutlich zwischen PNC Größenfraktionen. Alle Modellschätzer waren weitgehend robust für die Adjustierung mit PM_{10} und NO_2, nur für das Modell mit ordinalem Interaktionsterm verringerte NO_2-Adjustierung die Schätzwerte insgesamt.

Diese Studie lässt auf eine mögliche Erhöhung des Risikos für NCM, CVM und RM durch UFP (und PNC) schließen. Die beobachteten Assoziationen unterschieden sich substantiell nach PNC Größenfraktion und zeigten sich unabhängig von PM_{10} und NO_2. Die RR-Änderungen durch das Fahrverbot in der UEZ deuten auf eine mögliche Zurechenbarkeit hin. Die Ergebnisse motivieren eine Ausweitung größenspezifischer PNC Messungen zur Analyse von Gesundheitseffekten und Interventionsfolgen, bestenfalls mit hoher zeitlicher Auflösung und zusätzlicher Indikatoren für eine Quellenzuordnung.

Abstract

A growing number of epidemiological studies identify possible adverse associations between periods with elevated ultra-fine particle (UFP, particle diameter <100 nm) concentrations and short-term mortality. Diesel exhaust particles (DEPs) have shown to be especially toxic. Diesel-powered on-road vehicles (DPVs) are hence being regulated, particularly through exhaust filtration. It remains unclear how DPV exhaust filtration may modify short-term mortality associations with UFP. This time series study investigated the developments of size-specific, particulate number concentrations (PNCs) between 2009 and 2019, their associations with short-term mortality, and potential effect modification by European diesel exhaust regulation.

Daily mean, size-specific PNC (electric mobility diameter of 13.8-500 nm), fine particles (PM_{10}, aerodynamic diameter < 10 µm) and nitrogen dioxide (NO_2) concentrations from a central urban background station in Mülheim-Styrum (Germany), and daily natural-cause (NCM), cardiovascular (CVM) and respiratory mortality (RM) counts for adjacent municipalities (Mülheim, Essen, Oberhausen) were analysed across 2965 days. Immediate (aggregate lag0-1 days, lag1-2; 0-2 days after exposure), medium-term (lag2-3, lag3-4) and delayed (lag4-5, lag5-6, lag6-7) mortality risk ratios (RR) (95% confidence interval (CI)) per interquartile range (IQR) increase of size-specific PNCs were analysed by Poisson regression. The size fraction of 30-120 nm (PNC_{30-120}) was chosen to represent most DEPs. The models were adjusted for time and meteorological variables, as well as, for sensitivity analyses for PM_{10} and NO_2. To test effect modification by the European exhaust regulation "Euro-4" norm, that requires most DPVs to install diesel particulate filters (DPFs), multiplicative interaction terms were used: a dichotomous one for banning non-compliant DPVs from entering urban environmental zones (UEZs), and an ordinal one for annual DPF prevalence increase among DPVs.

Medians (IQR) for daily mean PNC_{30-120} and total PNC were 4970 (3189) and 11000 (5630) PNC/cm^3, respectively; with simple linear regression estimates ***(β)*** (95% CI) for daily PNC of -0.63 (-0.73; -0.56) and -0.86 (-1.01; -0.71). Size-specific PNCs were associated with short-term NCM, CVM and RM. RRs estimates (95% CI) of PNCs were with NCM immediately (lag0-1) and delayed (lag4-5, lag5-6, lag6-7) up to 1.0121 (1.0023; 1.022), with CVM delayed (lag4-5, lag5-6, lag6-7) to 1.0199 (1.005; 1.0351) and with RM immediately (lag0-1, lag1-2) and delayed (lag5-6, lag6-7) up to 1.0333 (0.9971; 1.0707). Upon non-Euro-4-compliant DPV banning in the local UEZ upon 01.07.2014, RR for NCM, CVM, RM estimates decreased among PNCs up to particle size 100 nm (including for PNC_{30-120}), 30 nm and 50 nm, respectively, while RR for larger particle sizes increase. The model with the annual interaction term in the context of an increase in DPF-equipped diesel-powered on-road vehicle prevalence (from 49 to 88%) showed no gradual RR change over time, including for PNC_{30-120}. Overall, RRs differed greatly between PNC size-fractions. All model estimates were largely robust for PM_{10} adjustment, except for the model with the annual interaction term for which NO_2 adjustment caused a slight downsizing of estimates.

This study indicates that short-term UFP and PNC exposure may increase the risk of NCM, CVM and RM. Observed associations differed substantially depending on PNC size range, while they were robust to adjustment to the two main co-pollutants PM_{10} and NO_2. Effect modification over time in relation to the UEZ banning of non-Euro-4-compliant vehicles indicates potential accountability of the UEZ regulation for human mortality. The findings motivate the extension of size-resolved PNC measurements for basic epidemiological and for accountability studies, ideally with high temporal resolution and additional indicators for source apportionment.

Abbreviations

A40	German interstate #40
AAP	ambient air pollution
AQG	Air Quality Guidelines (by WHO)
CI	confidence interval
CPC	condensation particle counter
CVM	cardiovascular mortality
DAG	directed acyclic graph
DEP	diesel exhaust particle
df	degrees of freedom
DOC	diesel oxidative catalyst
DPF	diesel particulate filter
DPV	diesel-powered (on-road) vehicle
EAD	exhaust aftertreatment device
EC	European Commission
EEA	European Environment Agency
EU	European Union
Euro	European vehicular emissions standard
GAM	general additive model
GIS	geographic information system
GPS	geographic positioning system
GUAN	German Ultrafine Aerosol Network
IARC	International Agency for Research on Cancer
ICD	International Statistical Classification of Diseases and Related Health Problems
IQR	interquartile range
IT.NRW	official data provider for the state of North Rhine-Westphalia
IUTA	Institute for Energy and Environmental Technology. V.)
KBA	Federal Motor Transport Authority
km	kilometer
LANUV	State Agency for Nature, Environment and Consumer Protection of North Rhine-Westphalia
m	meter
MPSS	mobility particle size spectrometer
µm	micrometer or micron
NCM	natural-cause mortality
nm	nanometer
NH_3	ammonia
NO_x	nitrogen oxides
NO_2	nitrogen dioxide
NRW	North Rhine-Westphalia
OP	oxidative potential
OSM	Open Street Map
PAH	polycyclic aromatic hydrocarbons
PM	particulate matter
$PM_{2.5}$	PM with an aerodynamic diameter smaller than 2.5 µm
PM_{10}	PM with an aerodynamic diameter smaller than 10 µm
PNC	Particle number concentration
$PNC_{13\text{-}30}$	PNC range for electric mobility diameter 13.8-30nm (also: d13-30nm)
$PNC_{13\text{-}500}$	PNC range for electric mobility diameter 13.8-500nm (also: d13-500nm)
$PNC_{30\text{-}50}$	PNC range for electric mobility diameter 30-50nm (also: d30-50nm)
$PNC_{50\text{-}100}$	PNC range for electric mobility diameter 50-100nm (also: d50-100nm)
$PNC_{100\text{-}120}$	PNC range for electric mobility diameter 100-120nm (also: d100-120nm)
$PNC_{120\text{-}250}$	PNC range for electric mobility diameter 120-250nm (also: d120-250nm)
$PNC_{250\text{-}500}$	PNC range for electric mobility diameter250-500nm (also: d250-500nm)
Q-Q	quantile-quantile (probability plot)
RM	respiratory mortality
RR	risk ratio (or, synonymous: relative risk)
SCRs	selective catalytic reduction systems
SO_2	sulphur dioxide
(S)VOC	(semi-)volatile organic compound
UBA	Umweltbundesamt (*translates to:* German Environmental Agency)
UEZ	urban environmental zone
UFP	ultra-fine particle(s) sized smaller than 0.1 µm
WHO	World Health Organization

Table of contents

1. Introduction

1.1 Motivation

Short-term exposure to elevated ambient air pollution (AAP) concentrations adversely affects cardiovascular and respiratory health (Héroux *et al*., 2015; Thurston *et al*., 2017, WHO EURO, 2013). In comparison with other environmental risk factors, AAP is currently deemed most health critical by a global ranking (Cohen *et al.*, 2017; IHME, 2019). The contribution of individual AAP constituents for its overall health risk is still being unravelled. An improved understanding of the relative health risk for individual AAP constituents can be critical for designing (more) effective and equitable interventions on AAP to improve human health (e.g. Benmarhnia *et al*., 2014; Boogaard *et al*., 2019; Hoffmann *et al.,* 2020). Substantial developments in measurement technology and overall data availability, among other factors, allow researchers nowadays to differentiate more and more precisely the adverse effects of individual AAP constituents, as well as AAP intervention accountability (e.g. Abbas *et al.*, 2018; Kelly & Fussell, *et al*., 2020; Yang *et al., 2*019).

One group of AAP constituents of particular concern and subject of political and scientific debate are particles emitted by diesel-powered (on-road) vehicles (DPVs), also known as diesel exhaust particles or DEPs (e.g. IARC, 2013; Steiner *et al.*, 2016; Ris *et al., 2*007; Weitekamp *et al.*, 2020). Many people worldwide are exposed to varying concentrations of road-traffic emitted DEPs in their neighbourhood (Anenberg *et al.,* 2019). Studies by toxicologists, exposure scientists and epidemiologists have found evidence suggesting that DEP exposure may cause short-term health effects and constitute a risk factor for premature death (e.g. Hachem *et al., 2*020; Mehus *et al.,* 2015; Ris *et al*., 2007 or Tousoulis *et al*., 2020), beyond the established associations with long-term health effects (e.g. IARC, 2014). Some research findings imply that DEPs per number of particles may have greater short-term health effects than particles from (most) other sources (e.g. Farina *et al*., 2019; IARC, 2014; Park *et al*., 2018).

The reduction of DEP emissions caused by vehicular traffic, among others, is a priority of (national) government policy worldwide (Sanchez *et al.*, 2020). Yet, the understanding of regulation effects on size-specific particulate number concentration (PNC) levels in (urban) residential areas and possible associations with improved health status of populations remains limited to date (e.g. Burns *et al.,* 2019; Hulkonnen *et al*. (2020); Krecl *et al.,* 2020). In the case of DEPs, precise source apportionment outside controlled environments is complex (e.g. Zeraati-Rezaei *et al.*, 2020). The ongoing debates on on-road vehicle emission regulations (e.g. Pries & Wacken, 2020) may benefit from a strengthened evidence base for informed decisions and the design of optimal interventions.

1.2 Air pollution

1.2.1 Air pollutant categories

The management of pollutants in our environment has become institutionalised in societal norms, institutional structures and academic fields. The industrial revolution, among others, has sustainably increased the complexity of pollution management in different media, including vegetation, soil, water and air (e.g. Markham, 1994 or Candelone, 1995). One critical development was the introduction of combustion-based engines, which particularly affected AAP concentrations and composition (e.g. Mosely, 2014). Still today, over a century after the invention of the diesel-motor in 1892, debates on

the effectiveness of exhaust regulation for DPV (e.g. Gross & Sonnberger, 2020; Fujitani *et al.*, 2020) illustrate the topicality of (air) pollution management.

Ambient air can carry various pollutants from anthropogenic and natural sources and spread them further and quicker than any other environmental media (WHO, 2016). AAP may be defined as gaseous, solid and liquid or volatile substances that are either not naturally present or typically only present in lower concentrations in the atmosphere (Daly & Zannetti, 2007).

The constituents of AAP are typically distinguished based on its physico-chemical properties, but also on its source. Primarily, AAP can be differentiated into gaseous and particulate, including liquid constituents (WHO, 2016). The sub-group of AAP in focus of this study, diesel exhaust particles or DEP, largely falls under the categories of particulate, ultra-fine (<100 nm in particle diameter), and combustion-formed AAP, as schematically outlined in Figure 1 (Di *et al.*, 2017; Huang *et al.*, 2013; Wang *et al.*, 2019).

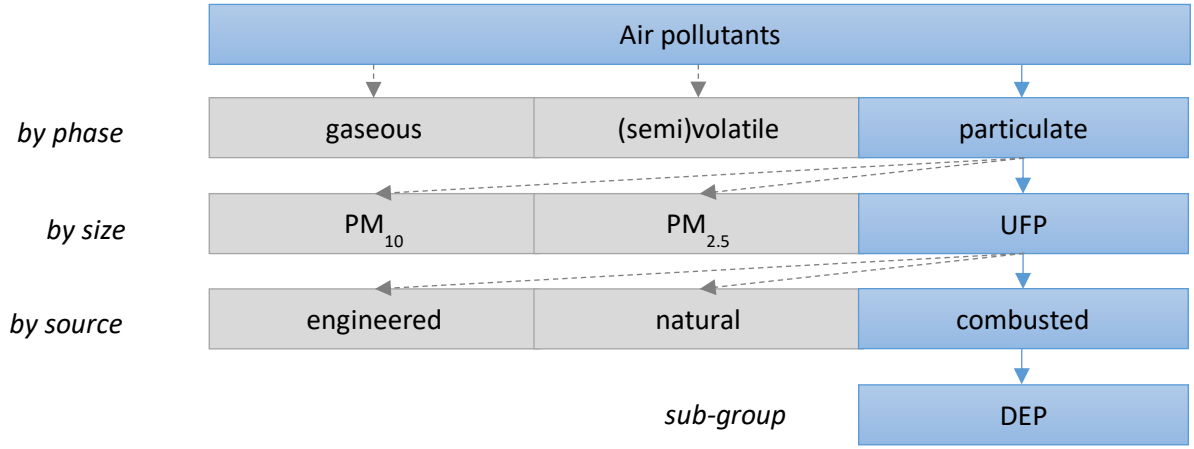

Fig. 1: Simplified classification of diesel exhaust particles among common air pollution categories (by phase, size and source). Source: own design based on WHO (2016) and Wang et al. (2019).

1.2.2 Particulate matter

The particulate constituents of AAP are typically referred to as particulate matter (PM). Notably, the abbreviation "PM" is frequently used synonymously with particulate matter mass concentration, which is the most common measure for air-borne particles (WHO, 2016). For this study, however, the basic definition of PM without specification of its measure is utilised.

PM includes primary pollutants as emitted by natural and anthropogenic sources as well as secondary pollutants formed by precursor substances in the air (Zhang *et al.,* 2018). Precursor substances mainly include nitrogen oxides (NO_X), (semi) volatile organic compounds ((S)VOCs), ammonia (NH_3) and sulphur dioxide (SO_2) (Koolen & Rothenberg, 2019; Ali *et al.*, 2019).

PM is typically measured in mass concentration per unit volume of air (e.g. $\mu m/m^3$) for defined particle size fractions. Two key measures of PM for epidemiological studies are the category of coarse particles with its common measure defined as PM with an aerodynamic diameters of 10 microns (µm) or less, typically denoted as PM_{10}, and of fine particles for PM with 2.5 µm or less in aerodynamic diameter, typically denoted as $PM_{2.5}$ (WHO, 2006). The mass measured is usually conducted with gravimetric metering devices, among others, with common devices described, for example, by Ameral *et al.* (2015).

1.2.3 Ultra-fine particles

The smallest category of PM defined for atmospheric sciences are particles with an electric mobility diameter (size) of less than 0.1 µm. This category is commonly referred to as ultrafine particles or UFPs (HEI Review Panel, 2013; Kwon *et al*., 2020). Air-borne UFPs can change in size, both growth and degrowth processes over short periods of time, mainly depending on temperature, humidity and air pressure (e.g. Kwon *et al., 2*020; Saha *et al.*, 2019). Some researchers therefore use an extended definition to also include particles sized slightly above 0.1 µm, but substantially below 1 µm with the label "quasi-UFP" (WHO 2006; HEI Review Panel, 2013). PM slightly larger than 100 nanometer (nm) can be considered similar enough in atmospheric behaviour and interaction with the human body to justify a slight extension of the official definition (e.g. Saha *et al., 2*019; Ameral *et al*., 2015).

Due to their low weight relative to larger particles such as PM_{10} or $PM_{2.5}$, UFPs are typically not measured in mass concentration, but in PNC per unit volume of air, typically expressed in PNC per cm^3, as also applied in this study (e.g. HEI Review Panel, 2013). Another possible, but less common, measure is the surface area, for which similarly the ratio to mass concentration is much larger for UFPs than larger particles (e.g. Kumar *et al.*, 2013a).

Most UFPs are produced in the context of combustion processes (e.g. HEI Review Panel, 2013; Li *et al*., 2018a; Zhao *et al*., 2020). Some UPFs originate as industrially manufactured particles, sometimes also referred to as nanoparticles in material sciences (e.g. HEI Review Panel, 2013). The particle size categories for PM below 1.0 µm are often differentiated into the nucleation mode (particle diameter < 30 nm), the Aitken mode (30 nm < particle diameter < 100 nm) and the accumulation mode size fractions (100 nm < particle diameter < 1 µm) (e.g. Kwon *et al*., 2020).

The composition of UFPs depends on their source and genesis. One may differentiate primary and secondary UFPs, as for PM, with secondary referring to formation by gaseous and (semi)volatile precursor substances in the air (e.g. Kwon *et al*., 2020). Rivas *et al*. (2020) characterised the urban background UFP composition for four European cities and found photo nucleation, traffic emissions and secondary particles as the three most common sources of UFP concentration. Thereby, traffic sources in combination contributed to 71-94% of PNCs. For Germany, based on data gathered by the European Environment Agency (EEA), on-road traffic-related emissions were the largest contributor to fine particles ($PM_{2.5}$), dominated by passenger vehicle emissions (over 90%) (EEA, 2020b).

1.2.4 Diesel exhaust particles

Overall, on-road motorized traffic is a main source of ambient UFP in Western Europe and elsewhere (e.g. Anenberg *et al.*, 2019). In many urban areas, on-road traffic has been identified as the dominant source of UFPs (e.g. Karagulian *et al.*, 2015; Li *et al.*, 2018b; Kumar *et al.*, 2014). "*Motor vehicles, especially those powered by diesel engines, have often been cited as a leading source of ambient UFP emissions and of human exposure*," concluded the HEI Review Panel (2013, p. 1). In Chinese cities, for example, DEPs are estimated to have been responsible for over 80% of on-road vehicular PM emissions in around 2010 (Deng *et al.*, 2017). Dallmann & Harley (2010) estimated that over a quarter of mobile sources of $PM_{2.5}$ attributes to DPV emissions between 1996 and 2006 (notably thus based largely on a vehicular fleet not equipped with diesel particulate filters (DPFs)).

Diesel-engine exhaust typically contains gaseous, (semi)volatile, liquid and solid fractions. Non-filtered diesel engine exhaust contains SVOCs and VOCs, as well as DEPs which comprises soot particles that

are coated with organic compounds such as polycyclic aromatic hydrocarbons (PAHs) and its derivates, nitrogen and sulphur oxides, alkanes, alkenes and aldehydes, as well as ash with its various metallic compounds (e.g. Wang *et al.,* 2019; Ris *et al*., 2007). The particulate proportion of diesel exhaust, i.e. DEPs, are regarded as one of the most health-critical components (e.g. IARC, 2014; Mills *et al., 2*021). Besides residential wood burning, DEPs are also considered the primary contributor to carcinogenic PAHs and nitro- and di-nitroarenes emission, amongst other substances (e.g. Karagulian *et al.*, 2015; Manoli *et al.*, 2016).

One may differentiate DEPs into: "[1] *primary UFPs formed in high temperature,* [2] *delayed primary particles formed as gaseous compounds nucleate during the cooling and dilution process and* [3] *secondary nanoparticles formed from gaseous precursors via the atmospheric photochemistry* (Rönkkö & Timonen, 2019, p. 15)". Upon emission at the exhaust pipe, in a supersaturated zone, soot and other primary PM become covered with condensated and adsorbed SVOC like PAHs (e.g. Keskinen & Rönkkö, 2010). Black carbon is also a part of DEPs, the definition includes but is not equal to (diesel) soot, contrary to common source apportionment simplifications (Buseck *et al.*, 2012; Watson & Valberg, 2001; Müller *et al.*, 2006). The high PNC in the air right behind the tailpipe also favours coagulation of primary PM to larger PM sizes (e.g. Wehner *et al.*, 2009). Jathar *et al.* (2017) estimate that the proportion of secondary compared to primary organic aerosol leans strongly towards secondary as aging time increases with increases of an order of magnitude and more. Real-world studies have shown the proportion of secondary aerosols to be more prominent in urban background than sites than at emission, e.g. roadside, sites (e.g. Taiwo *et al.*, 2014).

The size DEPs roughly ranges between 10 to 150 nm in size – representing both primary and secondary particles (e.g. Martos *et al*., 2020). Highest PNCs for fresh diesel exhaust emitted by on-road vehicles equipped with a DPF were found within a size fraction of 10 to 30 nm (e.g. Rivas *et al.*, 2020). For on-road vehicles without a DPF, the vast majority of its PNC were estimated between 30 to 120 nm in size based on an unsystematic review of available literature for this study (including estimates by Agudelo-Castañeda *et al*., 2019; Rivas *et al.,* 2020; Harrison, 2018; Zeraati-Rezaei *et al.*, 2020; Martos, 2020). Exact concentration patterns can depend on engine and vehicle operation properties, exhaust after treatment, fuel properties, as well as, typically time-varying, environmental factors (Martos *et al.*, 2020; da Silveira Fleck *et al.*, 2020; Rivas *et al.*, 2020; Wang *et al.*, 2019). Thus, the temperature and humidity of the dilution air may affect particle size distributions (e.g. Keskinen & Rönkkö, 2010). Due to the volatility of particularly nucleation-mode particles, some studies assume that particle size may reduce over time on a neighborhood scale (up to 1 kilometer (km)) due to evaporation (Nikolova *et al.* (2018).

Explicitly or implicitly the majority of studies on DPV particle emissions focus on DEPs or at least diesel engine exhaust while, DPVs also cause other particulate emissions, such as from brake and tire wear, including associated road wear. Such PM are assumed to largely range outside the UFP size fraction. The scientific debate on these traffic related particles is ongoing, with recent findings on brake wear having found minor contributions to the total UFP emission of DPVs through heat induced UFP emissions from braking (e.g. Jeong *et al.,* 2019 or Kwak *et al*., 2013).

1.3 Concentration and human exposure of air pollution

AAP concentration values in the ambient air are typically basis for estimates of individual or population-level AAP exposures. The measurement of AAP concentrations and estimation of human

exposures differ between locational settings, time perspectives and in-focus pollutants (groups). The estimation of an individual's air pollution exposure is naturally limited in accuracy and precision as discussed by (Dias *et al*., 2018) with a summary of the challenges in covering spatial and temporal dynamics for air pollution exposure assessments. Exposure sciences and other disciplines have developed measurement protocols and modelling approaches for various purposes, with an overview for urban air pollution exposure provided e.g. by Jerrett *et al.* (2005) and Xie *et al.* (2017) and for road traffic by Khan *et al.* (2018). Koolen & Rothenberg (2019) provides an overview of air pollutant concentrations for the European Union (EU). The majority of AAP concentration measurements stems from fixed, high-cost air pollution measurement stations, while the introduction of low-cost and mobile, e.g. on-person, sensors is developing rapidly (e.g. Maag *et al.*, 2018; Karagulian *et al.*, 2019).

1.3.1 Ultra-fine particles

Measurements of UFPs are relatively expensive and technically complex. For PNC estimation, currently the two main measurement types are condensation particle counters (CPCs) for high temporal resolutions of total UFP counts and differential mobility analysers or mobility particle size spectrometers (MPSSs) for differentiating counts between several UFP size fractions. To date, there is not standard measuring device and the lower detection limits of available measurement devices (including CPCs and MPSSs) differ – often between 5 and 20 nm (e.g. Ameral *et al*., 2015). UFPs are currently neither part of one of the key global guidelines, such as the World Health Organization (WHO) Air Quality Guidelines (AQG) (WHO, 2006), nor regulated by the EU or German legislation. Thus, typically no reporting duty on UFPs is in place, nor in turn, systematic government exposure measurements exist.

As UFPs are known to be highly dynamic in time and space, the differentiation of near-emission-source, often roadside, and urban or rural background concentrations is particularly relevant for exposure estimation. According to a recent study by Saha *et al.* (2019), the spatial heterogeneity of PNC (here: used simplified as a proxy for UFP) can be 2-3 times higher than of $PM_{2.5}$ mass concentration. As another illustration, a time series study in Ontario by Hilker *et al.* (2021) for the years 2004 to 2015, found local emissions such as from traffic were estimated to contribute relatively constantly to almost half of the urban background UFP concentrations). A study around the city of Strasburg (France) found significant differences between urban background and roadside concentrations of UFPs in contrast to relatively stable PM_{10} concentrations (Chatain *et al*., 2021).

In Germany, the German Ultrafine Aerosol Network (GUAN) operates several measurement stations for UFPs across the country (Birmili *et al.*, 2016). The network has grown to 17 stations in 2020 (as of 31.12.2020; formatted as DD/MM/YYYY), of which six measure rural and seven measure urban and one measures high altitude background concentrations. Three stations measure roadside concentrations (Birmili *et al*., 2016). Typical PNCs are often over 10,000 per cm^3 in urban background conditions and below 5,000 and 500 for rural background and alpine regions respectively (Kumar *et al*., 2014; Birmili *et al*., 2016). In the Netherlands, for example, a large UFP modelling study found average measured UFP concentrations across 20 locations between 3,814 and 7,070 particles/cm^3 (Beek *et al.*, 2020). In Germany, in a city of similar size as the municipalities in the study area, annual mean UFP PNC were found at just below 8,000 for urban background and just above 16,700 in a busy street canyon (Giemsa *et al*., 2021).

Various types of concentration measurements of UFPs serve as a proxy for short-term exposures. For time series studies of population, exposure measurements from fixed stations is common, which uses short-term concentration measures (e.g. hourly or daily). This is feasible as changes in daily concentration averages have shown to be mainly due to meteorological conditions. The temporal correlations between different UFP background measurement stations within one city has been shown to be high, thus estimation of temporal exposure dynamics for a larger population is deemed possible based on a central measurement station (e.g. Cyrys *et al.*, 2008). Mobile measurement devices, e.g. installed on bicycles, cars or airplanes, can be used for spatial differentiation of exposure, e.g. across a defined trajectory, or exposure of individual persons or specific groups. Exposure measurements of UFPs have also included experimental determinations of deposited UFP in human respiratory tracts (e.g. Guo *et al.*, 2019).

1.3.2 Diesel exhaust particles

The measurement of DEPs typically takes place within a vehicle's exhaust system or at the tailpipe, while estimations of DEP concentrations in ambient air are difficult due to the complexity of source apportionment (Giechaskiel *et al.*, 2013). Different parts of the exhaust system filter different parts of diesel exhaust and inherent DEPs, thus influencing measurements. With distance to the tail pipe, the properties of DEPs may change through several processes, mainly depending on their size, including: (1) coagulation, as estimated to cause single-digit (e.g. 5% by (Harrison *et al.*, 2018) in a street canyon) reductions in DEP PNC numbers, depending on meteorological conditions and overall PNC levels; (2) deposition to surfaces, also estimated to reduce PNCs in the single digit range, as well as, (3) condensational growth, (4) evaporation (e.g. Dall'Osto *et al.*, 2011) and (5) further chemical reactions (e.g. Harrison *et al.*, 2018). Sometimes, DEPs are thus differentiated into fresh and aged, while the continuous process of aging does not allow a definite differentiation – and fresh DEPs theoretically start aging in the moment of leaving the tailpipe (e.g. Harrison *et al.*, 2018). DEP concentration estimations within AAP mixtures can be performed with different source apportionment approaches, with the precision depending on the available information including size-differentiated PNC at different time resolutions (e.g. daily or hourly) and chemical particle compositions besides gaseous co-pollutant concentrations.

1.4 Health effects of air pollution

1.4.1 Ambient air pollution

Public concern about AAP and health dates back to at least ancient Rome and Athens, with the 19th century often quoted as a game changer with the stark increase in emissions from combustion in the context of the industrial revolution (Mosely, 2014). Among possible human health outcomes, mortality is considered to have been studied the longest and most frequent (Anderson, 2009). In the winter of 1952, a smog episode in the city of London, and in following years similar events in Belgium and the United States, caused thousands of deaths. The "London Smog" is retrospectively regarded as a key event for AAP research, and could be traced back to elevated (ambient) AAP concentrations due to combustion emissions (mainly coal) in conjunction with a temperature inversion (Bell & Davis, 2001; Zhang *et al.*, 2015). Research on AAP has since advanced steadily, amongst others along improving exposure measurement and data analysis methods (e.g. Anderson, 2009).

Nowadays, epidemiologists basically differentiate between short- and long-term health effects of AAP (e.g. Sun & Zhu, 2019b). AAP has overall particularly and robustly been associated with elevated risk for cardiovascular (Lelieveld *et al.*, 2019; including e.g. elevated blood pressure (Yang *et al.*, 2018) or thrombosis (Robertson & Miller, 2018)) and respiratory diseases (e.g. for asthma (Orellano *et al.*, 2017)) and associated premature mortality (e.g. Thurston *et al., 2*017). AAP has also been observed to cause potentially adverse effects on the central nervous system (including risk increase for stroke and carotid artery disease (Babadjouni *et al.*, 2017), for cognition (de Prado Bert *et al.*, 2018), for dementia (Peters e*t al.*, 2019) and for other mental health syndromes (Braithwaite *et al.*, 2019). Furthermore, evidence suggests potential adverse effects on the metabolism (including diabetes (e.g. Ikenna *et al*., 2015; Liu *et al.*, 2019; Yang *et al.*, 2020)) and by pregnancy exposure for neonatal health (e.g. for lower birth weight, congenital anomalies and preterm birth (e.g. Jacobs *et al.*, 2017 ; Conforti *et al.*, 2018).

Today, it is widely acknowledged that the quality of the air we breathe is of critical health relevance (Sun & Zhu, 2019a; Global Health Metrics, 2018). Effects on the cardiovascular system are estimated to cause the largest proportion of the disease burden (e.g. Lee *et al*., 2018). Air pollution overall has recently been estimated as the 4th most important health risk (behind blood pressure, malnutrition and smoking) and thereby as the leading environmental health determinant globally (Cohen *et al.*, 2017), even if such rankings are to be interpreted with care as they only include a limited number of environmental risks. Current estimates suggest that ambient PM may cause the majority of the AAP disease burden, as reflected in the latest ranking as the 7th most important health risk (IHME, 2019).

1.4.2 Particulate matter

The main exposure pathway for PM is inhalation, while ingestion and dermal, including soft tissue, contact can also be relevant (Hamanaka & Mutlu, 2018). However, the biological mechanisms behind identified associations between PM exposure and human health are not fully understood (e.g. de Kok *et al.*, 2006; Mudway *et al.*, 2020). PM theoretically can enter the human body through skin and mucosal contact, ingestion, inhalation into the lung and through the nose into the olfactory bulb. The main pathway is estimated to be inhalation through the lung with the following biological effect chains commonly hypothesized (e.g. Hamanaka & Mutlu, 2018; Fiordelisi *et al.*, 2017): (a) oxidative stress and inflammatory responses in the lung induce systemic inflammation and associated effects; (b) activation of sensory receptors affect the autonomic nervous system with consequences e.g. for heart rate variability; (c) intrusion of PM into the blood circulation and body tissues can affect various organs.

The health effects of PM have been described repeatedly, e.g. by Rückerl *et al.* (2011). One may differentiate between different toxicities of PM, including genotoxicity, cytotoxicity and others. Several reviews concluded that smaller PM size fractions, relative to their weight, are more toxic and more radical-generating. Largely in mutagenicity in-vitro assays, the genotoxic effect has been confirmed by toxicologists, while several methods have confirmed cytotoxicity of PM (e.g. de Kok *et al.*, 2006). One proxy for PM's biological reactivity is the oxidative potential (OP). A recent review concluded that, while many OP-studies reported significant associations between OP and biological effects in humans, findings were not consistent (Øvrevik, 2019), while ANSES (2019) concluded that PM's OP is still a recent measurement with many non-standardized methods which could explain limitations in the evidence strength. The OP is considered highest among the smallest particles, e.g. UFPs. Therefore, PNC is likely a critical measure alongside the common PM weight per volume of air (e.g. Daellenbach *et al.*, 2020; Nováková *et al.*, 2020). However, neither particle mass nor size are sufficient information to estimate toxicity, due to the mentioned differences in composition that defines health-relevant

factors, like OP, which is e.g. by Bates *et al.* (2019) proposed as an alternative measure to particle weight and size.

Like for AAP in general, short- and long-term effects on natural and cause-specific mortality have been associated with PM exposure (e.g. Yang *et al.*, 2019). PM has particularly shown positive associations with higher risks of cardiovascular diseases (Rajagopalan *et al.*, 2018), such as acute myocardial infarction (e.g. Shin *et al.*, 2021), but also with respiratory diseases (e.g. Kyung *et al.*, 2020). A systematic review on dementia and Alzheimer's disease concluded on positive associations upon meta-analysis (Tsai *et al.*, 2019). PM has also shown to serve as an endocrine disruptor, with risk increases for metabolic diseases including diabetes mellitus or obesity, and thus indirectly for cardiovascular diseases (e.g. Yang *et al.*, 2020). Thereby, the overall epidemiological understanding of the relative health effects of individual PM constituents remains limited, as does the understanding of UFP constituents (e.g. Kwon *et al.*, 2020).

1.4.3 Ultra-fine particles

UFP in general have a larger surface area per weight than larger particles, with consequences for, among others, the potential to adsorb toxic compounds on their surfaces and thereby increase, among others, the particles' OP (e.g. Kwon *et al.*, 2020, Moreno-Rios *et al.*, 2021). The small size also increases UFPs pulmonary deposition efficiency compared to large size fractions of PM, as well as its deposition duration (e.g. Schraufnagel, 2020). The size of UFPs and its biochemical properties allow UFPs to pass the boundaries to the blood, lymphic, and nervous systems and even to enter cellular organelles and the placenta (e.g. Kwon *et al.*, 2020). Like for PM, the main exposure route is by inhalation into the lung and the alveoli, but also other pathways, including the direct passage through the olfactory bulb to the brain are investigated (e.g. Longhin *et al.*, 2020). The review by the HEI Review Panel (2013) differentiated cardiovascular and respiratory health effects upon deposition in the respiratory tract through adverse effects on the sensory nerves and ganglia, as well as, the epithelial cells and macrophages and associated consequences for respiratory tract function, endothelial function, acute phase response, blood coagulability and platelet activation. Upon UFPs entering the circulation, they can cause adverse effect in further organs, the bone marrow or the brain. The brain may also be affected when UFPs enter the olfactory bulb through the nose.

The US-EPA Integrated Science Assessment (USEPA, 2019) describes the biological logic for UFP induced health effects, including on natural morbidity and mortality, and the plausibility of epidemiological findings in a comprehensive review. In addition, Hadrup *et al.* (2020) described acute phase response as a biological mechanism-of-action for UFP-induced cardiovascular disease, while Leikauf *et al.* (2020) summarized the biological mechanisms behind respiratory health effects of UFPs. Several studies, including those on purposely produced UFPs, or nanoparticles, discuss the difference in health effects by physico-chemical properties, including composition (e.g. Ajdary *et al.*, 2018).

Epidemiological and toxicological studies have found indications that UFPs can cause various adverse short-term and long-term health effects, with potentially significantly larger effects by mass concentration and possibly even by number than larger particles (HEI Review Panel, 2013; Kwon *et al.*, 2020; Meng *et al.*, 2013; Ohlwein *et al.*, 2019; WHO EURO, 2013). An increasing number of studies have investigated associations between short-term UFP exposure, with a recent review by Ohlwein *et al.* (2019) identifying more assessments of short- than of long-term effects with many studies assessing PNC size ranges beyond 100 nm. The assessed research suggested short-term associations with

adverse inflammatory and cardiovascular effects, and various outcomes without conclusive evidence or assessed independence of other air pollutants. Another review by Redaelli *et al.* (2019) concluded on "moderate" evidence levels for cardiovascular health and UFP exposure, while an expert consultation by ANSES (2019) rated the level of evidence for UFP and cardiovascular health association highest among respiratory mortality (RM) and natural-cause mortality (NCM). The review by Ohlwein *et al.* (2019), but also a multi-city and source apportioned study by Rivas *et al*. (2021) concluded in inconsistent and inconclusive observations for most quasi-UFP exposure and mortality outcome pairs. Notably, the patterns of effect estimates across lags 0 to 5 in the case of Rivas *et al.* (2021) differed notably between cities (less than for UFP sources/groups), e.g. concave vs. convex patterns, even for the same source-apportioned quasi-UFP group.

NCM was found statistically significantly associated 4, 5 and 6 days (lag4, lag5, lag6) after exposure to elevated PNC by Staffogia *et al*. (2017), for lag2 to elevated total PNC and for lag5 to traffic-source PNC with a size range 40-140 nm by Rivas *et al*. (2021), for lags 0 and 2 for UFP particles source apportioned to traffic exhaust by Tobías *et al*. (2018), as well as for aggregate lag of same day and previous day exposure of PNC size range 250-280 nm by Meng *et al*. (2013). The percentage changes in mortality risk were based on IQR increases of PNC, with converted estimates for absolute increases of 5000 particles/ml ranging between 1-5 %. Samoli *et al.* (2016) generally associated elevated UFP-exposure with elevated hospitalization rates. Studies on indoor and outdoor UFP exposure showed adverse associations with cardiopulmonary function particularly indicated by heart rate (variability) (Chen *et al.*, 2021; Rizza *et al.*, 2019).

Among the (few) observed statistically significant associations, Meng *et al*. (2013) observed increases in relative cardiovascular mortality risk for the moving aggregate lag of same day and previous day exposure, for lag0 and lag1 by Rivas *et al.* (2021), while Su *et al*. (2015) found increases for PNC sized 3-100 nm upon a 5-day average exposure. The percentage changes in mortality risk convert to percentage increases in mortality risk for PNC increases of 5000 particles/ml of between 4-6 %. Such findings may be linked to the experimental results of Soppa *et al*. (2019), who found increased arterial stiffness upon UPF exposure in an indoor experimental setting, or Soldevila *et al.* (2020) who found associations of blood pressure the day after elevated UFP exposure, as well as Chen *et al*. (2020) who observed statistically significant associations between myocardial infarction and same-day UFP exposure of several size ranges. As an indicator for adversely affected cardiovascular function, studies have also found associations between prolonged corrected QT intervals and short-term elevated UFP exposure (Lammers *et al.*, 2020). Núria *et al.* (2020) found significantly increase blood pressure upon lag1 elevated UFP exposure.

Significant associations between UFP exposure and RM were not identified by studies included in Ohlwein *et al*. (2019), but observed in a more recent study by Rivas *et al*. (2021) for traffic-source PNC with a size range of 40-140nm at lag1. A study on COPD mortality found weak, but statistically significant association with PNC of size range 1-300 nm (Yin *et al*., 2019). Also, a multicentre study in Europe found that increased 6-day average UFP exposure was associated with a higher risk of respiratory hospital admissions (Lanzinger *et al., 2*016). Also, a lagged effect (here lag2 and lag3) for short-term UFP exposure were found associated with respiratory hospital admissions by a recent meta-analysis (Samoli *et al.*, 2020). Several studies, for example by Samoli *et al.* (2020), have found associations several days after elevated UFP exposure, including on respiratory morbidity. Studies have found decreased forced vital capacity, as an indicator of lung function (Lammers *et al., 2*020). Adverse short-term effects of elevate UFP PNC were observed persons with asthma (Habre *et al.*, 2018).

On a side note, various long-term effects have been more or less robustly associated with UPF exposure, including cardiovascular and respiratory illnesses, neuronal and cognitive malfunctioning, as well as cancers (e.g. Downward *et al., 2*018; IARC, 2013; Ohlwein *et al.*, 2019). One key limitation for a better evidence base on long-term effects is the relative to other AAP reduced availability of long-term concentration datasets.

1.4.4 Diesel exhaust particles

Among the constituents of diesel exhaust, DEPs have been assessed as critical for diesel-exhaust induced health effects (e.g. IARC, 2014; Mills *et al.*, 2011; Zerboni *et al.*, 2021). The majority of DEPs fall within the UFP size range, and are thus subject from a size perspective to the biological mechanisms described above for UFPs. In addition, as the physico-chemical composition of DEPs differ from other UFP sources, several studies have described biological mechanisms for DEPs separately, particularly for short-term effects, such as Cardenas *et al.* (2021), Rankin *et al.* (2021) and Tousoulis *et al.* (2020), even if study designs that compare DEPs with UFPs of other sources to facilitate reliable comparisons are rare. Tseng *et al.* (2017), for example, described cellular mechanisms possibly responsible for the toxic effects of DEPs, while biological mechanisms for adverse respiratory effects through DEPs (e.g. allergic rhinitis or asthma) are described by (Riedl & Diaz-Sanchez, 2005). Toxicological studies have e.g. observed DEPs producing reactive oxygen species (superoxide and hydroxyl radicals) without biological activating systems, as required for some other UFPs (Sagai *et al*., 1993). The presence of DEPs in an UFP mixture may also interact adversely with other compounds, such as metal oxides, as e.g. assessed by Zerboni *et al*. (2019). The expert consultation by ANSES (2019) concluded on a "high" evidence level for black carbon, which is also a constituent of unfiltered DEPs, and its association with NCM, cardio-vascular mortality (CVM) and RM. For PAHs, however, they rate the level of new evidence since WHO EURO (2013) as low.

While some toxicological studies have compared DEPs with other AAP, the epidemiological evidence on DEP associations with short-term natural and cause-specific mortality (e.g. Lammers *et al.*, 2020; Longhin *et al.*, 2016; Zhang *et al.*, 2009) hardly includes comparative effect estimates. However, due to a dominance of diesel-powered engines in certain occupational contexts (e.g. mining sector), quasi-experimental setups largely excluding other emission sources are possible. Consistent with UFP studies, also DEP studies reported associations with NCM, CVM and RM or the respective morbidities (Andersen *et al.*, 2019; Ris *et al.*, 2007; Mehus *et al.*, 2015). Notably, both primary and secondary DEP have been observed as respiratory irritants (Ris *et al.*, 2007; Salvi *et al.*, 1997).

For long-term health effects, the evidence on the relatively high toxicity of DEPs is more established (e.g. Silverman *et al.*, 2012), such as a risk factor for cancer (IARC, 2014). In 1989, the International Agency for Research on Cancer (IARC), the specialized cancer agency of the WHO, evaluated DEP first as "*probably carcinogenic to humans (Group 2A) on the basis of limited evidence from epidemiological studies in humans and sufficient evidence for the carcinogenicity in experimental animals* (p. 33)". Today, IARC rates DEPs as an "class A"-carcinogen, the category with highest certainty, (IARC, 2014; Steiner *et al.*, 2016). Evidence for carcinogenic effects of DEP focuses on the primary emissions from engines without DPFs and thus high relative concentrations of polycyclic aromatic hydrocarbon (PAHs) (IARC, 2014; Abbas *et al.*, 2018).

Among UFPs differentiated by source, DEPs are estimated as the causing the greatest health effect per PNC (e.g. Park *et al.*, 2018). However, the evidence remains inconsistent, with limitations in

interpreting estimates due to the above-mentioned lack of effect comparisons between UFP sources within individual studies, that can hardly be replace by comparing individual studies of single UFP sources due to, among others, methodological differences. Notably, compared to other AAP caused by road traffic, DEPs and diesel exhaust in general are among the most extensively studied (ANSES, 2019). Above all, source apportionment of DEPs and robust differentiation of exposure to (mainly) DEP UFPs in contrast to UFPs to other sources, remains difficult, particularly outside (quasi-)experimental setups or occupational contexts (e.g. Hime *et al.*, 2018). A recent review concluded that the current evidence does also not allow a clear distinction between the health effects of unfiltered DEP and filtered DEP (Weitekamp *et al.*, 2020).

1.5 Policies on air pollution

1.5.1 European Union policy on air pollution reduction

For the protection of public health, ambient AAP concentration reduction is subject of laws and regulations in many countries and regions worldwide (e.g. Giechaskiel *et al.*, 2019). A key resource for defining AAP concentration limits are the guideline values provided by WHO (2006). The WHO lists PM as the primary group of concern among currently known air pollutants. To date, however, no WHO guideline value is available for UFPs (WHO, 2006).

In the EU, the policies on AAP consist of three main pillars, that are largely based on directives. In the logic of EU legislation directives set out legally binding goals, but allow member states to develop own laws and strategies to achieve these goals (in contrast to the EU legal instrument of regulations) (EEA, 2020a). The three pillars are:

(a) the "Ambient Air Quality Directives" to define air quality standards and requirements for the assessment of air quality the implementation of air quality plans. The current Directive 2008/50/EC is, among others, based on the AQG. It includes previous daughter directives on specific pollutants except the separate Directive 2004/107/EC on arsenic, cadmium, mercury, nickel and polycyclic aromatic hydrocarbons and is extended in terms of monitoring by Directive 2015/1480/EC and information exchange by Commission Implementing Decision 2011/850/EU;

(b) the National Emissions reduction Commitments Directive (2016/2284/EU) to establish national emission reduction commitments; and

(c) the source-specific legislation to establish specific emission and energy efficiency standards for selected AAP sources, including the so-called "Euro-norms" for on-road vehicle exhaust limits.

1.5.2 Regulation of on-road vehicle exhaust in the European Union

Among the source-specific regulations, the Euro norms for vehicles for on-road vehicle emissions specifically date back over 50 years (see Table 1). In 1970, for the first time, a coherent European directive, the Council Directive 70/220/EEC, on exhaust limits for carbon monoxides and hydrocarbons in the European Economic Community (EEC), later converted into the EU, was agreed upon (EEC, 1970). In 1992, the EEC introduced the emission norm "Euro" as part of the Council Directive 91/441/EEC with its first set of limit values known as "Euro-1" (EEC, 1991).

Table 1: Overview of European Union policies on vehicle emission standards (Euro norms). Source: own design based on UBA (2015) and EEC (1970).

Legal document	*Euro norm*	*Year of taking (first) effect for passenger vehicles*
70/220/EEC	pre-Euro	1970
91/441/EEC and 93/59/EEC	Euro-1	1992
94/12/EC and 96/69/EC	Euro-2	1996
98/96/EC	Euro-3	2000
98/691/EC and amendment 2002/80/EC	Euro-4	2005
Various	Euro-5	2009
Various	Euro-6	2014

These Euro norms have become the key tool for regulating on-road vehicle emissions in the EU (UBA, 2015). Most legislation on the Euro norms and its implementation have been decided as directly binding regulations. Besides the vehicular emission legislation, the above-mentioned Ambient Air Quality Directives (currently: 2008/50/EC) and its associated national legislation for implementation set limits for AAP, which particularly affects urban areas due to a concentration of emission sources, including gaseous and particulate on-road vehicle exhaust. Road traffic was rated the main target of AAP reduction measures in European cities by a recent study (Viana *et al.*, 2020). Table 1 outlines the different Euro norms with its associated legal documents in chronological order.

Another regulatory intervention alongside the exhaust limits concerns fuel composition based on EU's "EN-590" norm (e.g. Giechaskiel *et al*., 2019). One main change since concerned continued reductions of the diesel's sulphur content (from 0.2% for Euro-1 to 0.001% for Euro-5) and slight increase in cetane number (from min. 49 for Euro-1 to min. 51 for Euro-5). The diesel fuels with lower sulphur content were gradually introduced at filling stations, with the last upgrade in terms of sulphur content on January 1st, 2009. These changes thus occurred before this time series, while studies estimate overall a small effect of fuel composition changes, particularly sulphur content, on PNC in comparison with DPFs (e.g. Kontses *et al*., 2019).

In the EU and in its member states, the key measures taken for DPV emissions include regulations on diesel fuel composition, diesel particulate filters (DPFs) and so-called "low emission zones" or "urban environmental zones" (UEZ) in urban areas (Cyrys *et al.*, 2014; Cyrys *et al.*, 2018; Reşitoɬlu *et al.*, 2015) (see Tab. 2). The key intervention on DEP in the EU in the past two decades was thereby the introduction of the DPF, which were installed in the vast majority of vehicles that were to comply with Euro-4 norm. "(…) *the application of aftertreatment devices (mainly: DPF) not only reduces the emitted particle mass but also leads to significant changes in the nature of the particles, such as a relative increase in the volatile fraction*," concluded Burtscher (2005, p. 897). In association with the Euro norm introduction and implementation of Directive 2008/50/EC, Germany, amongst others EU member states, introduced and gradual upgraded and extended UEZ in selected urban areas (Cyrys *et al.*, 2014). All UEZs in Germany that have so-called "level-3" requirements require on-road vehicles to comply with Euro-4 and for DPVs thus in the vast majority of cases to be equipped with a DPF (UBA, 2020a).

Table 2: Overview of relevant on-road passenger vehicle exhaust policies with year of introduction in Germany with regulatory limits for PM. Source: own design based on UBA (2015) and (2020a) and Cyrys *et al.* (2014)

Intervention	*Level*	*Year*	*Regulatory specification*
(1) Euro emission standards (gradually tightening)	Euro-1	1992	
	Euro-2	1996	PM: 0.08g/km
	Euro-3	2000	PM: 0.05g/km
	Euro-4	2005	PM: 0.025g/km
	Euro-5	2009	PM: 0.005g/km
	Euro-6	2014	PM: 0.0045g/km
(2) Environmental zones (gradually tightening)	L1	2008/2012	only Euro-2,3,4
	L2	2013	only Euro-3,4
	L3	07.2014	only Euro-4
(3) Diesel particulate filter	Euro-4	2005	
(4) Truck driving ban (on Sundays and holidays)	n.a.	1956	

The modifications of DPVs through exhaust aftertreatment devices (EADs) started with the introduction of catalysts, that were required for all on-road vehicles in the study area before the study's first measurements. The diesel oxidative catalyst (DOC) and the selective catalytic reduction systems (SCRs) particularly aimed at carbon monoxide and hydrocarbons (Chirico *et al.*, 2010). Subsequently, the introduction of the DPF aimed at reducing particle mass, but also PNC. The DPF effectively leads to a burning and gasification of compounds previously emitted as solid particles, a large fraction of which containing soot. DPFs are typically "regenerated" periodically to remove trapped PM. Over time, DPFs also accumulate ash particles, that cannot be regenerated in the same way, but may require replacement of the DPF (Valverde & Giechaskiel, 2020).

Also, driving bans for certain heavy-duty on-road vehicles on Sundays and public holidays are an additionally exposure-relevant intervention in several countries, including Germany (§ 30 sections 3 and 4 of the German road traffic regulation). This measure took effect well before 2009 (see Intervention No. 4 in Tab. 2) and thus the beginning of the time series at hand.

1.5.3 Composition change of diesel exhaust upon regulations

The DPFs were developed and refined as EAD to meet the ordinally more restrictive Euro norms (Euro-4 and higher) for DPVs, especially the limits for particle mass and later also for PNC (Chirico *et al.*, 2010). The DPF is estimated to trap most primary PM or non-volatile particles (e.g. Reijnders *et al.*, 2018). Karjalainen *et al.* (2019) estimated a 98% reduction in PM by the latest EADs, with DPFs as the key intervention for PNC reduction, thus leaving mainly SVOCs as potential UFPs, as also illustrated by experiments (e.g. Chirico *et al.*, 2010; Platt *et al.*, 2017; Kontses *et al.*, 2019). Qadir *et al.* (2013) found the contribution of traffic to particulate organic compounds, a component of PM and PNC, to have decreased by 60% upon UEZ introduction, and thus non-DPF equipped DPV banning, in the German city of Munich.

The PNC concentrations in the exhaust of DPF-equipped vehicles were shown to be mainly based on secondary particle formation through precursor gases right at the tail pipe and in the ambient air (e.g. Platt *et al*., 2017; Zeraati-Rezaei *et al.*, 2020). For the remaining primary PM emitted by vehicles with DPFs, Su *et al.*, (2004) observed smaller and differently shaped, rather fullerene-like, soot particles in primary particulate exhaust. Thereby, Young *et al.* (2012) suggests that non-volatile particle reduction by DPF does not depend on whether normal fuel or biofuels are used. The PNC size ranges emitted by DPF-equipped DPVs, even if taking nucleation processes right behind the tailpipe are estimated to be below 30 nm (e.g. by Rivas *et al*., 2020)

1.6 Research gap

The epidemiological evidence base on UFP and PNC associated health effects remains fragmentary and inconsistent, including a need for further investigation of short-term mortality associations with size-differentiated PNCs (HEI Review Panel, 2013; Ohlwein *et al*., 2019). A limiting factor has been the availability of long-term UFP concentration data representative for sufficiently large study populations and thus assessable number of deaths; besides frequently missing adjustments to co-pollutants, particularly NO_2 and PM_{10} (Kwon *et al*., 2020; Ohlwein *et al*., 2019).

Ambient UFP and PNC concentrations remain without specific regulation worldwide, to our knowledge; which motivates accountability assessment for existing AAP interventions. One PNC size range of particular interest due to potentially high toxicity is the one containing high proportions of DEPs – as largely associated with DPV traffic emissions. Coincidently, traffic emissions are regarded as the UFP source with the potentially highest intervention potential (e.g. Rakowska *et al*., 2014; Burns *et al*., 2019), and traffic interventions have also been identified as the most popular AAP intervention (Burns *et al.*, 2019). At the same time, Hulkonnen *et al*. (2020) concluded that traffic intervention effects on PM (or UFP) concentrations and associated mortality remain hardly assessed. Also, accountability studies for AAP interventions for periods exceeding a few years and reaching beyond a local scale remain scarce (Boogard *et al*., 2017).

To fill these research gaps, the German Ruhr Area was identified as a particularly suitable area for studying both the size-differentiated PNC associations with short-term mortality of a relatively large population (about one million inhabitants within a 25km radius of an AAP monitoring station), and the accountability of regulations targeting DPV traffic due to the co-location with one of Europe's largest UEZ. Two key regulatory measures on DPVs, the introduction of level-3 restrictions banning non Euro-4 norm compliant vehicles from the UEZ and a gradual prevalence increase of Euro-4 compliant DPV fall within the decade of simultaneously available PNC and mortality datasets. The investigation of two regulatory actions, development of ambient AAP concentrations and development of mortality rates for this study thereby aligns with the first, third and fifth stage of the accountability framework by HEI (2003).

1.7 Study objectives and hypotheses

This study's objective was to investigate how size-differentiated PNCs were associated with short-term NCM, CVM and RM. In addition, we wanted to assess how size-differentiated PNCs developed over time and whether traffic exhaust regulations for diesel-powered on-road vehicles modified PNCs short-term mortality associations. We operationalised the study's objective through the following research questions and hypotheses:

(1) Has the daily average, size-specific particle number concentration changed during the observation period (2009-2018)? The underlying hypothesis is that the particle number concentration for the size fraction that includes most diesel exhaust particles has decreased.

(2) Are size-specific particle number concentrations associated with short-term natural-cause, cardiovascular and respiratory mortality? The underlying hypothesis is that mortality increases following exposure to elevated particle number concentrations.

(3) Is time an effect modifier for the exposure-outcome associations considering implementation of regulatory measures on particulate matter exhaust for diesel-powered on-road vehicles? The underlying hypothesis is that mortality risk per fixed increment of particle number concentration for the size fraction that includes most diesel exhaust particles is decreasing over time.

2. Materials and methods

Statistical descriptions and analyses were conducted in five steps: (i) definition and retrieval of exposure, outcome and meteorological datasets, besides a literature and primary data search for auxiliary information; (ii) data cleaning and checking; (iii) computation of annual levels and temporal dynamics for exposure and outcome variables, alongside Spearman correlation estimation; (iv) modelling of average daily PNC fractions with short-term NCM, CVM and RM, including sensitivity analysis for co-pollutant adjustment; (v) estimation of effect modification by two traffic regulations with a dichotomous and an ordinal interaction term, respectively. In preparation, literature searches in "Web of Science" (Core Collection) and "Scopus" were conducted, primarily to inform methodological decisions and to define exposure and traffic intervention variables. Auxiliary data was compiled for auxiliary descriptions of traffic and study population properties and developments, including spatial calculations using a Geographic Information System (GIS).

2.1 Descriptive analysis of traffic regulation, composition and volume

2.1.1 Literature search on traffic context

In preparation, literature and primary data searches were conducted to gather auxiliary information for study design and result discussion. Targeted information included quantitative data on-road vehicular traffic, particularly of DPVs, and qualitative data on the DEP-related regulations applicable in the study area, specifically: DEP-related regulatory interventions on DPVs (including information to estimate the affected study population fraction), on-road vehicle registration numbers differentiated by fuel use (gasoline and diesel) and Euro-norm compliance (by level), traffic volume differentiated by vehicle type (based on counts for interstate A40). Thereby, on-road passenger vehicles below a permissible total weight of 3.5 tons were in focus as the largest contributor to $PM_{2.5}$ and assumedly UFP in the on-road traffic sector (EEA, 2020b). In addition, literature searches following methodological guidance by Grant and Booth (2009) were conducted in the databases of "Web of Science" (Core Collection) and "Scopus" on the effects of DPV regulation for DEP concentration and composition, with insights guiding the selection of PNC size ranges for analysis as elaborated upon in preceding Chapters 1.2.4 and 1.5.4.

The following information providers were identified as relevant sources, among others: (i) grey-literature by the European Union and its institutions, particularly the European Commission (EC) and the EEA; (ii) grey-literature and datasets by the German Ministry for Environment, Nature Conservation and Nuclear Safety and the German Ministry for Traffic and Digital Infrastructure with its respective subordinate institutions, particularly the German Environmental Agency (UBA) and the Federal Motor Transport Authority (KBA); (iii) peer-reviewed articles published in national and international scientific journals.

2.1.2 Definition of relevant traffic interventions

The time series period (2009-2018) included the introduction and gradual adoption of two key regulations for DEP emissions by on-road vehicles in the study area. Both regulations were designed, among others, to reduce PM exposure through DPF adoption for DPVs in response to EU directives. Implementation levels are represented by the variables defined in Table 3.

The first regulation is implemented through vehicle registration requirements, specifically EAT compliance of on-road passenger vehicles with Euro-4 and higher. Governmental vehicle registration data is thus differentiated by fuel-use and Euro standard of the EAT-system (see KBA, 2021). For auxiliary descriptive analysis, we compared annual registration numbers of passenger vehicles by strata of vehicles' Euro-norm compliance level, next to annual registration numbers by strata of vehicles' fuel use (gasoline vs. diesel).

The second regulation is implemented by access limitation for non-Euro-4-compliant passenger vehicles with the introduction of "Level-3 requirements" for urban environmental zones (UEZs). The UEZ requirements are applicable to any public road except interstates (or "Autobahn") in the defined UEZ perimeter. Notably, the restrictions exclude old-timers and certain public service vehicles, among others. The year in which "Level-3" took effect in the study area was defined as a break point in terms of regulatory measures in the context of this study.

Table 3: Indicator definition for key interventions related to diesel-powered on-road traffic exhaust with potential relevance for DEP PNC and human mortality.

Intervention indicator	*Unit*	*Time*	*Specification (and source)*
(1) Diesel particulate filter prevalence among registered vehicles	% of registered passenger vehicles	annually	Number of registered passenger-class DPVs compliant with Euro-4 or higher in the study area, based on (KBA, 2021)
(2) Diesel particulate filter requirement in urban environmental zone	dichotomous	annually	Year in which „Level 3" took effect for the UEZ in the study area to restrict access for most non-Euro-4-compliant passenger vehicles, based on (UBA, 2020a)

2.1.3 Urban environmental zone description using a Geographic Information System

The relevant "Ruhr Valley UEZ" at the time of this study was the largest UEZ in Germany and one of the largest in Europe (UBA, 2015. This UEZ spanned across 13 municipalities at the time. The study area partially fell within the UEZ, with the study municipalities constituting three of four municipalities that form the Western section of the UEZ - only missing the municipality of Duisburg on the Western edge (UBA, 2020a).

Exact dimensions of the UEZ in relation to municipal borders were reviewed for this study, particularly to estimate the approximate proportion of the study population residing within versus outside the UEZ to gauge relevance. This was conducted by basic spatial analysis using a GIS and publicly available data on population numbers per area and the outline of the UEZ. The statistical approximation of this population proportion was conducted using the software QGIS® (Version 3.16.8). As input data, publicly available Geographic Information System (GIS) layers for the boundaries of the three assessed municipalities, the UEZ (both vector data), and for population density (based on a 1 by 1 km raster dataset) were combined. The population dataset was based on governmental census data for the year 2011. The population layer was clipped firstly by the outline of the study area, and secondly by the

cropped outline of those parts of the study area that fell within the UEZ. In this process, only raster squares were selected that fell to more than 50% into the selected boundaries.

2.1.4 Data collection on traffic volume

The study region was crossed by one major, 4-lane interstate (*Autobahn 40* or *A40*) during the study period. AAP, including UFP concentrations are known to be affect by traffic counts, even background concentrations. Annual aggregate traffic counts were used as an indication of the long-term trend in on-road traffic volume. The A40 has an exit nearby the AAP monitoring station used for this study. Inherent limitations in this indicator's precision, but also in accuracy or relevance of actual overall (beyond interstates), long-term on-road traffic dynamics in the study area are to be considered. Traffic counts were described as annual aggregates of the daily averages stratified by weekdays and by basic vehicle types (passenger vehicles and vehicles with a maximum permissible weight above 3.5 tons).

2.2 Design of the time series study

The main analyses for this study were designed as a time series study. Time series studies are commonly used for predictive studies, but with an adapted methodology can also be used to estimate the retrospective association between AAP and human health. In preparation of the study design for this study, the methodological considerations of Bell *et al*. (2004), Bhaskaran *et al.* (2013), Chuang *et al*. (2011) and Dominici *et al*. (2004 and 2002) were consulted. For this study, the compiled time series data of AAP, mortality, meteorological and time variables span from 2009 to 2018.

2.2.1 Exposure assessment

Exposure data was sourced from GUAN's only site in the German state of North Rhine-Westphalia (NRW), located in Mülheim-Styrum (Global positioning system (GPS) coordinates: 51.453 459 °North and 6.865 05 ° East (ETRS89)) at an elevation of 37 meters (m) above sea-level (Birmili *et al.*, 2016). The installed MPSS (model TSI 3936) measures (size-specific) PNCs of both ultrafine (electric mobility diameter 13.8-100 nm) and fine (electric mobility diameter between 100-750 nm) particles, with details on measurement procedures described by Birmili *et al*. (2016). The station is managed by the (German) Institute for Energy and Environmental Technology e.V. (IUTA). Based on the required exposure variables defined in Table 4, datasets with daily average values for the period from 2009 until 2019 were obtained from IUTA upon formal data request. Exposure-data processing and cleaning was conducted based on the standard procedure by State Agency for Nature, Environment and Consumer Protection (LANUV) and the GUAN-Network as specific in Birmili *et al.* (2016; p. 370 ff.).

The GUAN station with its MPSS is co-located with a central urban background monitoring station of the regional air quality network, as managed by the LANUV (Hennig *et. al.,* 2018). This allowed the use of additional air quality indicators, including daily mass concentration values of PM_{10} and NO_2, which was also obtained upon request for the same time period.

The two co-located measurement stations in Mülheim-Styrum are positioned within a residential area and classified as urban background stations with the air inlet positioned at four meters height above ground (Birmili *et al*., 2016). The nearby area is characterised by scattered, low-rise buildings (Birmili *et al*., 2016). We measured approximate spatial distances using the GIS setup described in the preceding Chapter 2.1.3. Around the measurement stations, there is an interstate (A40) located within

a vegetation-lined depression running in East-West direction (in about 350 meter (m) north-ward distance) and a national road in North-South direction (about 500 m west-ward distance), as well as near several industrial sites in East and South-East direction (about 1000 m distance). Main wind directions are from the South/Southwest and from the North-East (Birmili *et al.*, 2016). The site is within one km of the municipal boundary of Mülheim and Oberhausen (all distance estimates based on GIS calculations; see Figure 2 with marked buffer areas using equidistant map projection).

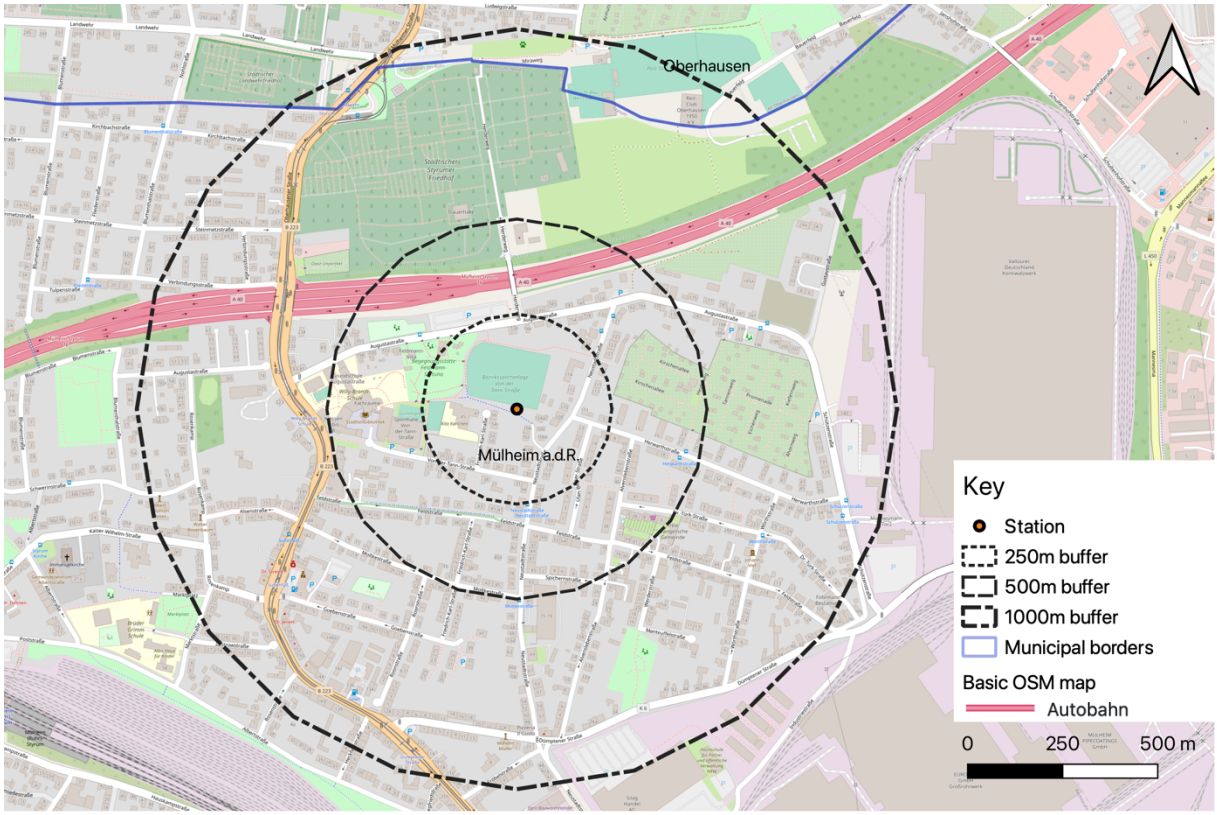

Fig. 2: Map of APP station in Mülheim-Styrum showing surrounding area with main roads and buffers of 250, 500 and 1000 m. The underlying OpenStreetMap (OSM) map broadly classifies areas with vegetation, including sportsgrounds as green, and areas with buildings as grey. The A40 as the nearby interstate ("Autobahn") is marked in red, while other main roads are marked in orange and yellow. Source: own design based on open-access OSM layers converted to an equidistant projection (ESRI 54032 World Azimuthal).

Upon the literature searches described in Chapter 2.1.1 (results presented in Chapter 1.2.4), the PNC size spectrum containing the majority of DEP PNCs was defined as 30–120 nm ($PNC_{30\text{-}120}$; largely Aitken mode, which covers the size fraction between 30–100 nm). This size range was differentiated into a small (30-50 nm), medium (50-100 nm) and large (100-120 nm) sub range. Further, a variable for the smallest measures size range of particles was defined, with the lower limit corresponding to the lower detection limit, specifically with a mean PNC of 13.8–30 nm ($PNC_{13\text{-}30}$) (equal to nucleation mode, which covers any particle sized below <30 nm). Finally, two PNC categories for larger and thus fine particles with size ranges 120-250 nm ($PNC_{120\text{-}250}$) and 250-500 nm ($PNC_{250\text{-}500}$) were defined for particles sized just above the DEP category. For comparison, the common variable of total PNC was defined for the size range of 13.8 to 500 nm ($PNC_{13\text{-}500}$). Again for comparison PNC results and for sensitivity analyses, we also included PM_{10} and nitrogen dioxide (NO_2) and thus the two variables concluded as most critical for UFP-associated mortality by Ohlwein *et al.* (2019) (for an overview of exposure variable definitions, see Table 4).

Table 4: Exposure variables defined for the time-series study.

Exposure (PNC size range)	*Unit*	*Time*	*Notes*
13.8-30 nm	PNC/cm^3	daily average	< 30 nm
30-50 nm	PNC/cm^3	daily average	within 30-120 nm
50-100 nm	PNC/cm^3	daily average	within 30-120 nm
100-120 nm	PNC/cm^3	daily average	within 30-120 nm
30-120 nm	PNC/cm^3	daily average	in-focus for DEPs
120-250 nm	PNC/cm^3	daily average	> 120 nm
250-500 nm	PNC/cm^3	daily average	
13.8-500 nm	PNC/cm^3	daily average	
PM_{10}	µg/m^3	daily average	
NO_2	µg/m^3	daily average	

2.2.2 Outcome assessment

As outcomes, daily counts of NCM, CWM and RM were defined, based on existing evidence on which mortality causes may affected by UFP or DEP exposure (e.g. Liu *et al*., 2019 or Ohlwein *et al*., 2019). For mortality cause classification, the 10th revision of the International Statistical Classification of Diseases and Related Health Problems (ICD) (WHO, 2015) was used (see Table 5). For each municipality, namely the cities of Mülheim an der Ruhr (Mülheim), Essen and Duisburg, and for each day of the study period (as available at time of study until 31.12.2018; with the start date defined by the availability of PNC exposure data) daily mortality counts were included in the time series. The data was retrieved upon formal written request from IT.NRW, the official data provider for the state of NRW in Germany. A small number of inconsistencies and an unclear differentiation between missing values and (cause-specific) mortality counts hidden for protection of privacy could be clarified with their staff. Overall, the data synthesis and data analyses were based on aggregate health data without personal information or information retraceable to individual persons, as secured by the statistical department of IT.NRW. Therefore, no ethical declaration was required.

Table 5: Outcome variables defined for this time series study.

Outcome (mortality)	*Unit*	*Time*	*ICD-10*
Natural-cause	deaths	daily total	A00 – R99
Cardiovascular	deaths	daily total	I00 – I99
Respiratory	deaths	daily total	J00 – J99

The approximate study population were the residents of the three municipalities located in the direct vicinity of the study's air-quality measurement station, for which mortality data were obtained. Both the trend in annual mortality counts and the association modelling is based, amongst other factors, on the assumption of relatively constant resident or study population numbers. Thus, as auxiliary information, the total number of residents based on municipal estimates was retrieved from IT.NRW

and compared for the beginning (municipal population estimates for 31.12.2008), middle (09.05.2011 and 31.12.2013) and end (31.12.2018) of the time series period to reconstruct potential population dynamics.

2.2.3 Covariates

Based on theoretical considerations of possible interactions and confounding factors for the relationship between UPF exposure and mortality, a list of potentially confounding, variables was developed using a directed acyclic graph (DAG) and split into meteorological and other time-variant variables. The DAG was informed by existing evidence on associations between PM, UFPs and short-term mortality. The lists were compared with the variable selections in previously published UFP time series analyses, including one study by Hennig *et al.* (2018) for the same study area.

Several meteorological variables describing daily weather variations can possibly influence measurements of urban background concentrations for UFPs and human mortality. Finally, the variable for adjustment included were air temperature and humidity among the meteorological variables, as UFP concentration and size distribution are known to be highly dependent on the air's temperature and humidity levels due to the processes, particularly photo-nucleation, described before (e.g. Giernsa *et al*., 2021). Also, a recent study showed that high air temperatures can enhance mortality effects of AAP, including UFP (Chen *et al*., 2018). The following Table 6 lists the variables deemed relevant based on the study's DAG and existing literature, such as Bismarck-Osten *et al.* (2013). The translation of the temperature factor to a suitable variable was based on the work of Hennig *et al.* (2018), which had evolved from the work of several biostatisticians on UFP time series. Air temperature was thus included through two variables: once as the same-day's mean temperature (lag0) and again as the mean temperature averaged across the aggregate lag of the three prior days (lag1-3) with each three degrees of freedom (df).

Meteorological variables were sourced from daily records of state-managed weather station, located in the nearby municipality of Duesseldorf in less than 20 km distance (GPS coordinates: 51.30° North, 6.77° East (ETRS89)) at a similar elevation (41 m above sea level), which was deemed representative of the conditions at in Mülheim-Styrum. The weather station is run according to standard protocols of the *Deutscher Wetterdienst*, a public institution under the German Federal Ministry of Transport and Digital Infrastructure.

Table 6: Meteorological variables selected as potential confounders for time series model integration.

Covariate (meteorology)	*Unit*	*Time*
Precipitation	mm	daily average
Relative humidity	%	daily average
*Temperature (same-day)**	°C	daily average
*Temperature (prior)**	°C	aggregate of the daily averages of the three prior days with 3 df

The following Table 7 lists the selected non-meteorological variables used to control for confounding by the day of the week, holidays and vacation periods, and the most relevant seasonal epidemic in the region during the study period, as posed by the influenza flu. Data on these time-dependent variables

were retrieved from official calendars and records as applicable for the state of NRW and converted to dichotomous and ordinal variables.

Table 7: Further time-variant variables selected as potential confounders for time series model integration.

Indicator	*Unit*	*Time*	*Specification*
Day of Week	ordinal (0-6)	daily	0= Sunday to 6= Saturday
Holidays	dichotomous (0;1)	daily	1= bank holiday in NRW
Summer population decrease	ordinal (0;1;2)	daily	1= school holiday in NRW; 2= 4-week period before and after school holiday in NRW; 0= all other days
Influenza	dichotomous (0;1)	weekly	1= week with influenza based on RKI, 2020

To allow estimation of effect modification for our model by time or the defined DEP-regulation variables, we defined two different time variables in Table 8: a dichotomous and an ordinal variable. The dichotomous variable was defined for the years before and after "level-3" of the urban environmental zone in the study area took effect (= 2014; precisely 01.07.2014). The ordinal variable used calendar years as a variable.

Table 8: Time variables defined for estimation of effect modification for this time series study.

Variable	*Unit*	*Explanation*
Dichotomous	dichotomous	before = years 2009-13; after = 2015-18
Annual	ordinal (year)	by year of the time series

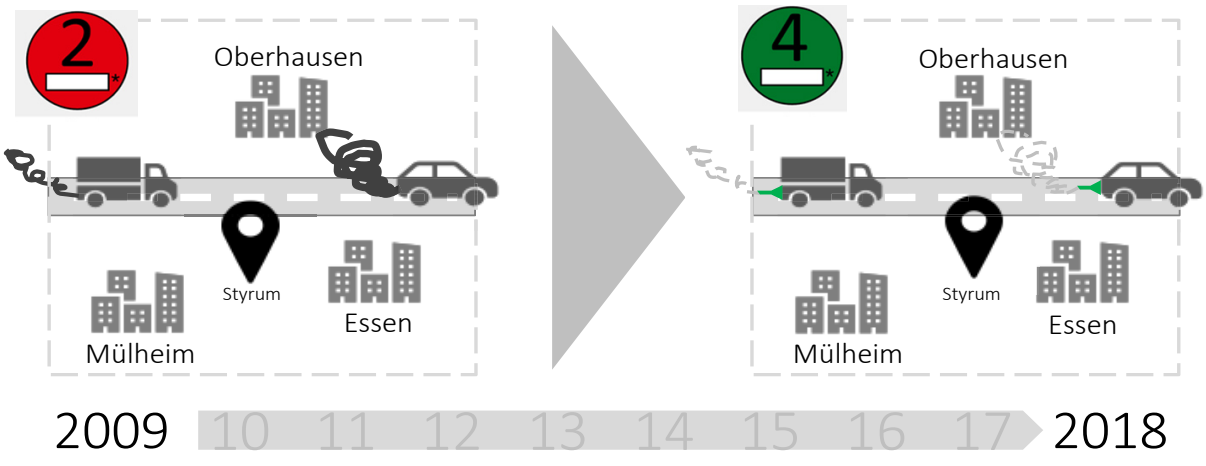

Fig. 3: Illustration of before/after scenario on vehicular traffic regulation for this time series study. Source: own design with illustrations by Microsoft Office and by Markus Baumer under Creative Commons license 2.0.

2.3 Statistical analysis

2.3.1 Dataset preparation

The primary datasets for the time series were combined in SAS®, then run through standard data cleaning and checking processes before transfer to R®, version: 4.0 (edited with R-Studio version: 1.4.1106; R Foundation for Statistical Computing). Identified data issues and unclarities in variable attribution were clarified with the respective administrators of the databases at IUTA and IT.NRW. Auxiliary data on traffic variables, sourced from online resources of KBA, were checked and analysed separately using Microsoft Excel®. The resulting study dataset was assessed for completeness to define suitable start- and endpoints of the time series period: only years with over 75% of daily data availability and only periods with less than a month of continuously missing data for mean PNC and mortality data were included. Missing values were left blanc and omitted for modelling purposes.

2.3.2 Descriptive analysis of dataset

For description and preparatory screening of the study dataset, the variables' means, medians, inter-quartile ranges (IQRs), maxima and minima were computed. We visualized daily mean PNC, PM_{10} and NO_2 values and NCM, CVM and RM mortality counts aggregated for the whole study region by plotting over the time series period. The plots were complemented with straight simple linear regression lines, based on computation using the "ln()" function of the "DPLYR" package (Version: 1.07) in R®. We further computed simple linear regression estimates *(β)* for the daily values of the main exposure and outcome variables.

In preparation of modelling, we computed Spearman's correlation coefficients (r) between and among exposure, outcome and (potentially) confounding variables. Variables with a correlation coefficient with key exposure and/or outcome variables of $r < 0.6$ were accepted as unrestricted for subsequent model integration.

2.3.3 Modelling of association between main exposure and outcome variables

We fitted general additive models (GAMs) defined to follow a Poisson distribution to estimate whether and how strong daily size-specific PNCs (alongside PM_{10} and NO_2) per interquartile range (IQR) change and natural and cause-specific mortality were associated across the whole time period. This is a common association model for AAP time series, which facilitates comparability of resulting estimates with similar study, and is deemed suitable for this study type (e.g. Chuang *et al.*, 2011; Ravindra *et al.*, 2019). In preparation, values for all exposure variables were converted to IQRs in R®.

The decision for using a Poisson distribution was based on the fact that exposure and outcome variables were count data. Notably, Poisson distributions require independence of adjacent variable values, an assumption that is not naturally met by neither PNC nor mortality data. Poisson distributions also assume the mean being equal to the variance, and thus the absence of overdispersion, an assumption that also requires consideration during model building. To check the assumptions underlying a time series model based on a GAM with a Poisson distribution, we assessed the (a) internal independence of exposure and outcome variables (i.e. absence or acceptable level of autocorrelation) and the (b) (quasi) absence of overdispersion, as recommended e.g. by Pan *et al*. (2018). The checks were computed using the "gam.check" function of the "mcgv"-package for the main

exposure ($PNC_{30\text{-}120}$) and all three outcomes, with a focus on NCM. First, we plotted a bar chart of autocorrelation residuals that should show a quasi-symmetrical, ideally bell-shaped distribution. Then, a scatter plot of model residuals and the linear predictor, which should show an even distribution around the null level. Further, a normal quantile-quantile (Q-Q) plot o residuals' deviances and theoretical quantiles, expected to lie on a more or less straight line. Finally, we plotted response values against fitted values expecting a roughly linear association, ideally on a 1 to 1 line.

We used splines to control for underlying time trends not controlled for by the other variables included to control for confounding, as specified below. Time trends, particularly by season, e.g. through the number of sun hours and the change in UFP source fractions have been shown relatedly as a critical factor (e.g. Giernsa *et al*., 2021), particularly for long-term, but also for short-term exposure (e.g. Kim *et al., 2*021). The used R® package "mgcv" (Version: 1.8-31) allowed specification of the adjustment level of the spline using a "k-value" that is to be interpreted similarly to specifying the number of knots or turns of the spline curve. As the time trend of the association between exposure and outcome was one of the study questions, the time trend adjustment was to be conducted carefully to avoid over-adjustment. The ideal k-value was approximated by testing the lowest logic value in terms of the number of major seasonal variable value changes, while being ideally dividable by the number of years (10) with a substantial minimization of residual autocorrelation (with a resulting value of k=30). Using $PNC_{30\text{-}120}$ as exposure and CVM as outcome variables, we plotted the resulting spline as a trend line for visual confirmation.

The association estimates were computed for aggregate lags as the time between the day of exposure and the day of recorded mortality. Prior to association computation, we transformed the exposure variables to IQRs. We then chose 2-day lag models to increase statistical power and buffer missing values and outliers, while presenting daily lags auxiliary in the annex. We computed the moving aggregate lag values for a period of up to seven days prior to the day of death. The aggregate lags included the immediate effect (lag0-1, lag1-2), a medium-term effect (lag2-3, lag3-4) and a delayed effect (lag4-5, lag5-6, lag6-7). Expecting associations strengths to be moderate at best, the plotted comparison among the aggregate time lags was to allow the identification of potential patterns or trends.

The coding of the main statistical model (full model) in R® using the "mgcv"-package to compute a GAM reads as follows (for variable coding see Table 9), with the first line introducing the spline, the second line the potential meteorological confounders, the third line the potential additional confounders, and the fourth line specifying the Poisson distribution and omittance of missing values:

```
gam(Outcome ~ Exposure + s(trend, k=30, bs='cr') +
ns(tempmean, df=3) + ns(ma13_tempmean, df=3) + rhmean +
as.factor(dow) + influenza + hday1 + as.factor(summernrwpopdecrease),
family=quasipoisson, data=data_final, na=na.omit)
```

Estimates were computed and visualised as point estimates with 95% confidence intervals (CI) to facilitate interpretation of the statistical significance of estimates. For results presentation, the estimates were grouped to facilitate comparison between the main size range $PNC_{30\text{-}120}$ with its sub-ranges (small, medium, large), with smaller ($PNC_{13\text{-}30}$) and larger ($PNC_{120\text{-}250}$, $PNC_{250\text{-}500}$) particles, as well as, with total PNC ($PNC_{13\text{-}500}$), PM_{10} and NO_2.

Table 9: Coding of variables for full model calculations in R®

#	*Variable*	*Coded name*
1	Outcome	e.g. mortnatuerl_gesamt ("gesamt" = aggregtae for study area)
2	Exposure	e.g. d13_8to30 nm
3	Time trend (using spline function)	s(trend,k=30,bs="cr")
4	Mean daily temperature on the same day (with 3 df)	ns(tempmean,df=3)
5	Average of mean daily temperature for the prior three days (with 3 df)	ns(ma03_tempmean,df=3)
6	Day of the week	as.factor(dow)
7	Relative humidity	rhmean
8	Influenza-flu (based on official health statistics for each year of the time series)	influenza
9	Official holidays (for state of NRW)	hday1
9	School summer holidays with travel (for state of NRW)	as.factor(summernrwpopdecrease)

2.3.4 Effect modification by traffic regulations

The time series ran in parallel with changes in the EAT required for the registration of vehicles and for vehicle access to urban areas like our study area. To recall, the basic hypothesis was that in the beginning of the study period, when less vehicles on most roads of the study area were equipped with DPFs, the association of size-specific $PNC_{30\text{-}120}$ with mortalities were stronger than later, after a higher percentage of vehicles used DPFs and the UEZ in the study area started to ban non-DPF equipped vehicles.

Bernal *et al*. (2017) propose interrupted time series regression to evaluate public health interventions, which is ideal for interventions that allow a definite pre- and post-intervention definition around one point or a limited period in time. As the intervention, i.e. the introduction of Euro-4 and in association installation of DPFs, took effect gradually starting from before and ending after the time series period, the potential of interrupted time series regression cannot be utilised fully. However, even if overlaid by the overall prevalence changes for DPF equipped vehicles, the introduction of "Level 3" for the local UEZ affecting large parts of the study population comes close to a "level" change, which we translated to the model with a dichotomous time variable for the period with and without "Level 3". To a limited extend, we also used ideas by Bernal *et al*. (2017) for the annual and quasi-continuous models which assume a "slope change". Resulting effect estimates were assessed for patterns and also compared with the full model estimates.

For interpretation of the model with the dichotomous interaction term, we produced the same figures as for the full model. Figure 3 illustrates in a simplified manner the before/after scenario (as mainly represented by the dichotomous variable) for DEP-relevant interventions during the study period in the study area. We assessed effect modification by patterns across lags, rather than p-values and used the rule-of-thumb (e.g. Austin and Hux, 2002) that two estimates only overlapping with the CIs or not

overlapping at all may indicate a statistically significant difference at 95% confidence level, while noting that coincidental statistical significance is to be considered when running a larger number of models. For statistical analysis, we added a multiplicative interaction term for a dichotomous variable (exposure * time period) aggregating estimates for the time periods 2009-2013 versus 2015-2018.

To check for effect modification by the gradually increasing DPF among DPV, we chose an ordinal variable was defined as equal to the year variable estimating the risk ratios or relative risks (RRs) for each year (2010-2018) in comparison with the base-year (2009). As the focus was on pattern analysis of annual estimates, we aggregated lags without overlaps (lag0-1, lag2-3, lag4-7) to facilitate year to year estimate comparison. For statistical analysis, we added a multiplicative interaction term with an ordinal variable equalling the year of study (exposition * year) to compute relative risks for the years 2010-2018 in relation to the base-year 2009.

2.3.5 Sensitivity analyses

For each of the main statistical analysis steps, selected results were checked for robustness. The sensitivity analyses included the following calculations:

For assessing sensitivity of descriptive analyses of exposure variables, the simple linear regression estimates ***(β)*** for exposure were calculated without the year 2012 to check robustness against the potential effects of an interstate reconstruction phase (A40) on exposure estimates that took place during several months of 2012. For outcome variables, the descriptive overview of the development of resident counts in the study municipality was deemed sufficient to exclude potential effect modification by large population changes.

For assessing sensitivity of the estimate from Poisson regression models, for all exposure, outcome and aggregate-lag combinations, models separately adjusted for NO_2 and PM_{10} were calculated. Further, additional single-lag models were calculated for comparison with the main two-day aggregate lag models. Already as an integral part of the main result presentation, the calculation of models for the sub-ranges of $PNC_{30\text{-}120}$ (namely, $PNC_{30\text{-}50}$, $PNC_{50\text{-}100}$, $PNC_{100\text{-}120}$), next to the ranges for smaller and larger particles ($PNC_{13\text{-}30}$ and $PNC_{120\text{-}250}$) were used to gauge sensitivity for a differing size range definition of $PNC_{30\text{-}120}$.

For assessing sensitivity of effect modification models, calculations with an alternative break point, i.e. before and after 2013 instead of 2014, for the model with the dichotomous interaction term were performed. For the model with the dichotomous and the ordinal interaction terms, potential sensitivity for the separate adjustments by the two key co-pollutants, PM_{10} and NO_2, was gauged for the relevant exposure, outcome and aggregate-lag combinations.

3. Results

3.1 Description of on-road traffic developments

3.1.1 Temporal development of on-road traffic

As a proxy for traffic dynamics in the study area, Figure 4 displays the daily average vehicular traffic counts for both directions of traffic on the A40 interstate. The values are displayed as average daily counts for each year, with the daily averages based on counts for the whole week (Monday to Sunday; figures on the left-hand side), for the main workdays (Monday to Friday figures in the centre) and for Saturday only (figures on the right-hand side). For both passenger vehicles (top row) and trucks with a total permissible weight above 3.5 tons (bottom row), the overall traffic counts increased across the time series period, except for the year of 2012, which included several months of road closure due to construction. The year 2012 is thus highlighted in blue and subject of a sensitivity analysis for linear regression of exposure trends. When comparing the year-to-year change in daily average counts for different days of the week, the overall trend shows similar patterns of increasing vehicular counts. The average daily counts for weekdays are substantially higher than for Saturday or the whole-week average.

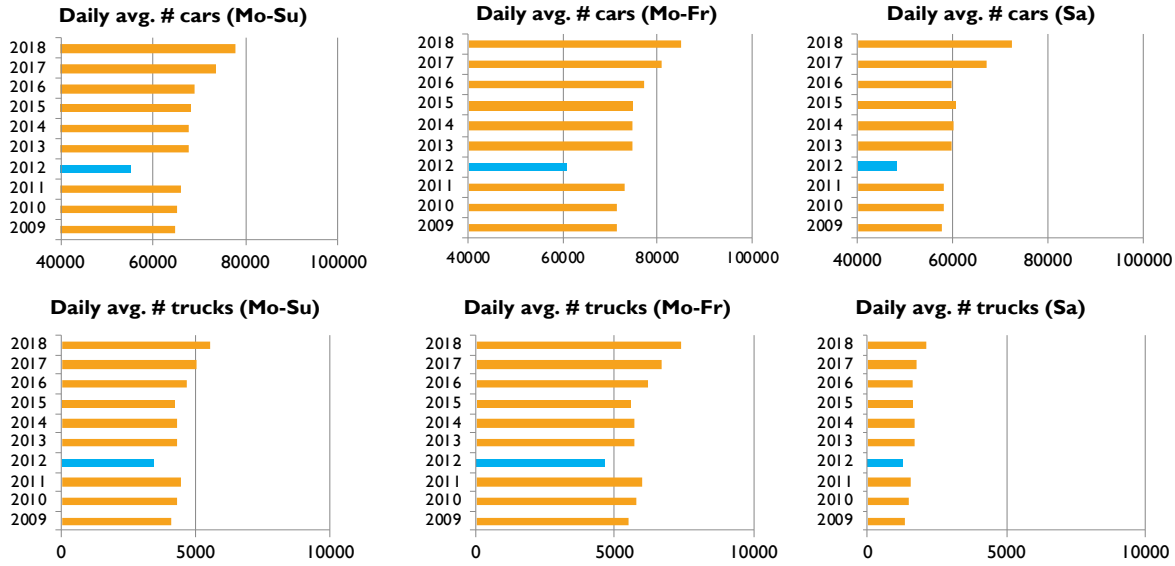

Fig. 4: Six graphics depicting the traffic counts for passenger vehicles and trucks on the study region's interstate (A40) on different days of the week as defined by graphic titles. Note: The reduced number of vehicular traffic in 2012 was due to a major construction work on the A40. Source: own design based on data by KBA, 2021.

3.1.2 Relative proportion of diesel-powered vehicular on-road traffic

The following Figure 5 depicts the proportion of DPVs relative to the total number of diesel- and gasoline-powered registered vehicles in the study area. The proportion of DPVs compared to all registered fuel-powered vehicles in the study region increased slightly from 22% (2009) to 26% (2018) within the 10-year study period.

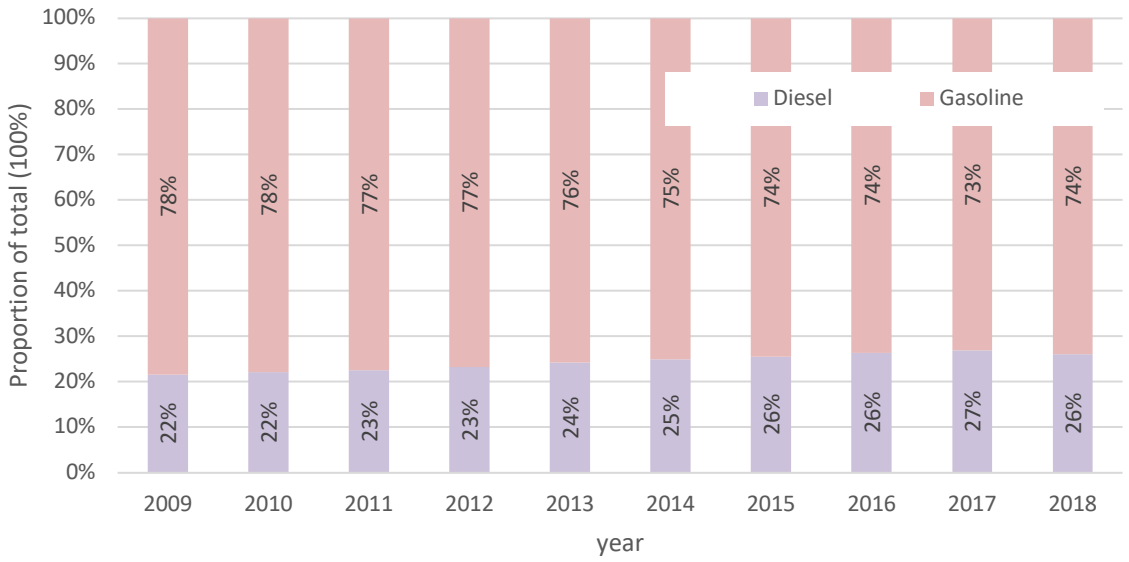

Fig. 5: Proportion of diesel-powered vehicles among total number of registered vehicles in the study region. Source: own calculations based on data by KBA (2021)

3.1.3 Status and temporal dynamics of diesel-powered vehicular on-road traffic

The absolute number of registered passenger-class DPVs increased steadily in the study region until 2017 (see Figure 6) from 90,170 (01.01.2009), just before the study period, by 25% to 121,755 (01.01.2019). In the same period, the number of all fuel-powered passenger class vehicles increased from 441,094 by 10% to 491,141. Among the passenger-class DPVs, the absolute number of vehicles compliant with Euro-4 and higher increased steadily. Across the whole study period, the proportion of passenger-class DPVs compliant with Euro-4 or higher increased from 49% at the beginning of 2009 (01.01.2009) to 88% at the end of 2018 (01.01.2019).

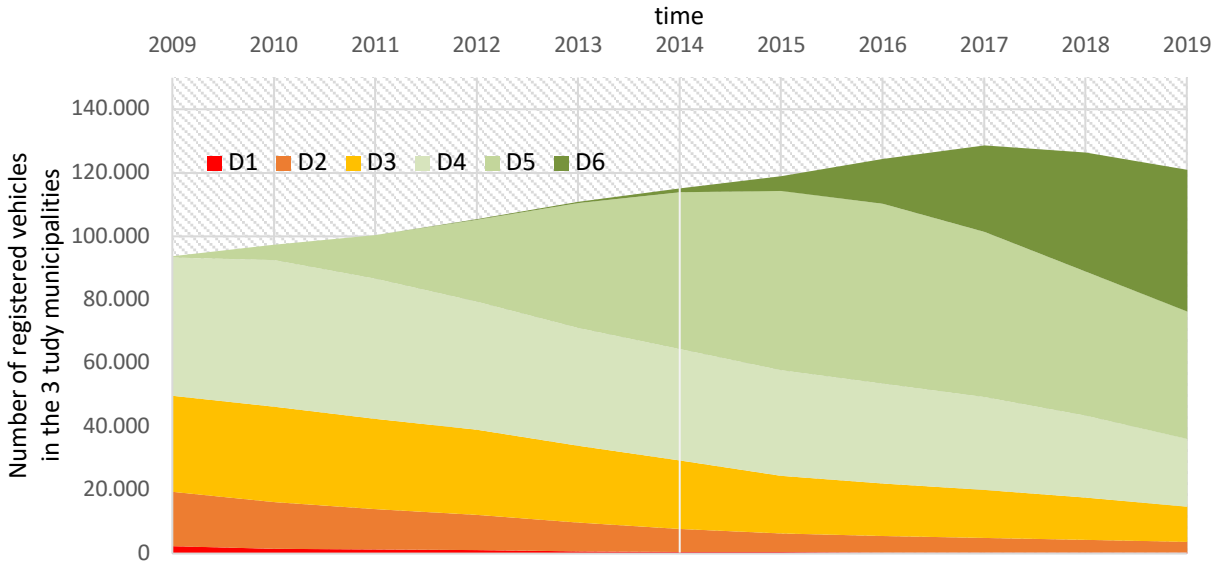

Fig. 6: Time trend (2009-2019) of number of registered diesel vehicles (only passenger vehicles) in the study area. Colour-coded classification along Euro-Norm I to VI (here: displayed as D1 to D6). Source: assembled based on data by KBA (2021).

3.1.4 Urban environmental zone in the Ruhr Valley

The “Ruhr Valley UEZ” was enacted on 01.10.2008 – and thus shortly before our time series period. Since 01.07.2014, only vehicles meeting Euro-4 norm or higher and thus for DPVs almost exclusively those equipped with DPF could access the study municipalities, with regulatory exceptions summarized in UBA (2020a). Figure 7 shows an overlay of the map layers for the study region (in grey) and for the UEZ (in green), with large parts of the study region falling within the UEZ, as well as, within a 25 km perimeter of the AAP measurement station in Mülheim-Styrum.

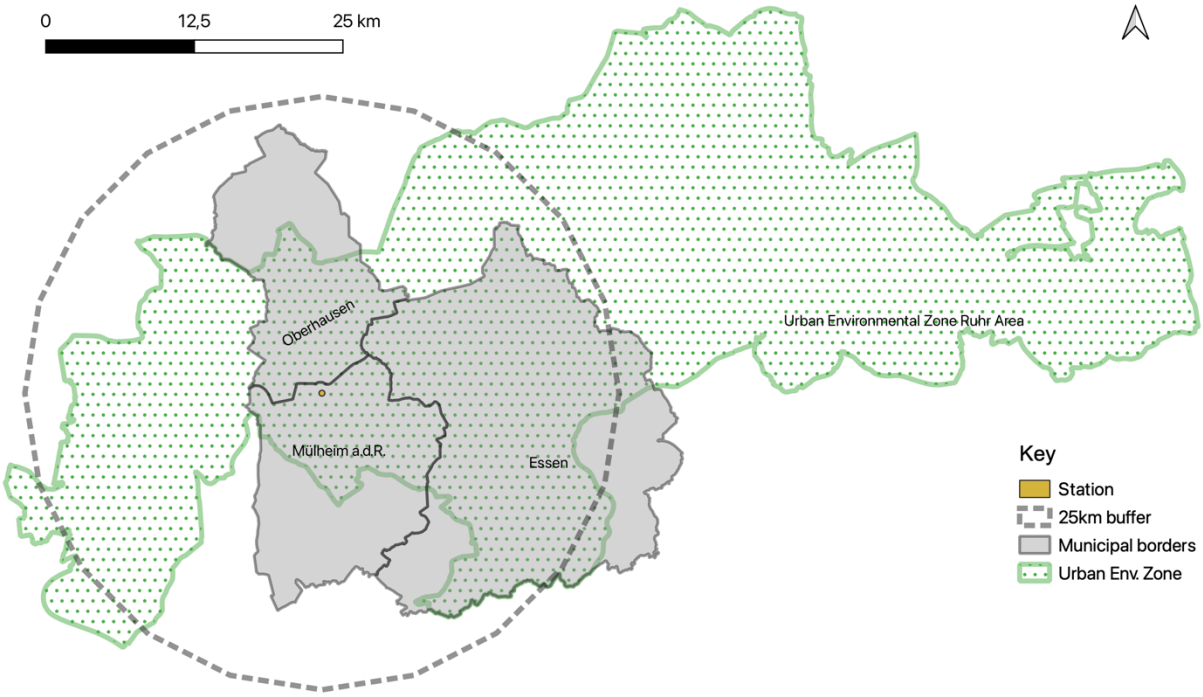

Fig. 7: Map of air pollution monitoring station in Mülheim-Styrum with a 25km buffer around over municipal and urban environmental zone boundaries. Explanations: “Station” is AAP monitoring station in Mülheim-Styrum; “Urban Env. Zone” is the urban environmental zone of the Ruhr Valley. Source: own design based on open-access OSM layers converted to equidistant projection (ESRI 54032 World Azimuthal)

The GIS-based population estimate for the whole study area was 999,712 persons and for the cropped study area, representing the area within the UEZ, 878,183 persons, with the relevant measure being the percentage of the estimated total population that resides within the UEZ: 87.84%. Due the data format (1x1km raster) and QGIS statistics assuming homogenous population distribution within individual raster squares for calculating population values of partial squares, the estimates bear a certain level of imprecision. The total number (999,712) based on 2011 census data only deviates about 5.56% from the actual census values officially attributed to the study area (Fig. 8). With a 5% deviation, the actual proportion would remain between 83.45% and 92.23%. Overall, the study population remains stable in total resident numbers during the study decade (Tab. 10).

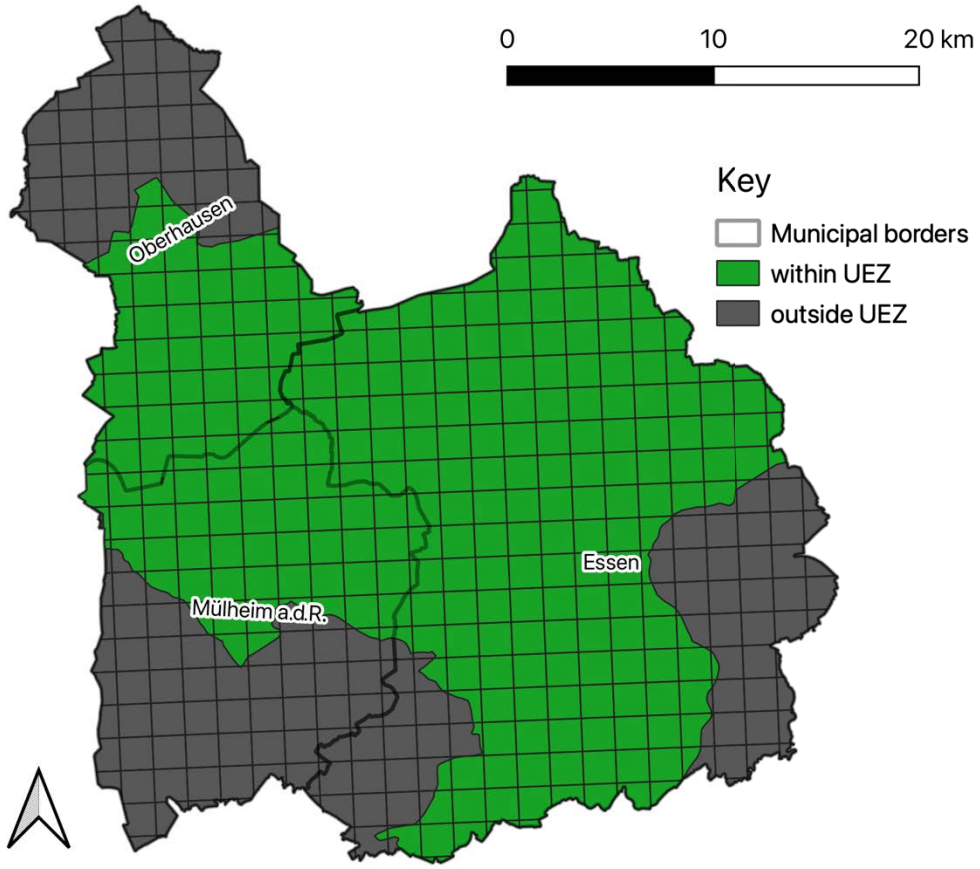

Fig. 8: Map of proportion of study area (aggregate three municipalities) located inside and outside the urban environmental zone of the Ruhr Area. Raster squares equal population data as saved in 1 by 1 km raster format. Source: own design based on open-access OSM layers converted to equidistant projection (ESRI 54032 World Azimuthal); population data by ESRI open source based on census data for the year 2011 by the German statistical offices of the federal and state governments.

Table 10: Overview of population sizes in study municipalities. Source: www.landesdatenbank.nrw.de/ldbnrw/online?operation=abruftabelleBearbeiten&levelindex=1&levelid=1616426124757&auswahloperation=abruftabelleAuspraegungAuswaehlen&auswahlverzeichnis=ordnungsstruktur&auswahlziel=werteabruf&code=12411-01i&auswahltext=&werteabruf=starten#abreadcrumb; last accessed on 06.08.2021.

Municipality	*Start in 2009* *Population on 31.12 2008*	*Official census* *Population on 09.05.2011*	*Half-time in 2014* *Population on 31.12.2013*	*End in 2018* *Population on 31.12.2018*
Essen	579,759	566,201	569,884	583,109
Mülheim	167,471	166,865	167,640	170,880
Oberhausen	214,024	210,216	209,097	210,829
Study region total	961,254	943,282	946,621	964,818

3.2 Descriptive analysis of time series

3.2.1 Levels and temporal development of exposure variables

Figure 9 depicts periods with missing values for PNC exposure data of the required size fractions between 13.8-500 nm. January and February 2009 did not meet the requirement for data completeness with only individual days covered, thus 01.03.2009 was defined as the start date of the dataset. The maximum percentage of missing values in one year was recorded for 2017 with 21.9% of daily values missing for the PNC measurements, while the minimum percentage, with no missing values, was in 2014. In exchange with IUTA, we discussed interpretation of larger periods of missing values and identified them as data missing due to either technical repairs or irregular maintenance work on the sensor - and thus at random.

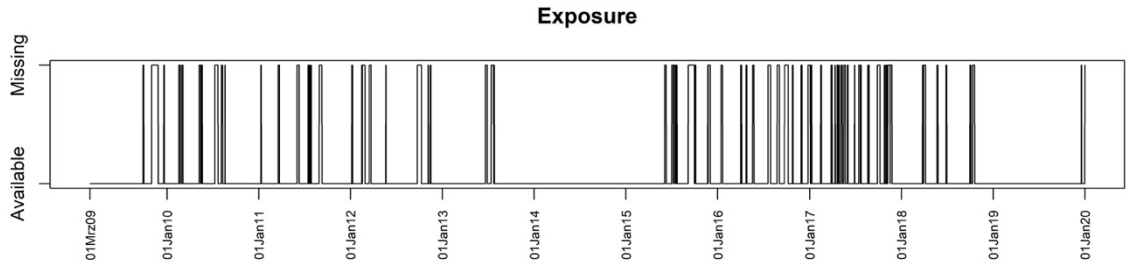

Fig. 9: Overview of missing PNC exposure values (all PNC size ranges) between 01.03.2009 and 31.12.2018.

The basic descriptions of the variables used for modelling are listed below (Tab. 11). The particle size fractions of $PNC_{13.8\text{-}30}$, $PNC_{30\text{-}120}$, $PNC_{120\text{-}250}$ and $PNC_{13.8\text{-}500}$ had median (IQR) PNC per cm^3 values of 4,268 (2,334), 4,970 (3,189), 749 (575) and 10,400 (5,630) respectively for the whole time period.

Table 11: Basic description of measured variables included in the time series models (exposure, mortality, meteorology). Table includes means, standard deviations (SDs), medians, interquartile ranges (IQRs), minima (min) and maxima (max).

Parameter	*Mean*	*SD*	*Median*	*IQR*	*Min*	*Max*
(Exposure)						
PNC 13.8-30 nm	4,630	2,070	4268	2,334	726	20,800
PNC 30-50 nm	2,620	1,070	2,460	1,480	443	8,190
PNC 50-100 nm	2,350	1,180	2,130	1575	258	9,370
PNC 13.8-100 nm	9,600	3,780	9,000	4,942	1,790	29,600
PNC 100-120 nm	376	233	324	273	40	1,990
PNC 30-120 nm	5,340	2,340	4,970	3,189	806	17,500
PNC 120-250 nm	863	3,780	749	575	108	5,810
PNC 250-500 nm	199	142	169	163	16	1,960
PNC 13.8-500 nm	11,000	4310	10,400	5,630	2,050	31,800
PM_{10}	22.3	12.9	19.0	12.7	3.7	132
NO_2	28.3	12.1	27.2	17.1	2.2	82
(Mortality)						
Natural-cause mortality	32.3	6.6	32.0	8	13	60
Cardiovascular mortality	11.3	3.7	11.0	5	1	29
Respiratory mortality	3.0	2.0	3.0	2	0	14
(Meteorology)						
Mean temperature	11.5	6.9	11.5	10.5	-8.55	30.2
Mean relative humidity	77.1	12.8	78.5	19.7	33.7	99.9

Figures 10-12 show the PNC dynamics with seasonal variations for selected size fractions ($PNC_{13.8\text{-}30}$, $PNC_{30\text{-}120}$, $PNC_{120\text{-}250}$, $PNC_{13.8\text{-}500}$ in Fig. 10), the sub-fractions of $PNC_{30\text{-}120}$ ($PNC_{30\text{-}50}$, $PNC_{50\text{-}100}$, $PNC_{100\text{-}120}$ in Fig. 11) and PM_{10} and NO_2 (Fig. 12) graphically, with a simple linear regression line fitted to the daily values to illustrate the overall time trend. The daily average PNCs slightly decreases for all size fractions, as expressed by the statistically significant linear regression estimates *(β)* listed in Table 12.

Table 12: Simple linear regression estimates *(β)* with confidence intervals for all modelled PNC size fractions

Exposure (PNC by size fraction)	*Linear regression estimate (B) (2009-18)*	*Confidence interval (2.5%; 97.5%)*
PNC 13.8-30 nm	-0.221	-0.307; -0.133
PNC 30-50 nm	-0.272	-0.316; -0.228
PNC 50-100 nm	-0.303	-0.352; -0.255
PNC 100-120 nm	-0.056	-0.066; -0.047
PNC 30-120 nm	-0.632	-0.728; -0.562
PNC 120-250 nm	-0.130	-0.151; -0.108
PNC 250-500 nm	-0.036	-0.042; -0.030
PNC 13.8-500 nm	-0.862	-1.011; -0.713

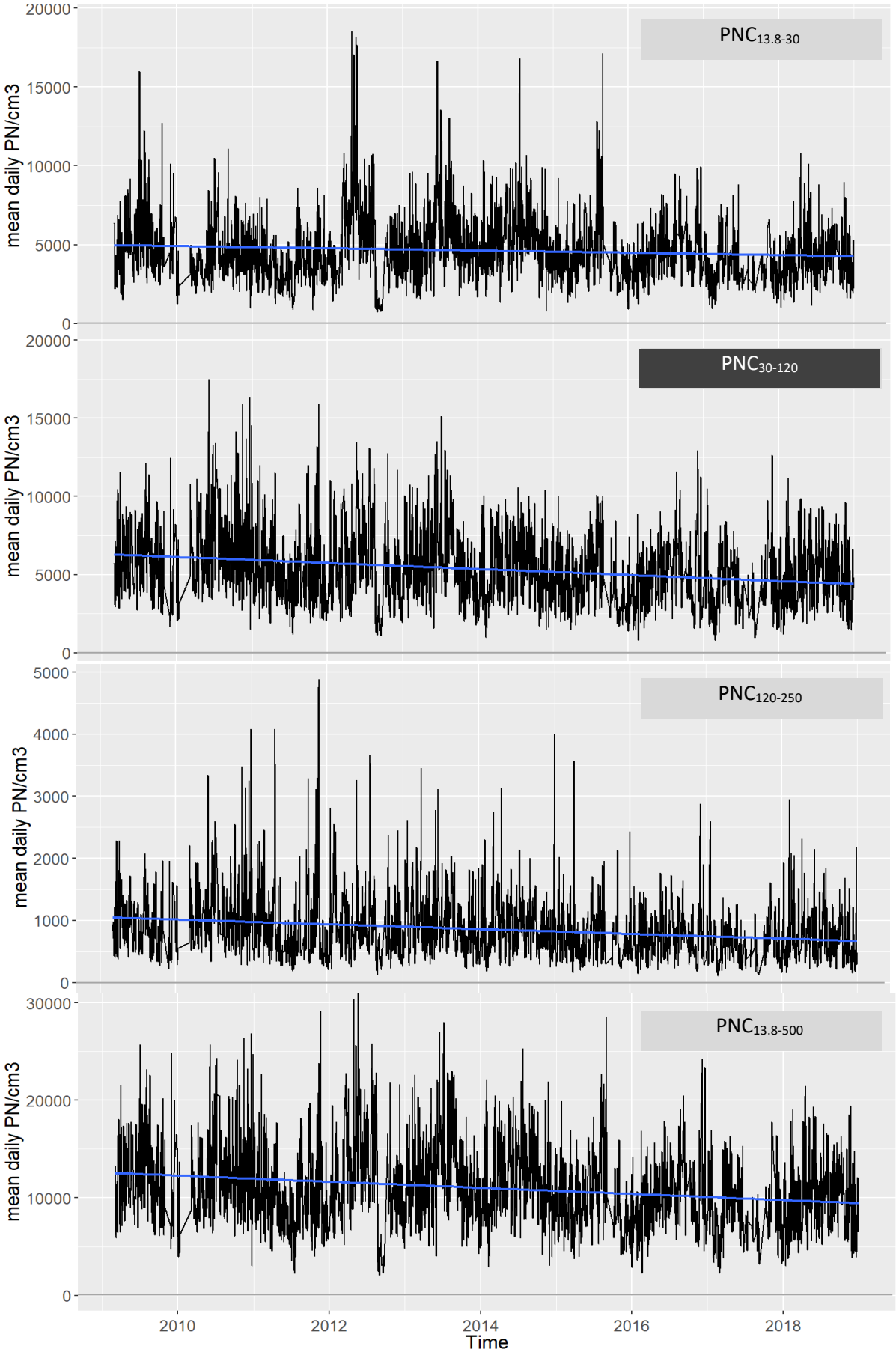

Fig. 10: Daily mean particle mass concentrations over time at Mülheim-Styrum for variables $PNC_{13.8\text{-}30}$, $PNC_{30\text{-}120}$, $PNC_{120\text{-}250}$ and $PNC_{13\text{-}500}$. Simple linear regression estimate displayed as straight line in blue.

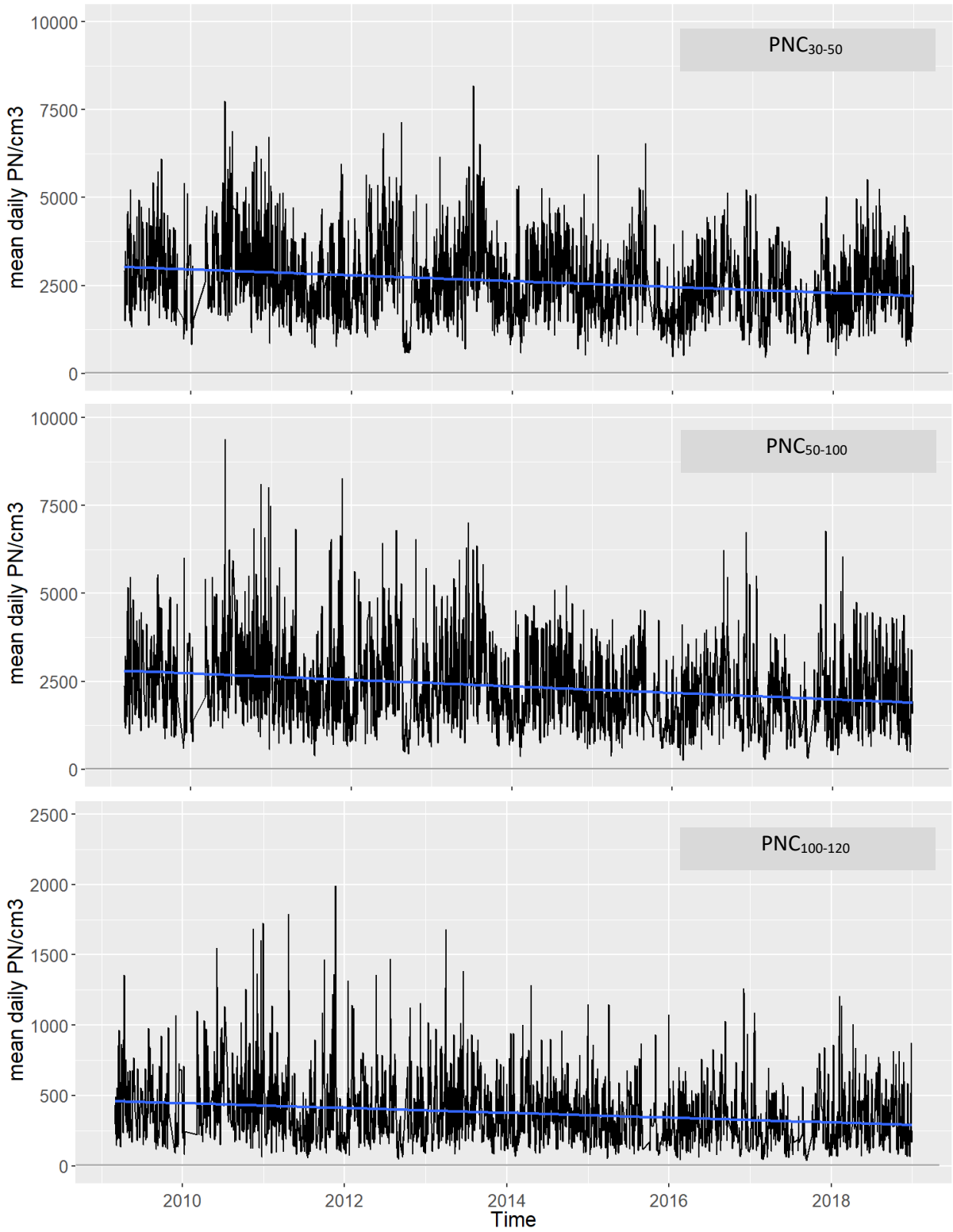

Fig. 11: Time trend in daily PNC means for the three sub-size fractions of the particle range between 30-120nm: PNC_{30-50}; PNC_{50-100}; $PNC_{100-120}$.

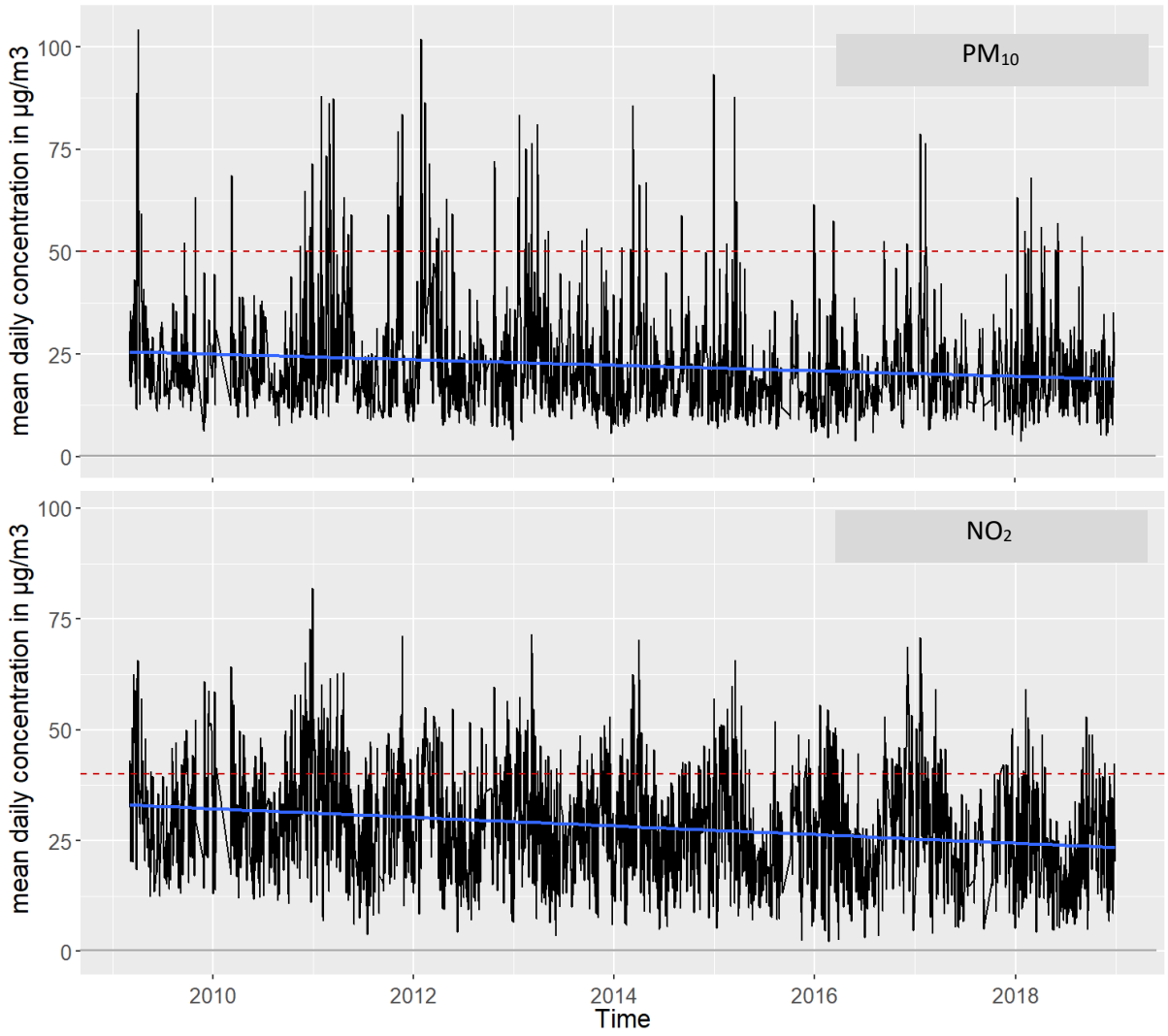

Fig. 12: Daily mean mass concentrations for PM_{10} and NO_2. Simple linear regression estimate displayed as straight line in blue. WHO guideline value (Source: WHO, 2006) marked as (red) dotted line.

3.2.2 Levels and temporal development of outcome variables

The mortality counts among the population in the study area (absolute numbers as registered by the three selected municipalities) show seasonal dynamics for NCM, CVM and RM (Fig. 13). CVM (median 11; IQR 5) and RM (median 3, IQR 2) together account for almost half (43.8%) of the total NCM (median 32; IQR 8) in the region. The total counts for NCM, CVM and RM causes during the 2965 days included in the analyses were 95,867, 33,432 and 8,967, respectively.

Figure 13 depicts the temporal development of the three assessed mortality categories based on aggregate, daily reported values for the study region. For NCM, the (linear) regression estimate revealed a significant, minimally positive trend of 0.00061 with a CI of 0.00038 to 0.00085 (CI 2.5%-97.5%). For CVM, the calculation showed a significant, minimally negative trend of -0.00058 with a CI of -0.00070 to -0.00048 (2.5% - 97.5%). Finally, for RM, the regression calculated a non-significant, minimally positive trend of 0.000045 with a CI of -0.000025 to 0.00011 (2.5% - 97.5%).

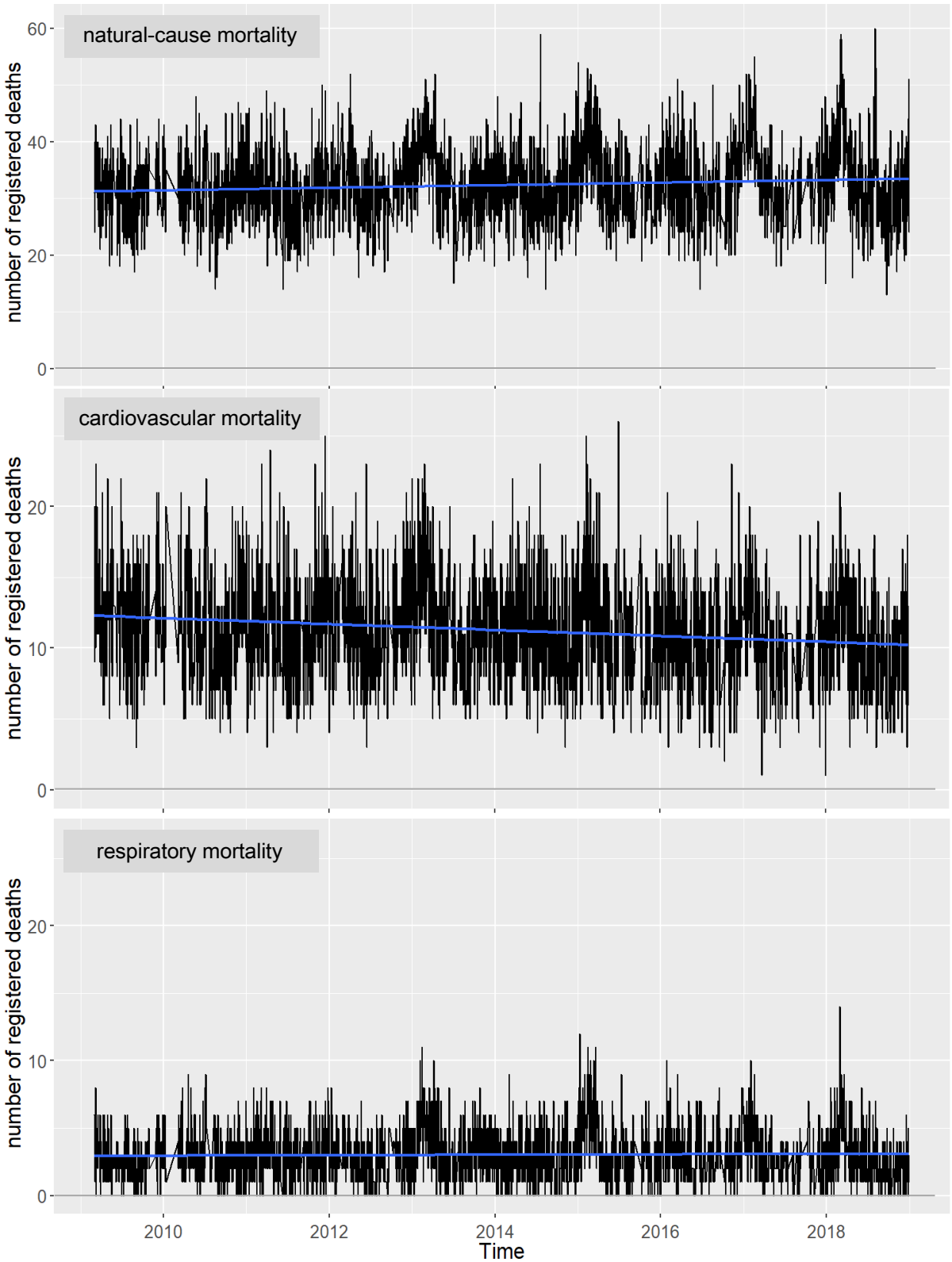

Fig. 13: Daily mortality counts for the three mortality categories (natural-cause, cardiovascular and respiratory mortality) in the study region (aggregates for the municipalities of Mülheim, Essen and Oberhausen). Simple linear regression estimate displayed as straight line in blue.

3.3 Correlation analyses for time series

We derived the following results from computing correlation matrices with Spearman "*r*" values for exposure (Tab. 13), outcome (Tab. 14), and meteorology (Tab. 15).

(i) The exposure variables show relatively high correlation coefficients (including above 0.6) among the PNCs. NO_2 showed a maximum correlation with $PNC_{120\text{-}250}$ at 0.59 and PM_{10} with $PNC_{250\text{-}500}$ at 0.84.

(ii) The study-region based mortality variables showed *r* values of 0.61 between NCM and CVM, of 0.45 between NCM, RM and 0.16 between CVM.

(iii) The time variables did not exceed a correlation coefficient of 0.31 with the main outcome or the main exposure and among each other of 0.12.

(iv) The meteorological variables did not exceed a correlation coefficient of -0.30 with the main exposure or outcome and of 0.49 among each other, except for the two temperature variables, as to be expected, of 0.91.

Among the measured variables finally used for adjusting the full model (see underlined variables), none exceeded a correlation coefficient of 0.5, except the two adjustment variables for temperature.

Table 13: Correlation matrix (Spearman *r*) for key exposure variables

	$PNC_{13.8\text{-}30}$	$PNC_{30\text{-}120}$	$PNC_{120\text{-}250}$	$PNC_{250\text{-}500}$	NO_2	PM_{10}
$PNC_{13.8\text{-}30}$	1					
$PNC_{30\text{-}120}$	0.59	1				
$PNC_{120\text{-}250}$	0.26	0.72	1			
$PNC_{250\text{-}500}$	0.08	0.45	0.77	1		
NO_2	0.23	0.53	0.59	0.55	1	
PM_{10}	0.01	0.40	0.67	0.84	0.58	1

Table 14: Correlation matrix (Spearman *r*) for all outcome variables (municipality-specific and for total study region)

		Natural-cause mortality				*Cardiovascular mortality*				*Respiratory mortality*			
		Essen	Mülh.	Oberh.	Total	Essen	Mülh.	Oberh.	Total	Essen	Mülh.	Oberh.	Total
Natural-c.l mortality	Essen	1											
	Mülh.	0.08	1										
	Oberh.	0.07	0.08	1									
	Total	0.80	0.48	0.52	1								
Cardiovascular mortality	Essen	0.61	0.02	0.01	0.46	1							
	Mülh.	0.05	0.61	0.05	0.29	0.02	1						
	Oberh.	0.04	0.03	0.6	0.31	0.04	0.03	1					
	Total	0.50	0.27	0.3	0.61	0.79	0.44	0.49	1				
Respiratory mortality	Essen	0.44	0.08	0.08	0.39	0.13	0.03	0.09	0.15	1			
	Mülh.	0.06	0.28	0.04	0.16	0.04	0	0	0.03	0.06	1		
	Oberh.	0.06	0.05	0.35	0.22	0.03	0.04	0.08	0.07	0.09	0.02	1	
	Total	0.39	0.18	0.21	0.45	0.13	0.04	0.10	0.16	0.84	0.41	0.48	1

Table 15: Correlation matrix (Spearman *r*) for meteorological variables and one outcome (natural-cause mortality) and exposure variable ($PN_{C30-120}$). Note: variables included in the models are underlined; "*$Mean_{1-3}$" is the average of the mean daily temperatures during the three days before the day of exposure.

	Outcome	*Exposure*	*Wind*		*Humidity*		*Temperature*	
	Natural-cause^	PNC_{30-120}	Direct-ion	Speed	Precipi-tation	Relative Humidity	Mean	$Mean_{1-3}$*
*Natural-c.^*	1							
PNC_{30-120}	-0.05	1						
Direction	-0.07	-0.28	1					
Speed	0.11	-0.56	0.12	1				
Precipitat.	-0.01	-0.19	0.17	0.22	1			
Relative	0.08	-0.20	0.23	0	0.34	1		
Mean temp.	-0.24	0.14	0.11	-0.18	0.03	-0.48	1	
*$Mean_{1-3}$**	-0.30	0.15	0.14	-0.22	0.06	-0.39	0.91	1

3.4 Association modelling for exposures and outcomes

3.4.1 Full model validation

The gam.check function of R®'s "mgcv" package reported full model convergence, as one basic requirement for model validation. The visual check of the bar chart of autocorrelation residuals (Fig. 14) revealed the validation-supportive, quasi-symmetrical bell-shape distribution. The scatter plot of residuals and linear predictors showed a relatively even distribution around 0, while the normal QQ-plot of residuals' deviances and theoretical quantiles showed a relatively straight line, both in support of model validation (Fig. 15 and 16). Finally, the scatter plot of response and fitted values (Fig. 17) showed roughly the validation-supportive linear association, if not on an ideal 1 to 1 line. To check sensitivity of model validity to exposure and outcome variable selection, the plots were also produced for CVM and RM (Fig. 26 and Fig. 27 in the annex). We observed similar distributions; however, for RM, the outcome with fewest daily counts and thus the smallest data basis, the model fit criteria were not met as clearly, particularly in terms of the scatter plots for residuals versus linear predictors and for response versus fitted values.

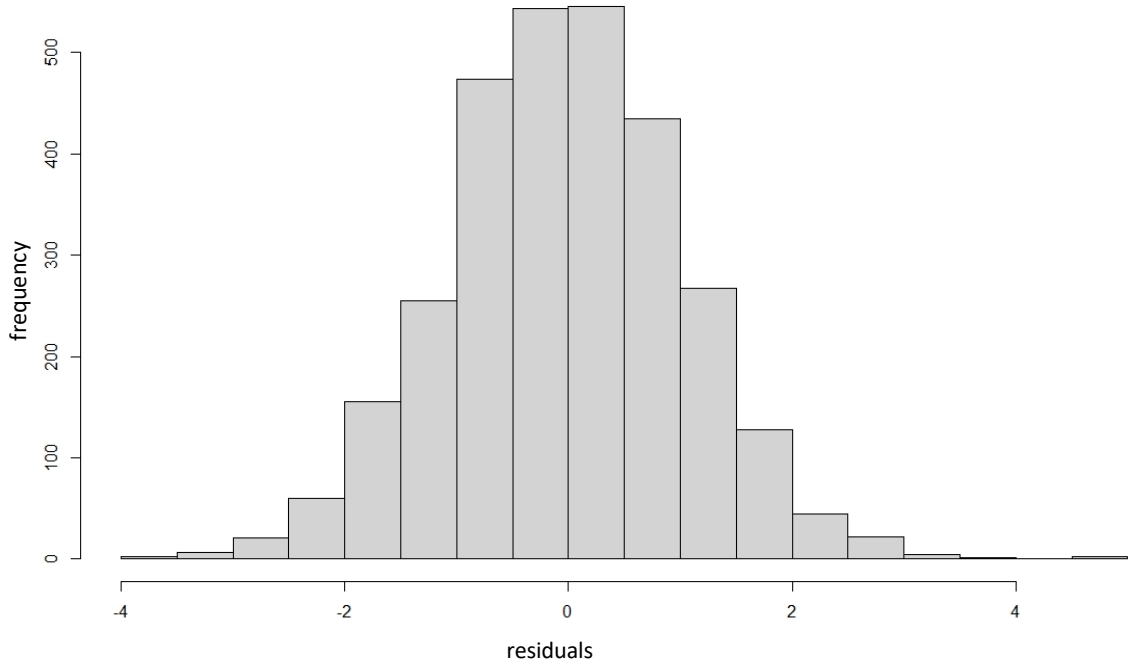

Fig. 14: Histogram of model residuals as bar chart for full model. The modelled exposure is $PNC_{30\text{-}120}$ and the outcome natural-cause mortality.

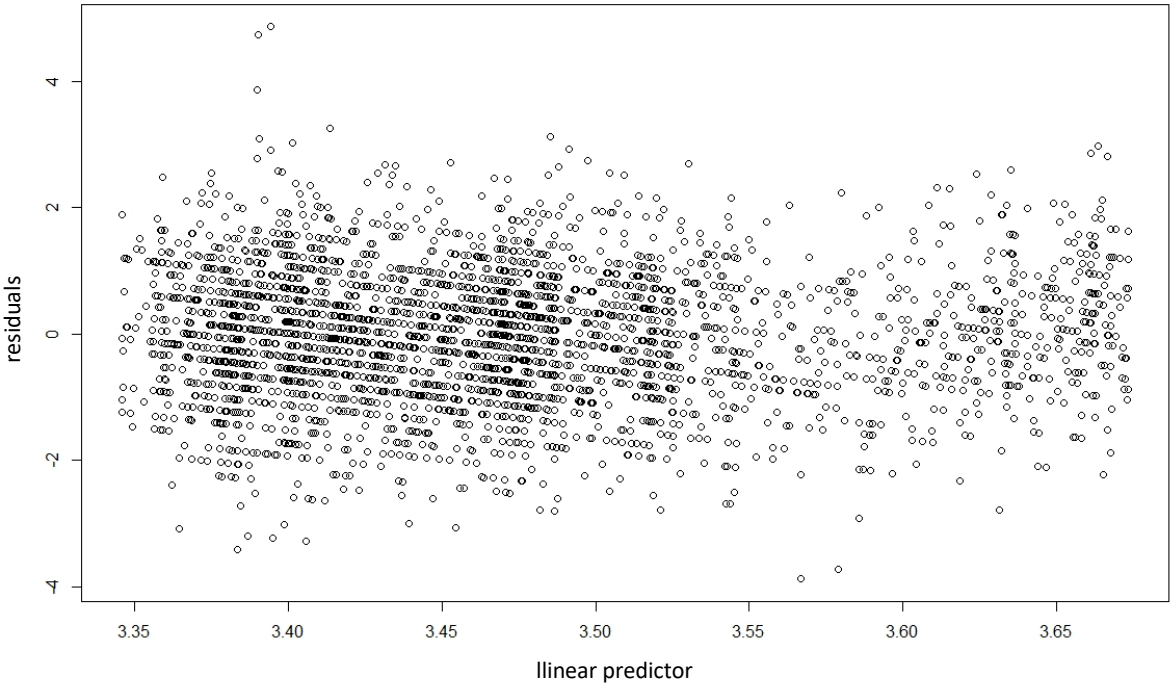

Fig. 15: Scatter plot of residuals and linear predictors for the full model (modelled exposure: $PNC_{30\text{-}120}$; outcome: natural-cause mortality). Full model adjusted for time trend, day of the week, holidays and summer population decrease, influenza, temperature and humidity.

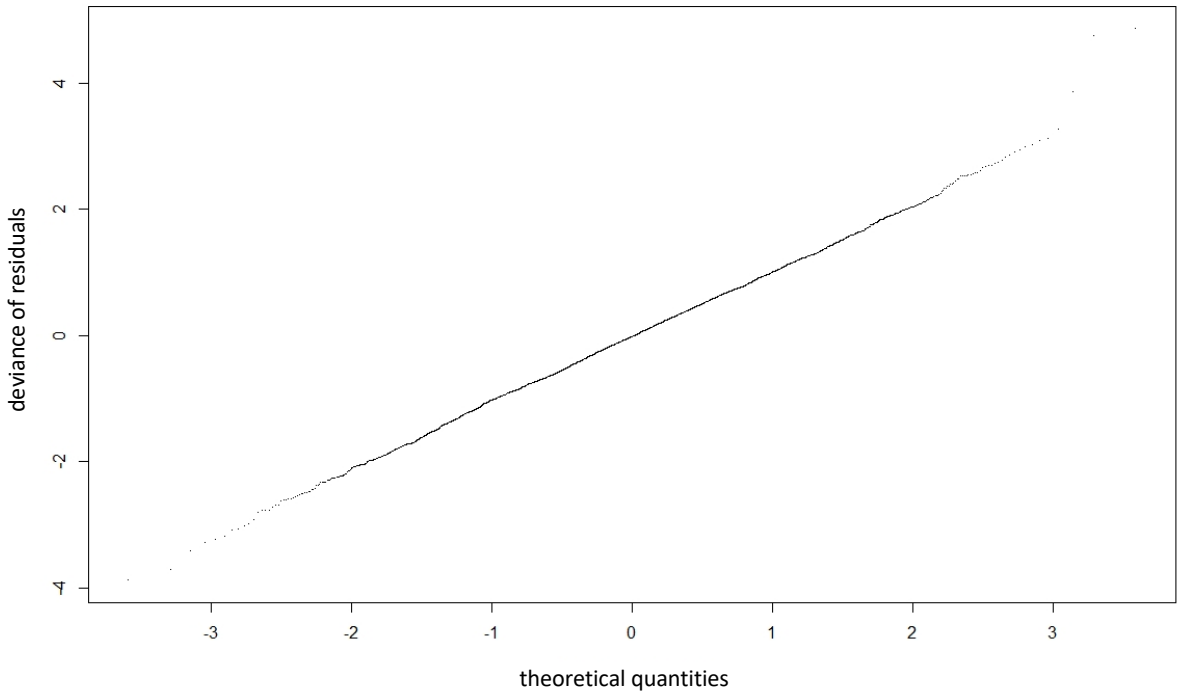

Fig. 16: Normal Q-Q plot of residuals' deviances and theoretical quantiles for the full model (modelled exposure: PNC_{30-120}; outcome: natural-cause mortality). Full model adjusted for time trend, day of the week, holidays and summer population decrease, influenza, temperature and humidity.

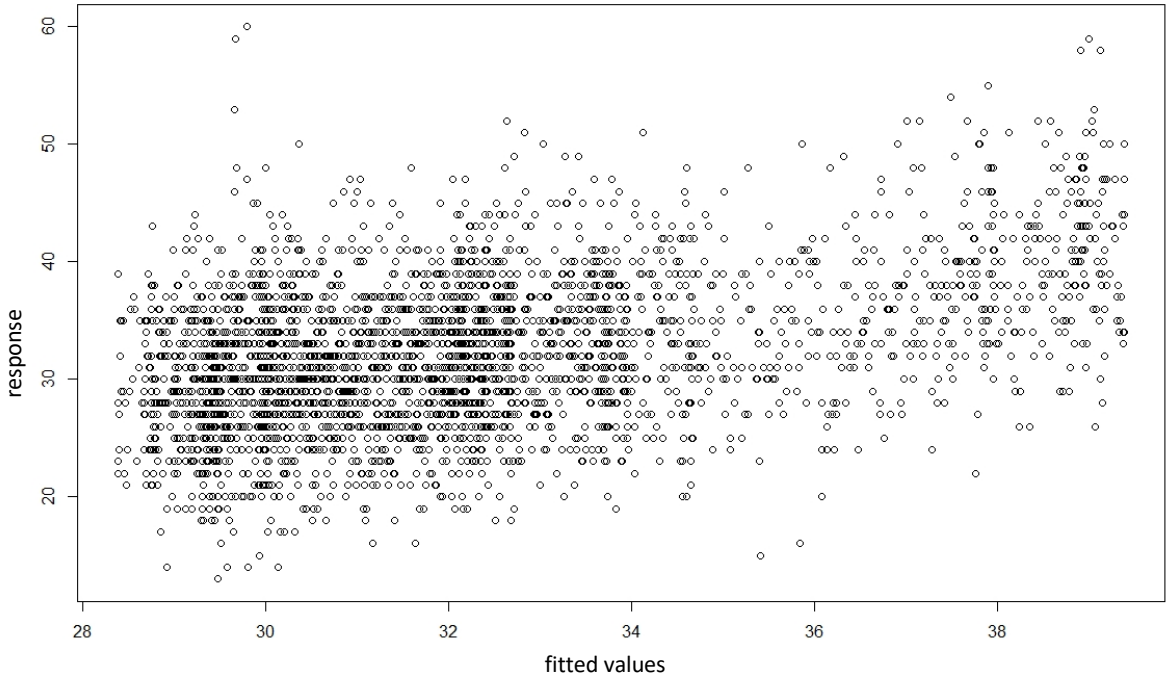

Fig. 17: Scatter plot of response and fitted values for the full model (modelled exposure: PNC_{30-120}; outcome: natural-cause mortality). Full model adjusted for time trend, day of the week, holidays and summer population decrease, influenza, temperature and humidity.

The trend line representing the spline function (k=30) for time trend adjustment is shown in Figure 18 along the days of the time series. The computed line shows about 20 turns, which corresponds to the main seasonal differences (summer vs winter) in each year and thus was appraised as sensible for this time series.

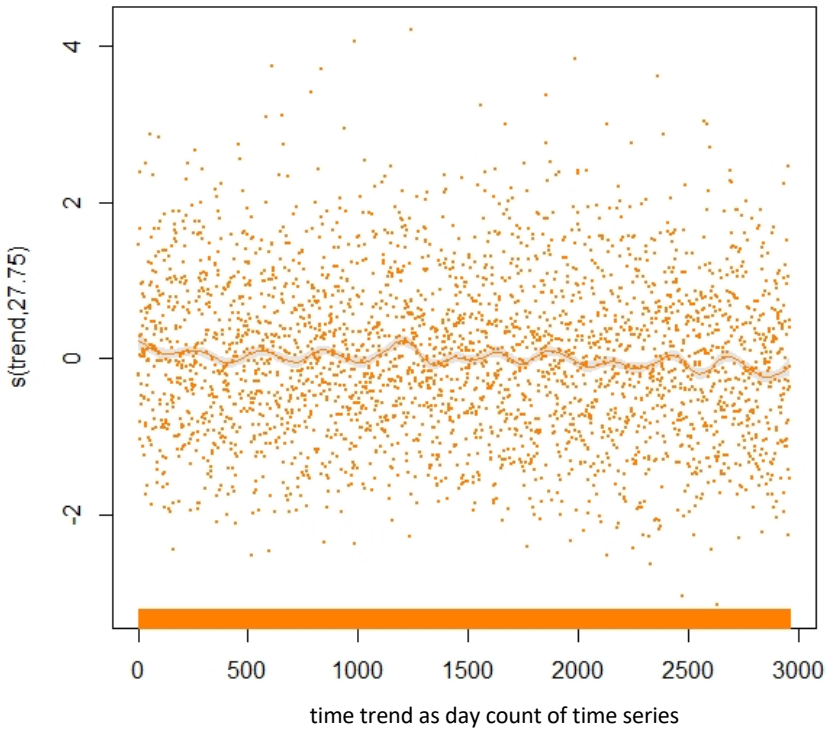

Fig. 18: Computed trend-line for spline adjustment (s(trend)) of time trend in the fully adjusted full model. The modelled exposure was $PNC_{30\text{-}120}$ and the outcome natural-cause mortality.

3.4.2 Association between exposures and outcomes for complete observation period

Based on the full model, the associations between the IQRs of PNC exposures and the three mortality categories at the level of the study region (aggregate numbers of all three municipalities) are shown for moving two-day aggregate lags ("lag0-1" to "lag6-7"), while single-lags are shown auxiliary in the annex (Fig. 27 and 28). Figure 19 shows the RRs for the PNC size fractions including DEPs ($PNC_{30\text{-}120}$) in comparison with larger ($PNC_{120\text{-}250}$ and $PNC_{250\text{-}500}$) particles, PM_{10} and NO_2. Figure 20 differentiates the RRs for the sub-ranges composing $PNC_{30\text{-}120}$, namely for the small ($PNC_{30\text{-}50}$), medium ($PNC_{50\text{-}100}$) and large sub-range ($PNC_{100\text{-}120}$), next to a comparison with smaller particles ($PNC_{13.8\text{-}30}$).

For NCM, we overall observed positive effect estimates, which for most exposures indicated relatively consistent values across lags. However, for $PNC_{30\text{-}120}$ we did not observe strong associations or evident patterns, with risk estimates for IQR of exposure meandering around the 1.00 line. This appears to be the composite result of the smaller sub-fraction ($PNC_{30\text{-}50}$), which shows slightly negative associations, the medium sub-fraction ($PNC_{50\text{-}100}$) with predominantly slightly positive associations and the larger sub-fraction ($PNC_{100\text{-}120}$) with positive associations throughout up to a RR of 1.0121 (1.0023;1.0220) for lag0-1 and 1.0094 (1.0001;1.0188) for lag4-5. This pattern of increasing RRs with increasing particle size is also reflected by the larger $PNC_{120\text{-}250}$ and $PNC_{250\text{-}500}$, as well as PM_{10}, which largely indicate significant positive associations, with small peaks at lag0-1 and overall peaks for $PNC_{120\text{-}250}$ at lag4-5 of 1.0106 (1.0021;1.0193), for $PNC_{250\text{-}500}$ at lag4-5 of 1.0117 (1.0026;1.0208) and for PM_{10} at lag6-7 of

1.0122 (1.0046; 1.0199). For NO_2, similarly, most estimates are significantly positive with a peak at lag4-5 of 1.0173 (1.0050; 1.0298).

For CVM, we observed largely delayed effects for PNC and PM_{10}. PNC_{30-120} shows a steadily increasing RR across aggregate lags with largely positive estimates peaking at lag6-7 with an estimate of 1.0171 (0.9978; 1.0368). Within its sub-ranges, the highest estimates are observed for $PNC_{100-120}$ at lag4-5 of 1.019 (1.0034; 1.0348), then slightly weaker for PNC_{50-100} at lag5-6 of 1.0182 (0.9997;1.0371) and again weaker for PNC_{30-50} at lag6-7 of 1.0147 (0.9941;1.0357). Minimal effect estimates are observed then for PNC_{13-30}, notably with lowest (below 1.00) estimates for lag5-6 and lag6-7. On the other hand, the larger particle ranges show stronger associations, with peaks at lag3-4 for both $PNC_{120-250}$ of 1.0174 (1.0027; 1.0322) and $PNC_{250-500}$ of 1.019 (1.0036;1.0345), as well as a second peak at lag6-7for $PNC_{250-500}$ of 1.0199 (1.005; 1.0351), that is also found for PM_{10} of 1.0206 (1.0079; 1.0335). For NO_2, most aggregate lag estimates are significantly positive, particularly immediate at lag0-1 of 1.0221 (1.0016;1.0431) and delayed at lag4-5 of 1.0248 (1,0039; 1.0461).

For RM, the first observation is that CIs are relatively large, at least partially explained by the smaller number of mortality cases to model from, with some short-term and delayed associations. The pattern for PNC_{30-120} vaguely resembles a “U” shape with two peaks: one at lag1-2 of 1.0248 (0.9846;1.0665) and one at lag6-7 of 1.029 (0.991; 1.0685), while lag3-4 show point estimates at 0.9698 (0.9316;1.0094). For the delayed associations at lag6-7, highest estimates estimate are observed for $PNC_{100-120}$ at 1.0304 (1.006;1.061), for PNC_{50-100} at 1.0333 (0.9971; 1.0707) and, slightly lower, for PNC_{30-50} at 1.016 (0.9758; 1.0578). For the larger size ranges, lag6-7 are at 1.027 (0.9999; 1.0548) for $PNC_{120-250,}$ at 1.0302 (1.0014;1.0599) for $PNC_{250-500}$ and at 1.0249 (1.008;1.0497) for PM_{10}. For the short-term associations, PNC_{30-50} at lag1-2 with 1.0283 (0.9861; 1.0723) and the smaller PNC_{13-30} at lag2-3 with 1.0256 (0.99; 1.0625) show highest RRs. For NO_2, the estimates resemble a “V” shape with peak estimates falling within the immediate associations at lag0-1 of 1.0421 (1.0024; 1.0834), and delayed association category, at lag6-7 with 1.0421 (1.0024; 1.0834).

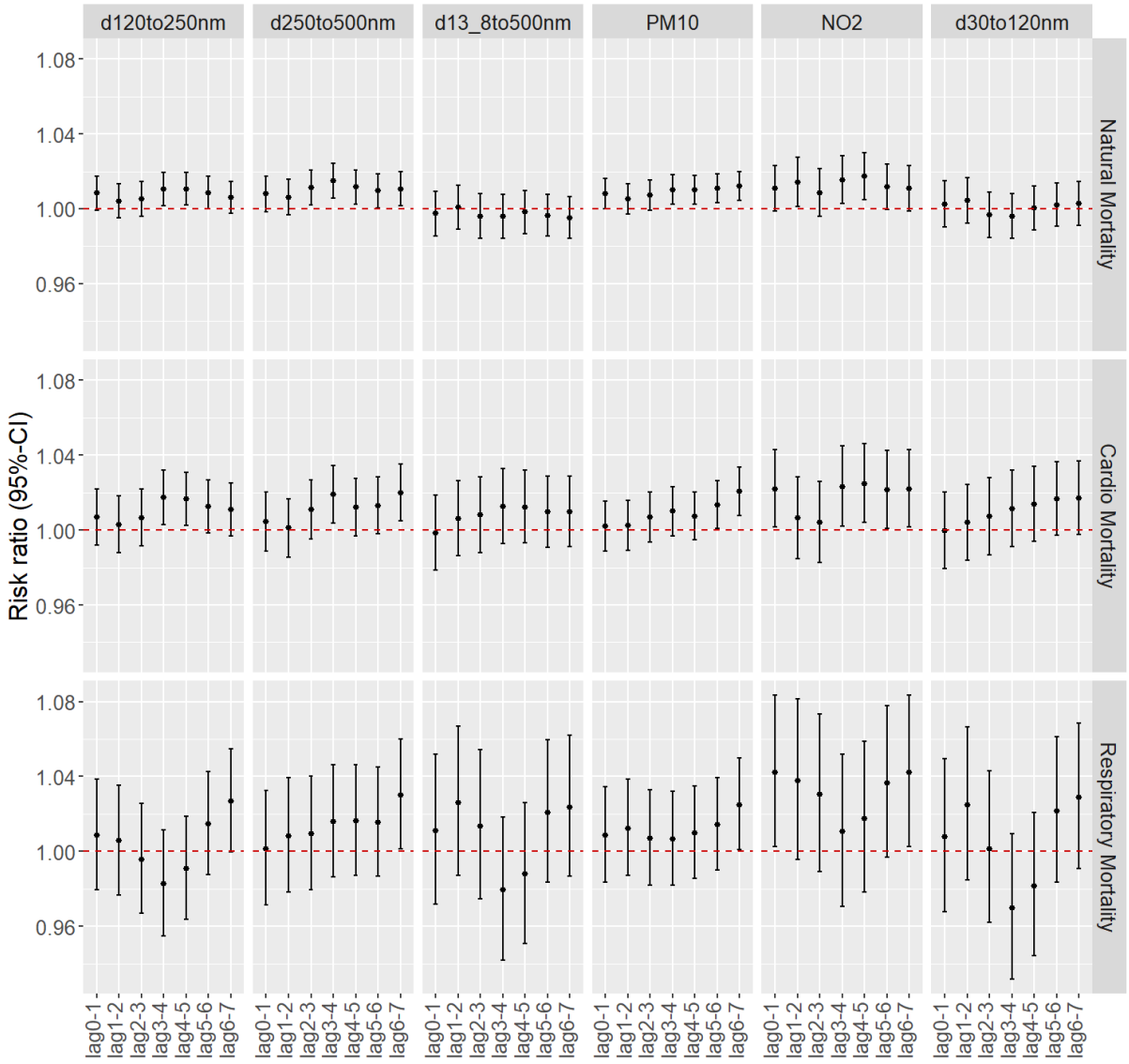

Fig. 19: Risk ratios with 95% CI based on the full model for PNC_{30-120} in comparison with larger particles ($PNC_{120-250}$, $PNC_{250-500}$), with total PNC as PNC_{13-500}, and with PM_{10} and NO_2 for two-day moving average aggregate lags over one week. Full model adjusted for time trend, day of the week, holidays and summer population decrease, influenza, temperature and humidity.

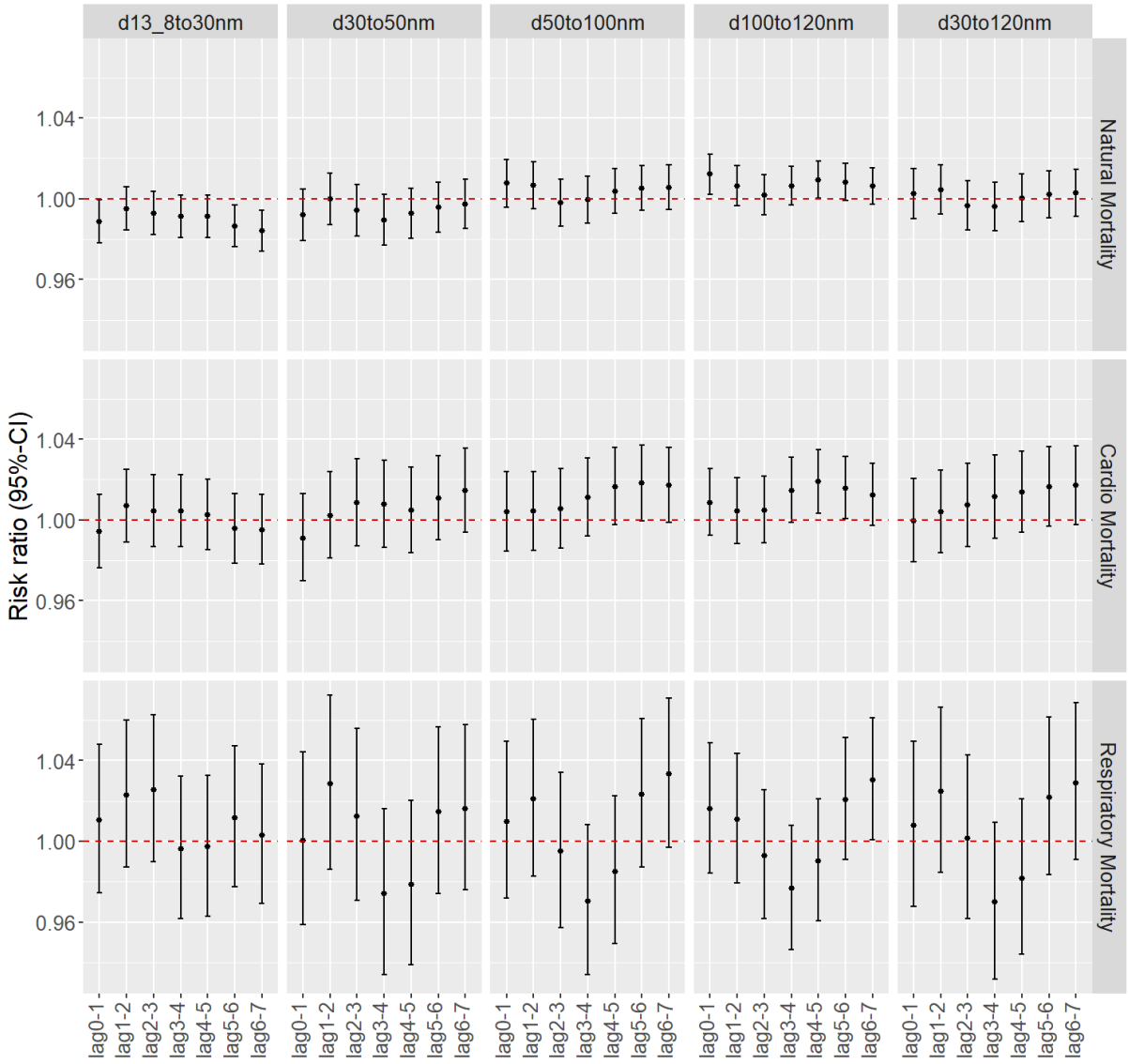

Fig. 20: Risk ratios with 95% CI based on the full model for PNC_{30-120} in comparison with its sub ranges (PNC_{30-50}, PNC_{50-100} and $PNC_{100-120}$) and smaller particles (PNC_{13-30}) for two-day moving average aggregate lags over one week. Full model adjusted for time trend, day of the week, holidays and summer population decrease, influenza, temperature and humidity.

3.5 Estimation of intervention effect on modelled associations

Through two interaction terms added separately to the full association model, we assessed whether and how the NCM, CVM and RM RRs for selected exposures may have changed over time in the context of traffic regulations. We show the estimates for the model with the dichotomous interaction term designed to account for the UEZ regulation banning non-Euro-4 compliant vehicles, and with an ordinal interaction term for annual estimates to monitor possible effect modification by an increasing DPF prevalence among registered DPVs.

3.5.1 Effect modification by UEZ regulation

The model with the dichotomous interaction term compared association estimates based on the years 2009-2013 with those of the years 2015 to 2018, thus leaving out the year during which the UEZ regulation changed. Figure 21 shows the RRs for the PNC size fraction assumed to include most DEPs

($PNC_{30\text{-}120}$) in comparison with larger particles ($PNC_{120\text{-}250}$ and $PNC_{250\text{-}500}$), PM_{10} and NO_2. Figure 22 differentiates the RRs for the sub-ranges composing $PNC_{30\text{-}120}$, namely the small ($PNC_{30\text{-}50}$), medium ($PNC_{50\text{-}100}$) and large sub-range ($PNC_{100\text{-}120}$), next to a comparison with smaller particles ($PNC_{13.8\text{-}30}$).

For NCM, $PNC_{30\text{-}120}$ shows minimal RR drops for 5 of 7 aggregate, with estimates for both periods meandering around 1.00, with a similar pattern as for the full model. These observed moderate differences appear to be the composite results of relatively strong drops in risk estimates for $PNC_{30\text{-}50}$, and little change for the larger sub-fractions $PNC_{50\text{-}100}$ and $PNC_{100\text{-}120}$. The possible reduction in RR observed for $PNC_{30\text{-}50}$ is more prominent among the smaller $PNC_{13.8\text{-}30}$ with maximum drops in RR of roughly 2.5% for delayed associations and with RRs for lag4-5, lag5-6 and lag6-7 overlapping only for parts of their CIs and thereby indicating statistical significance. At the same time, little changes, if leaning towards increases in RR are observed for $PNC_{120\text{-}250}$, while $PNC_{250\text{-}500}$ indicates more prominent increases for mid-term and delayed associations, with the RRs for lag3-4 indicate a statistically significant effect modification. Likewise, PM_{10} rather shows increases in RR, particularly for the delayed effects. For NO_2, no pattern can be observed, while the estimates for total PNC ($PNC_{13\text{-}500}$) roughly resemble the reductive pattern observed for the smallest PNCs such as $PNC_{13\text{-}30}$.

For CVM, the patterns across PNC size ranges show similarities to NCM associations, with the smallest $PNC_{13\text{-}30}$ showing reductions in RR, while already slightly larger particles in the range of $PNC_{50\text{-}100}$ show overall RR increases, particularly for delayed effects. The sub-ranges of $PNC_{30\text{-}120}$ show little repealing estimates across lags for $PNC_{30\text{-}50}$, and slight RR increases for $PNC_{50\text{-}100}$ and $PNC_{100\text{-}120}$. $PNC_{30\text{-}120}$ thereby indicates largest RR increases for delayed effects at lag5-6 and lag6-7. Overall, RR appears to increase with particle size, with $PNC_{120\text{-}250}$ and $PNC_{250\text{-}500}$ again showing largest increases for the delayed effects and minimal changes for the immediate effects, with the RR comparison at lag6-7 for $PNC_{250\text{-}500}$ indicating statistical significance. PM_{10} shows a similar pattern to the largest PNC size range, with the largest and statistically significant RR increase indicated for lag6-7. For NO_2, again, no evident pattern across lags could be observed, similarly as for the estimates of total PNC ($PNC_{13\text{-}500}$) that show neither a clear increase nor decrease.

For RM, again, patterns across PNC size ranges appear similar to the preceding mortalities: the two smallest size ranges ($PNC_{13\text{-}30}$ and $PNC_{30\text{-}50}$) rather show decreases in RR. $PNC_{50\text{-}100}$ and $PNC_{30\text{-}120}$ do not reveal a clear pattern across lags. Slight increases in RR are observed for $PNC_{100\text{-}120}$ and increasingly prominently for $PNC_{120\text{-}250}$ and $PNC_{250\text{-}500}$. Overall, as for the full model, and particularly for the pre-2014 estimates, the RRs roughly form “U” shapes for PNC size ranges between 30 and 250nm. The largest (positive) changes are observed for the medium-term and delayed effects, with substantial and statistically significant increases at lag2-3 and lag3-4 for $PNC_{120\text{-}250}$ and across most lags for $PNC_{250\text{-}500}$. Similarly, PM_{10} shows substantial and largely statistically significant increases across all lags, with a peak at lag6-7. Unlike for NCM and CVM, also NO_2 shows increases in risk, particularly for lagged effects, while total PNC ($PNC_{13\text{-}500}$) shows mixed effects, rather with decreases in RR, but without a clear pattern. Overall, the precision of estimates judged by the length of CIs is highest for NCM, over CVM and RM as expected based on the mean daily counts for the three mortalities.

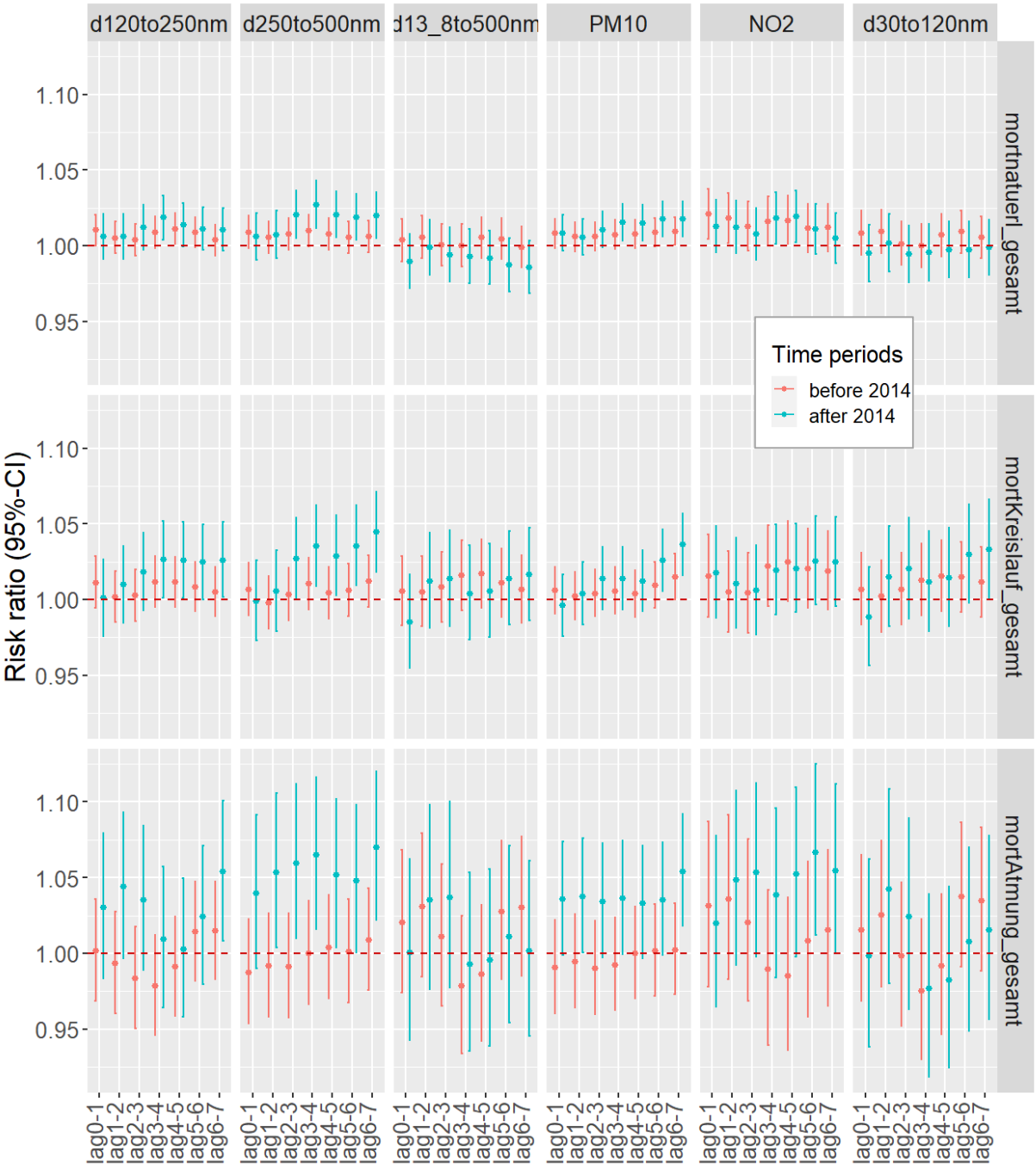

Fig. 21: Risk ratios with 95% CI based on the full model with the dichotomous interaction term for before and after 2014 for $PNC_{30\text{-}120}$ in comparison with larger particles ($PNC_{120\text{-}250}$, $PNC_{250\text{-}500}$), with total PNC as $PNC_{13\text{-}500}$, and with PM_{10} and NO_2 for two-day moving average aggregate lags over one week. Full model adjusted for time trend, day of the week, holidays and summer population decrease, influenza, temperature and humidity.

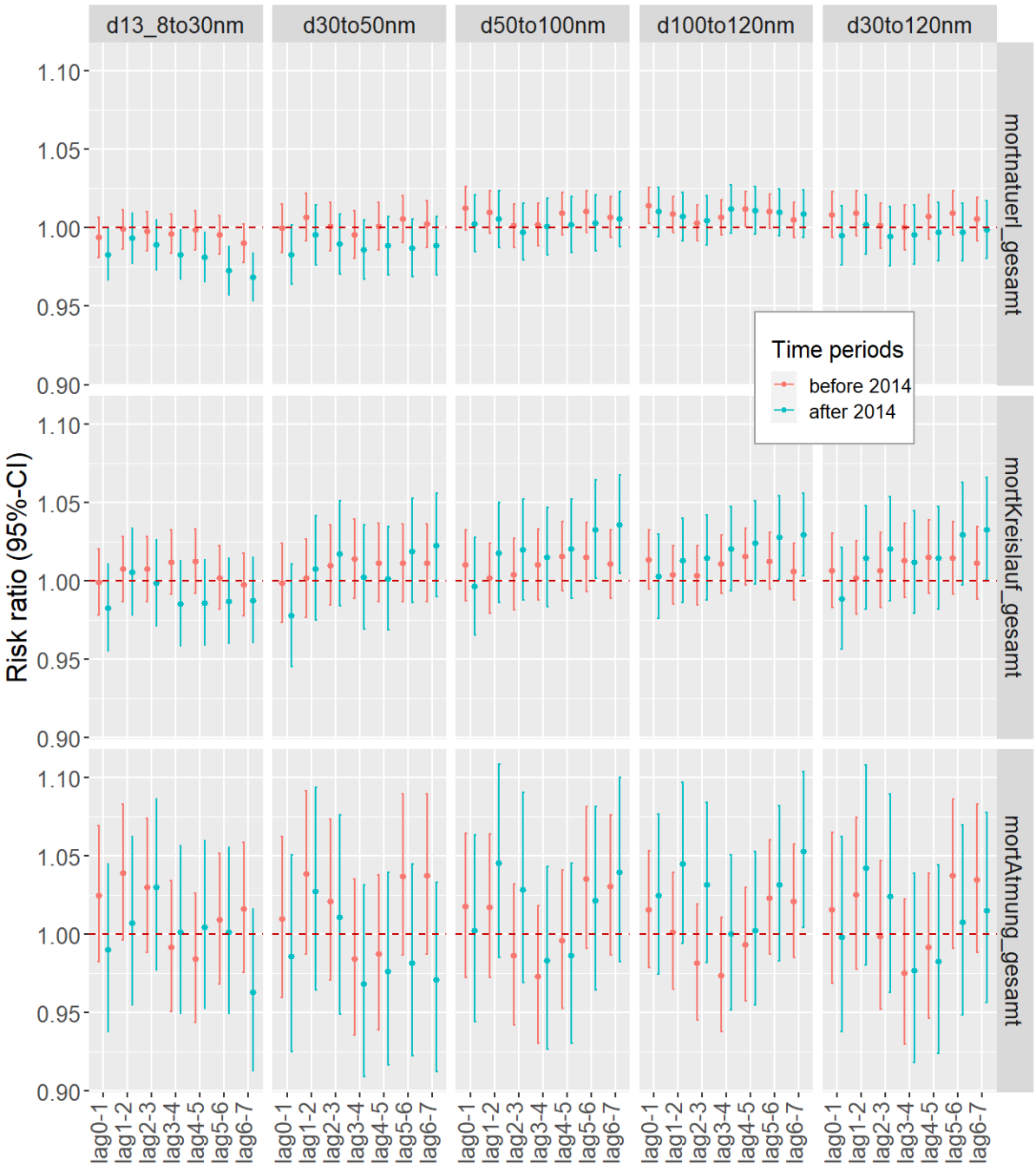

Fig. 22: Risk ratios with 95% CI based on the full model with the dichotomous interaction term for before and after 2014 for PNC_{30-120} in comparison with its sub ranges (PNC_{30-50}, PNC_{50-100} and $PNC_{100-120}$) and smaller particles (PNC_{13-30}) for two-day moving average aggregate lags over one week. Full model adjusted for time trend, day of the week, holidays and summer population decrease, influenza, temperature and humidity.

3.5.2 Effect modification by DPF prevalence

The model with the ordinal interaction term presents RR estimates for each year (2010-2018) in comparison with the base-year (2009). The analysis focuses on relative changes from year to year, and differences in patterns between exposures, rather than absolute RR differences with the base year. The models yield nine RR estimates for 2010 to 2018 per exposure, outcome and lag. In Figure 23, we present the smallest size range ($PNC_{13.8\text{-}30}$), total PNC ($PNC_{13\text{-}500}$), PM_{10} and NO_2 with a two-day aggregate lag for short-term (lag0-1), medium-term (lag2-3) and delayed (lag4-7) association. In Figure 24, we present the key exposure ($PNC_{30\text{-}120}$) with differentiation of its sub ranges, namely the small ($PNC_{30\text{-}50}$), medium ($PNC_{50\text{-}100}$) and large sub-range ($PNC_{100\text{-}120}$).

Overall, the estimates show neither gradually decreasing nor increasing RR patterns across the years, including for $PNC_{30\text{-}120}$. In contrast to the full model and the model with the dichotomous interaction term estimates, the RR patterns across the years do not differ as substantially between exposures, but rather between the immediate (lag0-1), medium-term (lag2-3) and delayed(lag4-7) aggregate lags. We observed two partial trend patterns, notably with inconsistencies and substantial uncertainty: firstly, a possible increasing trend among, mainly the delayed, NCM associations (lag4-7) for the final three years (2016-2018), and secondly, a change from an increasing to a decreasing trend halfway through the time period (around 2014) for medium-term and delayed RM association (lag2-3 and lag4-7).

As estimates are relative to one single year (2009), the non-gradual but aggregate changes for all annual estimates may contain more information about the year 2009 than about the subsequent years - with one, separate, observation appearing noteworthy: across exposures, the majority of annual estimates for immediate effects (lag0-1) lie around or below 1.0, for medium-term effects (lag2-3) around 1.0 and for delayed effects (lag4-7) slightly above 1.00.

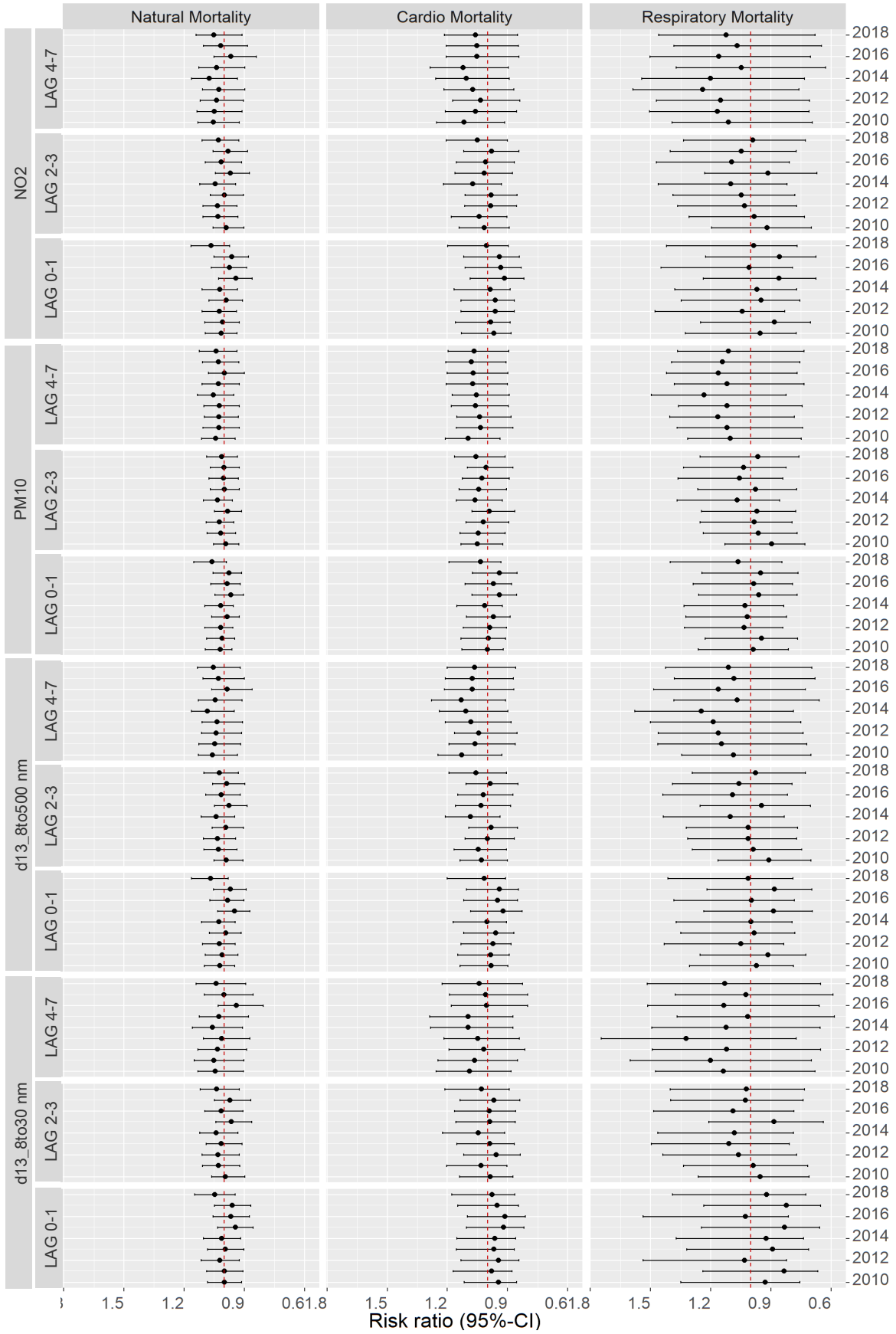

Fig. 23: Risk ratios compared with the base-year 2009 with 95% CI based on the full model with the ordinal (annual) interaction term for smaller particles (PNC_{13-30}), total PNC as PNC_{13-500}, PM_{10} and NO_2 for immediate (lag0-1), slightly lagged (lag2-3) and lagged (lag4-7) associations. Full model adjusted for time trend, day of the week, holidays and summer population decrease, influenza, temperature and humidity.

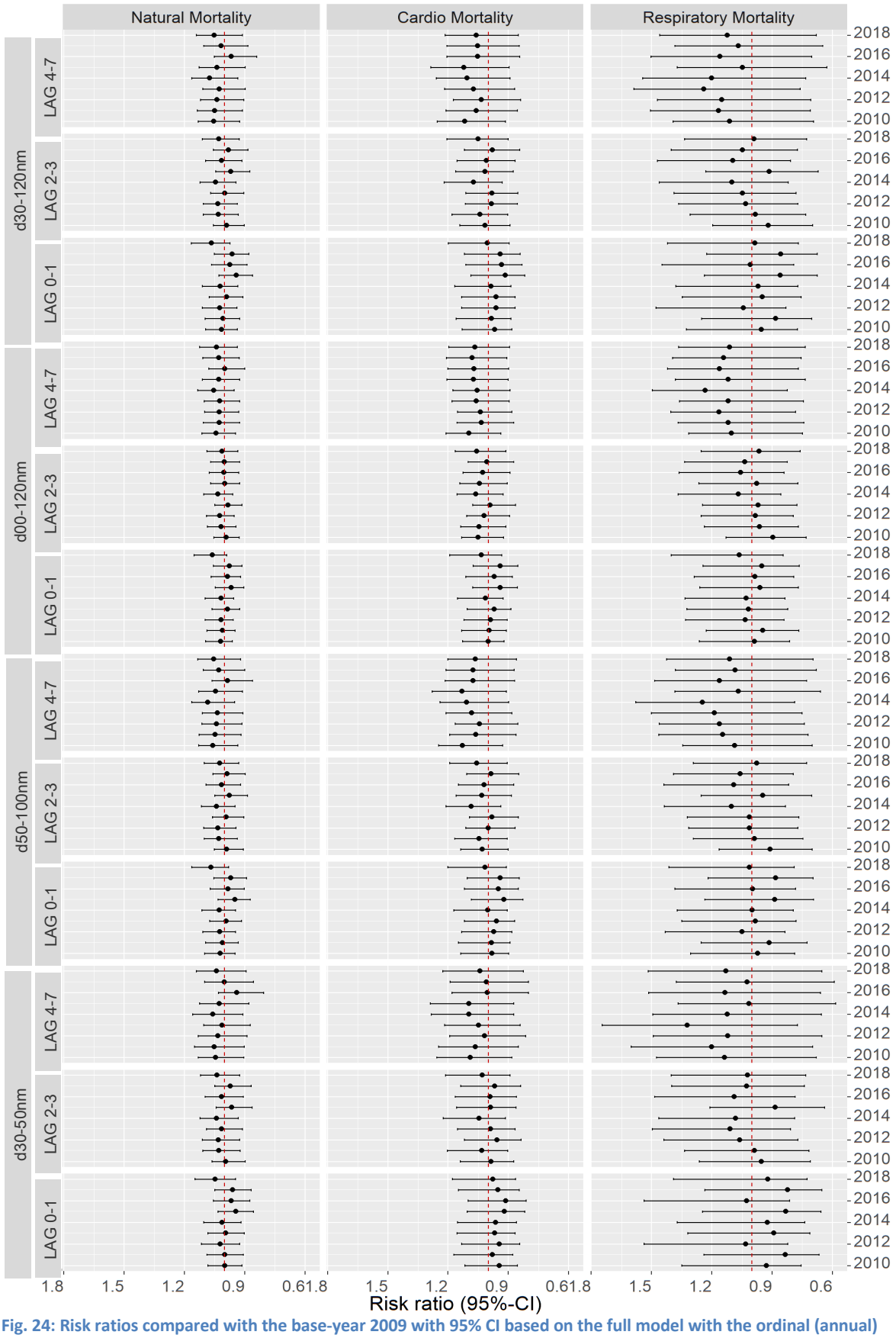

Fig. 24: Risk ratios compared with the base-year 2009 with 95% CI based on the full model with the ordinal (annual) interaction term for PNC_{30-120} in comparison with its sub ranges (PNC_{30-50}, PNC_{50-100} and $PNC_{100-120}$) for immediate (lag0-1), slightly lagged (lag2-3) and lagged (lag4-7) associations. Full model adjusted for time trend, day of the week, holidays and summer population decrease, influenza, temperature and humidity.

3.6 Sensitivity analyses

3.6.1 Exposure time trends

The following table compares the linear regression estimates for the complete time series with the one of an adapted time series, upon removal of all values for the year 2012, which included a several-month closure of the nearby interstate (A40) and thus a potential change in exposure. Table 16 presents the linear regression slopes alongside the CIs for both time series, with no substantial changes in the direction or magnitude of the trend.

Table 16: Linear regression estimates *(β)* with 95% CI for the whole time series, and as sensitivity analysis for the time series without 2012.

PNC size fraction	*Linear regression estimate (2009-18)*	*Confidence interval (2.5%; 97.5%)*	*Linear regression estimate (2009-18; EXCEPT 2012)*	*Confidence interval (2.5%; 97.5%)*
PNC 13-30 nm	-0.221	-0.307; -0.133	-0.205	-0.260; -0.152
PNC 30-50 nm	-0.272	-0.316; -0.228	-0.226	-0.256; -0.120
PNC 50-100 nm	-0.303	-0.352; -0.255	-0.245	-0.278; -0.212
PNC 100-120 nm	-0.056	-0.066; -0.047	-0.046	-0.053, -0.040
PNC 30-120 nm	-0.632	-0.728; -0.562	-0.517	-0.582; -0.453
PNC 120-250 nm	-0.130	-0.151; -0.108	-0.114	-0.128; -0.989
PNC 250-500 nm	-0.036	-0.042; -0.030	-0.036	-0.039; -0.032

3.6.2 Definition of DEP PNC size range

$PNC_{30\text{-}120}$ assumed as the range assumed to contain the vast number of DEPs, was split into three sub-fractions for separate model runs and comparison of respective estimates. For both the full and the model with the dichotomous interaction term, the three sub-fractions showed substantial differences for many mortality-lag combinations among each other, as well as, in comparison with $PNC_{30\text{-}120}$. Also, particularly the size range smaller than 30 nm, but also the one larger than 120 nm, partially showed substantially more pronounced estimates than $PNC_{30\text{-}120}$ or its small sub-range $PNC_{30\text{-}50}$. The model observations paired with the fact that particularly $PNC_{13\text{-}30}$ has a relatively high mean daily PNC, suggest that particularly an extension or shift of the $PNC_{30\text{-}120}$ to include smaller particle sizes could alter estimate size and patterns.

3.6.3 Full association model

The evidence-based selection of the PNC size fraction attributed to the majority of PNC emitted by DPVs without DPFs bears limitations in precision and possibly in accuracy, as explained in the introduction. Therefore, for the selected $PNC_{30\text{-}120}$ three sub-ranges were defined and computed alongside, while a smaller PNC range and two larger PNC ranges were used as comparators.

The preceding presentation of results allowed insights on the sensitivity of the effect estimates of the in-focus $PNC_{30\text{-}120}$. It was observed as sensitive to changes in the smallest size range $PNC_{30\text{-}50}$ – a

narrower definition of the PNC size range to represent most DEPs could have changed effect estimates substantially. Similarly, for the common total PNC indicator, here defined as $PNC_{13\text{-}500}$, substantial changes in the smallest sub-range, here $PNC_{13\text{-}30}$, were observed to affect the total PNC estimate, thereby supporting the observation made for $PNC_{30\text{-}120}$. Also, the comparison between aggregate two-day lags and single lags revealed sensitivity of single lags for missing data, as evident by outliers for lag0 for $PNC_{100\text{-}120}$ and $PNC_{250\text{-}500}$ that was not observable when using lag0-1. We otherwise did not observe substantial differences by equalization with two-day lags in comparison with daily single-lags (Fig. 27 and 28). The full model was observed as robust to separate adjustment for both PM_{10} (Fig. 29 and 30 in the annex) and NO_2 (Fig. 31 and 32 in the annex). Patterns and association directions remained constant across the PNC size ranges and for NO_2 and PM_{10}, respectively. RR-estimates for both adjustments were overall found slightly closer to the null-value of 1.00, without substantial changes in the number of statistically significant estimates.

3.6.4 Effect modification by traffic regulations

For the model with the dichotomous interaction term , we observed no substantial changes for the model computed with a different break point (2013 instead of 2014) was computed (Fig. 33 and 34 in the annex). The model thus showed to be robust to inclusion of the year 2014 as the year during which the UEZ regulation change took effect.

Both, the model with dichotomous and with ordinal (annual) interaction terms were also observed as largely robust to separate adjustment for both PM_{10} and NO_2. Patterns and association directions remained constant across the PNC size ranges and for PM_{10} (Fig. 35 and 36 in the annex) and NO_2 (Fig. 38 and 39 in the annex) respectively for the model with the dichotomous interaction term . For the model with the ordinal interaction term, estimates were found robust for PM_{10} adjustment (Fig. 39 and 40 in the annex), while NO_2 adjustment showed minimal changes in the pattern for PM_{10} estimates and RR-estimates substantial closer to the null-value of 1.00 for $PNC_{13\text{-}30}$ (Fig. 41 and 42 in the annex).

4. Discussion

4.1 Result summary

This study assessed the association between size-specific PNCs with NCM, CVM and RM, and potential effect modification by traffic regulation implementation over time. For the years 2009 to 2018, daily mean PNC, PM_{10} and NO_2 concentrations from a central measurement station in Mülheim-Styrum and daily NCM, CVM and RM counts for the adjacent municipalities (Mülheim, Essen, Oberhausen) were analysed across 2965 days. Poisson regression models built as GAMs were adjusted for time-varying covariates, including meteorological factors. $PNC_{30\text{-}120}$ was selected size range assumed to include the vast majority of DEP PNC. Dichotomous and ordinal interaction terms were used to evaluate effect modification by the banning of Euro-4 incompliant vehicles in the local UEZ and by gradual Euro-4 adoption among registered cars over time. Sensitivity analyses included adjustment for the co-pollutants PM_{10} and NO_2, as well as alternative time periods for simple linear regression of PNC trend regression and for the model with the dichotomous interaction term . In response to the three research questions, we gathered the following results and observations from the statistical descriptions and analyses:

(1) The level of daily average, size-specific PNCs showed reductive trends across size fractions during the observation period (2009-2018), including $PNC_{30\text{-}120}$. $PNC_{30\text{-}120}$ had a median (IQR) level of 4970 (3189) PNC/cm^3 with a linear regression estimate (95% CI) of -0.63 (-0.73; -0.56) for daily average PNC. For mortality, median daily counts (IQR) were 32 (8), 11 (5) and 3 (2), respectively for NCM, CVM and RM for a total of 95,867 deaths in the study period.

(2) Size-specific PNCs showed, partially statistically significant, associations with short-term NCM, CVM and RM. The RR for the investigated PNC ranges showed immediate (lag0-1) and delayed (lag4-5, lag5-6, lag6-7) association (95% CI) with natural cause mortality up to 1.0121 (1.0023; 1.022), delayed (lag4-5, lag5-6, lag6-7) association with CVM up to 1.0199 (1.005; 1.0351) and immediate (lag0-1, lag1-2) and delayed (lag5-6, lag6-7) association with RM up to 1.0333 (0.9971; 1.0707). Across particle size ranges, for NCM and CVM, we overall observed patterns of point estimates becoming more positive with increasing size of particles. For RM, patterns across particle size ranges were found relatively stable up to 250 nm with immediate and delayed associations, while for large particles and PM_{10} delayed associations prevailed. Overall, associations were relatively robust for PM_{10} and NO_2 adjustment. Single-lag estimates showed few differences in comparison to the main two-day aggregate lags.

(3) Effect modification by time in relation to regulatory measures on PM exhaust for DPVs could be partially observed for the UEZ regulation, but not for the increasing prevalence of Euro-4 compliant DPVs. The model with the dichotomous interaction term on effect modification by UEZ restrictions for NCM, CVM and RM showed decreasing point estimates for PNCs below 100 nm (including for $PNC_{30\text{-}120}$), 30 nm and 50 nm, respectively. However, PNCs above 120 nm, 50 nm and 100 nm respectively, as well as PM_{10} showed increases in RR, while NO_2 estimates only showed a RR change (increase) for RM. Estimates by the model with the dichotomous interaction term were robust to PM_{10} and NO_2 adjustment. The model with the ordinal interaction term showed no gradual RR decreases across years, including for $PNC_{30\text{-}120}$. Vague trend patterns could be observed among RM estimates across the time period and for delayed NCM associations for the years 2016-18. For the model with the ordinal

interaction term, estimates were largely robust for PM_{10} adjustment, with NO_2 adjustment causing a downsizing of estimates.

For interpretation of the main results, auxiliary variables on vehicular traffic properties in the study region revealed an increase in DPV traffic in the study period. Vehicle registration data (aggregate of study municipalities) show a substantial absolute increase (+25%) and a slight relative increase compared to gasoline-powered cars (from 22% to 26%). The traffic counts on interstate A40 showed a steady increase of car traffic, expect for a year with construction work (2012), for exception of which linear regression estimates showed to be robust. Approximately at half-time, upon 01.07.2014, the Ruhr Valley UEZ limited access largely to Euro-4-compliant on-road vehicles, which was estimated to have affected about 3/4th of the study population based on a GIS analysis. Across the study period, the proportion of DPVs equipped with DPFs, as approximated by registered vehicle compliance with Euro-4 in the study region, increased from 49% to 88%.

4.2 Levels and development of PNC size ranges over time

In terms of PNC levels, the observed median daily total PNC ($PNC_{13\text{-}500}$) value of 10,400 particles/cm^3 for our urban background station in Mülheim-Styrum is almost identical with the global average estimated by Schraufnagel (2020) of 10,760, while noting that total PNC definitions vary in their (more importantly) lower and upper limit. The median UFP PNC using the WHO definition (<100 nm) for UFP ($PNC_{13\text{-}100}$) with a value of 9,000 makes up most of the total PNC. A study by Birmili *et al.* (2015) showed means of about 6000 particles per cm^3 for comparable urban background stations on average in Germany (based on 7 measuring point across Germany), with Mülheim-Styrum listed as a station with relatively highest PNC values - as supported by our estimates.

For co-pollutant levels, the mean annual value for our study area of 22.3 µm/m^3 for daily PM_{10} concentration can be considered high for urban background stations in Germany, with national averages estimated between 17-22 for the years 2009-2018 (UBA, 2020b). For NO_2 concentrations, the study area mean of 28.3 µm/m^3 is even more strongly elevated compared to the annual means for German urban background stations estimate at 20-24 (UBA, 2020b).

In terms of PNC level development, the observation of generally decreasing PNC trends is consistent with a multi-city study for Germany by Sun *et al*. (2020), which found similar declines of 2.6 to 6.3% per year in PNC (20 – 800 nm) during an almost identical time period among five urban background measurement sites of the GUAN network. An earlier global study of PNC, including stations in Europe, North America, Antarctica and on Pacific Ocean Islands related their finding of decreasing PNC for the decade before the one of this time series (2001-10) mainly with reductions in anthropogenic emissions, particularly SO_2 as a particle precursor, while they did not long-term trends associated with surface temperature trends (Asmi *et al*., 2013).

For co-pollutant levels, a long-term decline fir PM_{10} is consistent with data from Germany (UBA, 2020b), and other European data, e.g. for a period of 2000-2017 in several European cities by Sicard *et al.* (2021), or for the city of Rome by Renzi *et al*. (2017). Also, the long-term decline in NO_2 similarly has been found elsewhere, e.g. for the urban background stations across Germany (UBA, 2020b).

4.3 Development of vehicular traffic

The reductive trend of daily mean PNC ran contrary to rising numbers of registered DPV and traffic volumes, besides a slight increase in the proportion of DPV over gasoline-powered on-road vehicles. This may be interpreted as contrary developments facilitated by the parallel and steady increase in the proportion of on-road vehicles complying with the Euro-4 norm, particularly among DPVs. A reductive trend was also observed for $PM_{10,}$ for which traffic emissions make up a relatively much smaller fraction compared to PNC, thus serving as a possible indication for additional APP reductions in other sectors. Notably, all studied PNC size fractions between 13.8 and 500 nm, and thus also outside the assumed DEP-size range, showed statistically significant reductive trends.

Jesus (de) *et al*. (2020), on the basis of long-term PNC decreases during a similar period, concluded on a reductive role of Euro-norm uptake, among others, for PNC values in 4 of 5 studies global cities. Meanwhile, Fujitani *et al*. (2020) for the similar period of 2004-17 concluded in an associated reduction in $PNC_{10\text{-}100}$ with DEP measures similar to the Euro norm, if with a slower than expected decline, which they reasoned with secondary PNC based on diesel-vehicle emitted SVOCs. In comparison with other areas in Germany, UBA (2015), for the time period of 2008 to 2013, found, similarly to our observations, overall increasing vehicle registration numbers across Germany – also with relatively stronger increases for DPVs than for those powered by gasoline.

Among the traffic variables, one trend pattern may raise questions, as only until 2017, the proportion of diesel-powered in comparison to gasoline-powered vehicles increased, before the trend reversed to a slight decrease. We interpret this pattern as possibly representative of a turning point associated with the delayed effects of public debates on diesel-engines in Europe and Germany, including the penalised manipulation practices for NOx emissions by the *Volkswagen AG* in 2015 and later by other car-markers (Gross & Sonnberger, 2020; Pries & Wäcken, 2020).

4.4 Association between PNC size ranges and mortality

We generally observed positive, partially statistically significant, associations for NCM, CVM and RM with size-specific PNC across size fractions for different lags, while the partially negative associations are not plausible based the current understanding of the underlying biological logic. The (statistical significance of) individual estimates (is) are to be interpreted with care, mainly due to the number of model-runs allowing significant estimates based on a p-value below 0.05 to occur by chance that we did not separately adjust for. As almost half of the NCM consists of cardiovascular and respiratory causes, the association pattern across the aggregate lags may be expected, as observed, to partially embody an attenuated composite of their RRs (e.g. as observed in Stölzel *et al.,* 2006).

For NCM, the RR of the investigated PNC ranges showed possible immediate (lag0-1) and delayed association (lag4-5, lag5-6, lag6-7). Rivas *et al.* (2021), who limited their analysis to lag0-5, found immediate associations (lag1, lag2) for total PNC and two size ranges below 60 nm in Barcelona and Helsinki, and delayed associations (lag5) for large size PNCs (around 80-300 nm) in Zuerich and Helsinki. Delayed associations were also observed in a study in eight urban areas in Europe, which found a NCM increase of 0.35% per 10,000 particles/cm^3 for total PNC that occurred 5-7 days before death (Stafoggia *et al.*, 2017). Stölzel *et al.* 2006 identified association for UFP PNC and larger size ranges up to 1000 nm highest at lag4, next to a smaller peak at lag0.

For CVM, mainly delayed association (lag4-5, lag5-6, lag6-7) were observed. This may be reasoned by biological mechanisms that trigger a delayed outcome. Rivas *et al.* (2021) observed delayed (lag5) associations across for various PNC size ranges in Zuerich, next to almost significant estimates for lag0. They also observed delayed associations for <20 nm PNC in Barcelona, where, however, the immediate associations prevailed. Lammers *et al.* (2020) on the other hand attributed short-term, adverse effects on cardiovascular function, here indicated by blood pressure, to particle sizes above 50nm, but not below 20nm.

For RM, immediate and delayed association were observed, with largest point estimates for immediate associations for the smaller size ranges (<100nm) and for delayed associations for the medium (>100nm) and the largest size range (>250nm). (Vaguely) similar associations were also found by studies in other European cities, which have observed possible associations between UFP PNC and RM, for example, the "UFIREG" study, which assessed UFP and RM association for six, vaguely comparable, cities in Europe found non-significant associations for lag0-6 of 9.9% [95%-CI: − 6.3%; 28.8%] with RM per IQR increase in UFP (20-100 nm) concentration (Lanzinger *et al.,* 2015). Rivas *et al.* (2021) observed, less prominent, "U" shapes for Zuerich and among some size ranges for Helsinki – with particularly Zuerich featuring a relatively comparable climate to our study area. Notably, for example Lammers *et al.* (2020) attributed short-term, adverse effects on respiratory function mainly to particle sizes below 20nm, and thus outside $PNC_{30\text{-}120}$. The estimates were robust against adjustment for PM_{10} and for NO_2, the key co-pollutants for traffic related UFP studies besides $PM_{2.5}$, thus supporting the conclusion observed associations to be likely independent of parallel AAP exposures.

4.5 Effect modification by traffic regulations and time

We observed effect modification over time for the change in UEZ regulation for most PNC size ranges (besides for PM_{10} and NO_2) with direction and magnitude of change dependent of the PNC size range. At the same time, no gradual decrease (or increase) of annual RR could be identified for any of the exposure, outcome and lag combinations.

For the model with the dichotomous interaction term the, partially substantial and statistically significant, decreases in RR for the smaller PNC size ranges and increases for the larger PNC size ranges and PM_{10} across mortality causes may indicate a change in PNC composition beyond the fraction attributed to DEPs ($PNC_{30\text{-}120}$). Differences between lags were also observed, but less pronounced than for size-range. For the exposure in focus ($PNC_{30\text{-}120}$), the modification differed by morality with overall - across aggregate lags - reductions for NCM, increases for CVM and mixed effects for RM. The differences could be disentangled when looking at the sub ranges of $PNC_{30\text{-}120}$ that show different "turning points" from a decreasing to an increasing RR, with the smallest size range ($PNC_{13\text{-}30}$) showing decreasing RR across mortality causes. $PNC_{13\text{-}30}$ is a range that has been associated by other studies with highest PNCs for primary gasoline exhaust particles, with typically lower PNC peaks than DEPs (e.g. Pant & Harrison, 2013), which were also targeted by Euro-4-related EAT systems. Overall, the strongest RR decreases were observed for NCM, thus, assuming correct mortality attributions, this suggests health effect changes outside CVM and RM causes. In contrast, the strongest increases in RR were observed for the largest PNC size range ($PNC_{250\text{-}500}$), which is not a range attributed typically to (on-road vehicle emitted) DEPs or other primary on-road vehicular traffic exhaust particles, especially when considering the parallel increase in PM_{10} RR. PM_{10} can despite its measurement as mass concentration be highly influenced by traffic-related particles, as conclude by Pant & Harrison (2013). Our observation raises the question, which particle source (and mixture), likely not on-road traffic-

exhaust, is responsible for such substantial increases in RR after 2014. Li *et al.* 2018 for another German city identified biomass burning (e.g. from power plants or residential heating) and biogenic organic secondary aerosols as main PNC contributor for larger particles (up to 360 nm), while Pant & Harrison (2013) reviewed (road) surface and tyre wear at a PNC mode of around 300 nm. At the same time, the strongest RR increases were observed among RM associations, including for NO_2, which for NCM and CVM showed mixed effects. The fact that strongest increases were observed for RM may be an indication for an AAP substance (mix) particularly relevant for respiratory health. One potential source are DEPs from ships, where the prevalence of EAT is lower, that also may proliferate NO_2 emissions, and PNC peaks are at larger particle sizes compared to DPVs (e.g. Moldanová *et al*., 2009). Unfortunately, epidemiological studies differentiating mortality associations for non-exhaust UFP and PNC sources remain rare for potential comparison, as the underlying source apportionment is not trivial, particularly for AAP measurements away from the source due to the relatively high temporal and spatial variability of quasi-UFP (e.g. Kumar *et al*., 2013b). Finally, the GIS analyses indicated UEZ relevance for over $3/4^{th}$ of the study area residents, with a stable level of the total (registered) population number across the time series period.

The model with the ordinal interaction term showed no gradual RR decreases across years, including for $PNC_{30\text{-}120}$, thus not confirming the hypothesis of a reduction in DEP toxicity being traceable by reductions in RR for NCM, CVM and/or RM. The vague trend patterns for RM estimates, with increasing before decreasing RR for the first and second half of the time period respectively, could, however, hypothetically be linked with the change in UEZ regulation around the time of the trend pattern's turning point. Although RR changes for RM associations were higher than for NCM and CVM for the model with the dichotomous interaction term, they differ substantially between PNC smaller versus larger than 120 nm, which the pattern in the model with the annual interaction term does not. Also, the delayed NCM associations with gradually increasing RR for the years 2016-18 took place in parallel with relatively larger increases in traffic counts (A40 interstate). However, also this pattern is not limited to a certain size range, and explicitly not to the ones estimated to include most PNC from gasoline or diesel exhaust – and an association thus hardly plausible.

Overall, the annual estimates are based on a much smaller data basis than the general (about 10 years) and dichotomous (4-5 years) models, which may partially explain the reduced robustness to co-pollutant, particularly NO_2, adjustment.

4.6 Strengths and limitations

4.6.1 Basic study setup

Overall, and relative to the current evidence base on UFP-associated health effects, this study bears a number of relevant strengths. The assessed size-resolved PNC data for a largely uninterrupted period of almost one decade (2965 days) in association with 95,867 deaths of exposure-relevant causes. The used exposure and mortality data were sourced from renowned institutions with well-established quality checks for data gathering and processing. The co-location of the PNC measurement station with a general air pollution monitoring station, allowed inclusion of both PM_{10} and NO_2 concentrations for the exact same location in comparative analyses, only missing $PM_{2.5}$ as a third, commonly used, variable.

The study area in the German Ruhr Valley is particularly suitable for assessing the association of urban background concentrations with a larger population (about 1 million residents within the study area), as permitted by the size and relative homogeneity of the combined agglomeration representing one of the largest urban areas in Europe. At the same time, the location of the study area was predestined for assessing time trends on DEP-related PNC exposures during the time of study: Germany was a country with an overall high absolute and relative prevalence of DPVs, while the very study area was part of one of the largest UEZ in Europe, with over 75% of the locations of residence of the study population falling within the UEZ perimeter. This is a rare situation for a UEZ, as at least in Germany, as they are typically smaller and limited to one city, rather than a larger agglomeration as the case of the Ruhr Valley. The analysis for effect modification by traffic regulation used three different models for two main regulatory developments. As an urban background station, the measurements are assumed to be representative of a large area and not influenced by individual roadways, despite the relative vicinity of the interstate A40, which is not part of the UEZ.

In view of study comparability, the study population was rather unspecific as it represents the total population of the respective municipalities. The municipality populations may overall have a slightly lower than average for Germany SES, as the area is highly urbanized, and also parts of the population are former coal-mining workers, with possible occupational UFP exposure (before the study period), which is however less relevant for short-term associations**.** The statistical power of this study was not assessed explicitly, but two decisive factors according to Winquist *et al.* (2012), namely series duration with almost 10 years and outcome counts with a study population of almost one million and three common mortality causes accounting to almost 100,000 deaths are relatively large.

4.6.2 Time series methodology

Historically, time series studies have typically been performed in econometrics with the main purpose of forecasting and data stationarity and autocorrelation as key issues for consideration. In environmental epidemiology, time series studies are rather used for retrospective analyses. Their use for statistical analyses of AAP associations with health outcomes remains subject to several methodological challenges (e.g. Dominici, 2004). Issues include the handling of independent effects by a particular pollutant amidst potentially confounding covariates and co-pollutants, and autocorrelation among both AAP and health data (Dominici, 2004; Dominici *et al*., 2002). Our time series, as any air pollution time series validates this requirement as outcome values are more likely similar for adjacent days than for days weeks, months or years apart within the time series. Such autocorrelation is typically not intrinsic to the outcome results, but largely explained by seasonality and other time-dependent variables, like meteorology. A detailed reflection on time series regression for environmental epidemiology can be found elsewhere, such as by Baskaran *et al.* (2013). We followed the guidance of renowned statisticians and environmental epidemiologists, including the above-mentioned resources and those named in Chapter 2.3.3 for the full model and Chapter 2.3.4 for the effect modification models. The controlling for time-dependent variables was performed based on a DAG in combination with previously established model correction factors for the same study region, while the sensitivity analyses for two main co-pollutants showed model robustness, particularly for the full mode and model with the dichotomous interaction term, and the conducted residual autocorrelation assessments for the used models fulfilled the criteria with minor limitations as expected for such AAP time series.

4.6.3 Statistical modelling approach

For the statistical analysis of time series, the use of GAMs with nonparametric splines for Poisson regression is well established in AAP epidemiology with several methodological debates among groups of epidemiologists and biostatisticians having advanced both the methodological elaboration and the software tools, i.e. code (packages) in R®. Poisson regression was a logic choice, as this time series used count data, although it theoretically requires observations to be independent. GAMs can be more flexible than generalized linear models, and in contrast to several other model types do not require assumptions on the nature/shape of the relationship between dependent and independent variables. However, early uses of GAM-functions in older statistical software had shown to potential overestimate AAP effects. For correction, the inclusion of smooth functions to adjust for underlying time trends confounding outcome and exposure have become an integral part of most AAP time series studies, e.g. through smoothing splines or natural cubic splines with a parameter defining the number of internal knots or degrees of freedom. Ravindra *et al.* (2019) reflected on the utilization of the GAM function used for this study in more detail by comparing several studies.

4.6.4 Limitations of the methodological setup and statistical modelling decisions

The estimates rendered by the full model may have been subject to the following potential limitations with the results of under- or overestimation associations:

(i) The basic methodological setup with the use of one urban background station for the AAP exposure of the population in three adjacent urban areas bears risk of exposure misclassification, i.e. the setup may have not been accurate and precise enough to detect actual differences in associations for individual size ranges. This may have been particularly relevant for the model with the ordinal interaction term with its limited data basis. As auxiliary information, the GIS analysis showed that the vast majority of municipalities' inhabitants lived within a 25 km radius of the central monitoring station.

(ii) DEPs have shown to be more toxic than UFP or PNC generally in terms of long-term effects, but as the evidence based on short-term toxicity remains relatively weak, other sources may cause UFPs that are relatively more toxic in the short-term. A limitation that may explain that particle size ranges with, relative to the assumed main DEP size ranges, smaller and larger particles showed partially higher mortality associations.

(iii) The selection of $PNC_{30\text{-}120}$ may not actually have included the majority of DEPs or at least the particularly toxic fraction of those DEP removed by DPFs installed to meet Euro-4 for whatever reason, e.g. particle size change over time and distance, or was dominated by other particles which rendered the changes in DEP concentrations irrelevant.

Few studies have performed source apportionments of UFPs, thus evidence for the proportion, spatial and temporal dynamics is relatively weak in comparison to larger PM (Li *et al.*, 2018b; Valverde & Giechaskiel, 2020). UFPs are known to generally be more dynamic in size and concentration over small distances and time periods than larger PM, however this concerns particularly the smallest UFPs within the nucleation range (0-30 nm). Overall, source apportionment for traffic has been rated inadequate by some (e.g. Pant & Harrison, 2013).

(iv) Short-term mortality may not be sensitive enough for the differences between PNC size ranges, possibly more imminent biomarkers, e.g. inflammation indicators, would have been more sensitive. Mortality causes are inherently at a higher risk of outcome misclassification than e.g. the measurement of inflammation markers.

(vi) The model may have missed to include or not adequately adjusted (e.g. not the right variable or measure) for critical confounders. Typical confounding variables for air pollution effects on human health like age or socio-economic status are estimated to remain constant over time, and thus should do not relevantly affect estimates. This may hold particularly for the models with respiratory mortality as an outcome due to the relatively lower validity of the model, likely linked with fewer mortality cases.

Finally, the misclassification risk for where persons resided (and were exposed) before death registration is considered less of an issue for study on short-term effects.

4.6.5 Limitations of effect modification models for traffic regulation accountability

For estimation of the effect modification over time by the change of UEZ regulation and/or the increase in DPF prevalence following additional, potential limitations are to be named:

(i) Changes in toxicity of diesel exhaust over time may have been too small for detection with our measurement setup and statistical model or hidden among changes in the toxicity or PNC proportion of other compounds or mixtures.

(ii) The two models to estimate effect modification may not have been able to detect the modification actually present: for the UEZ regulation, for example, due to the exemption of interstate traffic and wide-spread violations; for the DEP prevalence, for example, due to a misrepresentation of the actual traffic composition by the municipal vehicle registries.

(iii) The model smoothing terms (spline) and/or confounder adjustments (various) may have partly reduced the strength of an actual difference in association over time.

4.7 Public health relevance

4.7.1 Demand for epidemiological studies on UFP exposures

The health effects and relevance of UFPs (and PNCs) to date has not been as robustly quantified in contrast to more common AAP components like PM_{10}, $PM_{2.5}$ or selected gases. Epidemiological studies on UFP exposure and human health remain relatively few, particularly size-specific UFP studies are rare, among others due to data availability and measurement costs. The UBA recently assessed the current level of knowledge sufficient to call for UFP minimisation, but not for setting regulatory limit values (Wichmann-Fiebig, 2020), thus implicitly calling for further epidemiological evidence, as now provided by this dissertation and the peer-reviewed publication in preparation.

4.7.2 Demand for guidance on future monitoring requirements for UFP concentrations

As UFP data availability remains a key limitation for epidemiological studies, a logical first step towards improving the health relevance estimation of UFPs were monitoring requirements, as have been gradually introduced for other pollutants. To our knowledge, mandatory UFP monitoring has not been

introduced at the national level in any country. In anticipation of such requirements, latest upon introduction of limit values, our study strengthens the call for size-specific UFP and PNC measurements (i.e. also beyond 100 nm in particle size) at urban background stations, amongst other locations.

4.7.3 Informing future research on UFP exposure

This study, as have others, including those named in the introductory chapters, suggests that the health effect of UFP PNCs may vary substantially between size fractions and is not limited to PNCs of particles below 100 nm. The change in mortality association over time observed for the model with the dichotomous interaction term suggests a possible dependency of PNC RR on chemical, physical or biological composition and properties beyond size, likely attributable to respective sources. Although source apportionment remains complex, while requiring additional data, the study results raise the hypothesis that size ranges may not be the only dominant factor for UFP health effects.

The mortality associations for larger particle size ranges ($PNC_{120\text{-}250}$, $PNC_{250\text{-}500}$) in this study question the sensibility of limiting debate of PNC-associated health effects to particles smaller 100 nm, rather than defining the upper limit based on the biological logic, such as comparable biological logic, such as partially defined by the potential to cross blood, placenta or blood-brain barriers.

4.7.4 Contribution to research on policy effects for air pollution

The update of the WHO AQG to be published right upon completion of this study on 23.09.2021 is expected to draw attention to air quality interventions. Albeit a guideline value for UFP not being expected, changes in UFP concentrations and related mortality are one indicator for the success of interventions. The study overall included three of five stage in the accountability framework for AAP interventions by HEI (2003). Thereby this study assessed effect modification to approximate accountability for two key traffic-related AAP interventions and could identify possible effect modification by one of them. Traffic interventions, according to Burns *et al*. (2020), remain the dominant AAP interventions, motivating further investigations of its accountability.

4.8 Conclusions

This study indicates that short-term UFP and PNC exposure may increase the risk of NCM, CVM and RM. Observed associations differed substantially depending on PNC size range, while they were robust to adjustment to the two main co-pollutants PM_{10} and NO_2. Effect modification over time in relation to the UEZ banning of non-Euro-4-compliant vehicles indicates potential accountability of the UEZ regulation for human mortality, while the RR increases for larger particles and PM_{10} raise the question, which particle composition or source(s) this can be attributed to.

The study results add to the body of evidence on the health effects of size-differentiated PNC and on effect modification by time. The identified associations with substantial differences between PNC size-ranges call for more epidemiological studies on size-specific UFP and PNC exposures, ideally using datasets that facilitate additional adjustment for $PM_{2.5}$. The findings also motivate further research on traffic regulation accountability that may include: alternative effect modification models, PNC datasets with high temporal resolution and additional indicators to facilitate source apportionment, and outcome datasets allowing the comparison of mortality rates with, possibly more sensitive, biomarkers.

5. Literature

Abbas, I. *et al.* (2018) 'Polycyclic aromatic hydrocarbon derivatives in airborne particulate matter: sources, analysis and toxicity', *Environmental Chemistry Letters*. Springer International Publishing. doi: 10.1007/s10311-017-0697-0.

Agudelo-Castañeda, D. M. *et al.* (2019) 'Cluster analysis of urban ultrafine particles size distributions', *Atmospheric Pollution Research*. Elsevier B.V., 10(1), pp. 45–52. doi: 10.1016/j.apr.2018.06.006.

Ajdary, M. *et al*. (2018) 'Health Concerns of Various Nanoparticles: A Review of Their in Vitro and in Vivo Toxicity', *nanomaterials*, 8:9. doi: 10.3390/nano8090634.

Alfano, R. *et al.* (2018) 'The Impact of Air Pollution on Our Epigenome: How Far Is the Evidence? (A Systematic Review)', *Current Environmental Health Reports*, 5(4), pp. 544–578. doi: 10.1007/s40572-018-0218-8.

Ali, M. U. *et al.* (2019) 'A systematic review on global pollution status of particulate matter-associated potential toxic elements and health perspectives in urban environment', *Environmental Geochemistry and Health*. 41(3), pp. 1131–1162. doi: 10.1007/s10653-018-0203-z.

Ameral, S. S. *et al.* (2015) 'An Overview of Particulate Matter Measurement Instruments', *Atmoshpere*, 6(9). doi: 10.3390/atmos6091327.

Andersen, M. H. G. *et al.* (2019) 'Health effects of exposure to diesel exhaust in diesel-powered trains', *Particle and Fibre Toxicology*, 16(1), p. 21. doi: 10.1186/s12989-019-0306-4.

Anderson, H. R. (2009) 'Air pollution and mortality: a history', *Atmospheric Environment*, 43(1), p. 142-152. doi: 10.1016/j.atmosenv 08.09.026

Anenberg, S. C. *et al.* (2019) 'The global burden of transportation tailpipe emissions on air pollution-related mortality in 2010 and 2015', *Environmental Research Letters*. IOP Publishing, 14(9). doi: 10.1088/1748-9326/ab35fc.

ANSES (French agency for food, environmental and occupational health & safety) (2019) ' Particulate matter in ambient air. Health effects according to components, sources and particle size. Impact on air pollution of the technologies and composition of the motor vehicle fleet operating in France. Retrieved from: www.swisstph.ch/fileadmin/user_upload/SwissTPH/Institute/Ludok/Aktuelle_Berichte/ANSES2019_PM_HealthEffects.pdf (last accessed on 6 August 2021).

Asmi, A. *et al*. (2013) 'Aerosol decadal trends – Part 2: In-situ aerosol particle number concentrations at GAW and ACTRIS stations', Atmos. Chem. Phys, 13, p.895-916. doi: 10.5194/acp-13-895-2013.

Atkinson, R. W. *et al.* (2016) 'Short-term exposure to traffic-related air pollution and daily mortality in London, UK', *Journal of Exposure Science and Environmental Epidemiology*. Nature Publishing Group, 26(2), pp. 125–132. doi: 10.1038/jes.2015.65.

Austin, P. C. and Hux, J. E. (2002) 'A brief note on overlapping confidence intervals', *Journal of Vascular Surgey*, 36(1), p.194-5. doi: 10.1067/mva.2002.125015.

Babadjouni, R. M. *et al.* (2017) 'Clinical effects of air pollution on the central nervous system; a review', *Journal of Clinical Neuroscience*, 43, pp. 16–24. doi: 10.1016/j.jocn.2017.04.028.

Bates, J. T. *et al*. (2019) 'Review of Acellular Assays of Ambient Particulate Matter Oxidative Potential: Methods and Relationships with Composition, Sources, and Health Effects', *Environ. Sci. Technol*., 58:8, p. 4003-19. doi: 10.1021/acs.est.8b03430.

Beek, E. (van de) *et al.* (2020) 'Spatial and Spatiotemporal Variability of Regional Background Ultrafine Particle Concentrations in the Netherlands', *Environ. Sci. Technol*., 55(2), p. 1067-1075. doi: 10.1021/acs.est.0c06806.

Bell, M.L. & Davis, D.L. (2001) ' Reassessment of the lethal London fog of 1952: novel indicators of acute and chronic consequences of acute exposure to air pollution', *Environmental Health Perspectives*. doi: 10.1289/ehp.01109s3389.

Bell, M. L. *et al.* (2004) 'Time-Series Studies of Particulate Matter', *Annual Review of Public Health*, 25(1), pp. 247–280. doi: 10.1146/annurev.publhealth.25.102802.124329.

Benmarhnia, T. *et al.* (2014) ' Addressing equity in interventions to reduce air pollution in urban areas: a systematic review', International Journal of Public Health, 59: 933-944. doi: 10.1007/s00038-014-0608-0.

Bernal, J. L. *et al*. (2017) 'Interrupted time series regression for the evaluation of public health interventions: a tutorial', *Int J Epidemiology*, 46(1), p.348-355. doi: 10.1093/ije/dyaa118.

Bhaskaran, K. *et al.* (2013) 'Time series regression studies in environmental epidemiology', *International Journal of Epidemiology*, 42(4) p. 1187-1195. doi: 10.1093/ije/dyt092.

Birmili, W. *et al.* (2015) 'Long-term observations of tropospheric particle number size distributions and equivalent black carbon mass concentrations in the German Ultrafine Aerosol Network (GUAN)', *Earth System Science Data Discussions*, 8, p. 935-993. doi: 10.5194/essdd-8-935-2015.

Birmili, W. *et al.* (2016) 'Long-term observations of tropospheric particle number size distributions and equivalent black carbon mass concentrations in the German Ultrafine Aerosol Network (GUAN)', *Earth System Science Data*, 8(2), pp. 355–382. doi: 10.5194/essd-8-355-2016.

von Bismarck-Osten, C. *et al.* (2013) 'Characterization of parameters influencing the spatio-temporal variability of urban particle number size distributions in four European cities', Atmospheric Environment, 77, p. 415-429. doi: 10.1016/j.atmosenv.2013.05.029.

Boogaard, H. *at al*. (2017) 'Accountability Studies on Air Pollution and Health: the HEI Experience', *Current Environmental Health Reports*, p. 514-522. doi: 10.1007/s40572-017-0161-0.

Boogaard, H. *et al.* (2019) ' Air pollution: the emergence of a major global health risk factor', *International Health*, 11(6), p. 417-421. doi: 10.1093/inthealth/ihz078.

Braithwaite, I. *et al.* (2019) 'Air pollution (Particulate matter) exposure and associations with depression, anxiety, bipolar, psychosis and suicide risk: A systematic review and meta-analysis', *Environmental Health Perspectives*. ehp.niehs.nih.gov, 127(12). doi: 10.1289/EHP4595.

Burns, J *et al.* (2019) 'Interventions to reduce ambient particulate matter air pollution and their effect on health', *Cochrane Database of Systematic Reviews*, CD010919(5), pp. 1–243. doi: 10.1002/14651858.CD010919.pub2.

Burtscher, H. (2005) 'Physical characterization of particulate emissions from diesel engines: A review', *Journal of Aerosol Science*, 36(7), pp. 896–932. doi: 10.1016/j.jaerosci.2004.12.001.

Buseck, P. R. *et al.* (2012) 'Are black carbon and soot the same?', *Atmospheric Chemistry and Physics Discussions*, 12(9), pp. 24821–24846. doi: 10.5194/acpd-12-24821-2012.

Candelone, J-P. (1995) 'Post-Industrial Revolution changes in large-scale atmospheric pollution of the northern hemisphere by heavy metals as documented in central Greenland snow and ice', *Journal of Geophysical Research - Atmospheres*, 100(D8), p.16605-16616. doi: 10.1029/95JD00989.

Cardenas, A. *et al.* (2021) ‘Controlled human exposures to diesel exhaust: a human epigenome-wide experiment of target bronchial epithelial cells’, *Environmental Epigenetics*. Edited by J. Goodrich, 7(1). doi: 10.1093/eep/dvab003.

Chatain, M. *et al*. (2021) ' Simultaneous Roadside and Urban Background Measurements of Submicron Aerosol Number Concentration and Size Distribution (in the Range 20–800 nm), along with Chemical Composition in Strasbourg, France', *Atmosphere*, 12(1). doi: 10.3390/atmos12010071.

Chen, K. *et al*. (2018) 'Two-way effect modifications of air pollution and air temperature on total natural and cardiovascular mortality in eight European urban areas', *Environmental International*, 116:186-196. doi: 10.1016/j.envint.2018.04.021.

Chen, C. *et al.* (2021) ‘Increasing cardiopulmonary effects of ultrafine particles at relatively low fine particle concentrations’, *Science of the Total Environment*. Elsevier B.V., 751, pp. 1–11. doi: 10.1016/j.scitotenv.2020.141726.

Chen, K. *et al.* (2020) ‘Hourly exposure to ultrafine particle metrics and the onset of myocardial infarction in Augsburg, Germany’, *Environmental Health Perspectives*, 128(1), pp. 1–10. doi: 10.1289/EHP5478.

Chirico, R. *et al.* (2010) ‘Impact of aftertreatment devices on primary emissions and secondary organic aerosol formation potential from in-use diesel vehicles: results from smog chamber experiments’, *Atmospheric Chemistry and Physics Discussions*, 10(6), pp. 16055–16109. doi: 10.5194/acpd-10-16055-2010.

Chuang, Y. H. *et al.* (2011) ‘Generalized linear mixed models in time series studies of air pollution’, *Atmospheric Pollution Research*. Elsevier, 2(4), pp. 428–435. doi: 10.5094/APR.2011.049.

Cohen, A. J. *et al.* (2017) ‘Estimates and 25-year trends of the global burden of disease attributable to ambient air pollution: an analysis of data from the Global Burden of Diseases Study 2015’, *The Lancet*. The Author(s). Published by Elsevier Ltd. This is an Open Access article under the CC BY 4.0 license, 389(10082), pp. 1907–1918. doi: 10.1016/S0140-6736(17)30505-6.

Conforti, A. *et al.* (2018) ‘Air pollution and female fertility: a systematic review of literature’, *Reproductive Biology and Endocrinology*, 16(1), p. 117. doi: 10.1186/s12958-018-0433-z.

Cox, L. A. T. (2017) ‘Do causal concentration–response functions exist? A critical review of associational and causal relations between fine particulate matter and mortality’, *Critical Reviews in Toxicology,* 47(7), pp. 603–631. doi: 10.1080/10408444.2017.1311838.

Cyrys, J. *et al*. (2008) 'Spatial and temporal variation of particle number concentration in Augsburg, Germany', *Science of the Total Environment*, 401:1-3, p. 168-175. doi: 10.1016/j.scitotenv.2008.03.043.

Cyrys, J. *et al.* (2014) ‘Low emission zones reduce PM10 mass concentrations and diesel soot in German cities’, *Journal of the Air and Waste Management Association*. Taylor & Francis, 64(4), pp. 481–487. doi: 10.1080/10962247.2013.868380.

Cyrys, J. *et al.* (2018) ‘Low emission zones in Germany: A reliable measure for keeping current air quality standards?’, *Bundesgesundheitsblatt - Gesundheitsforschung - Gesundheitsschutz*, 61(6), pp. 645–655. doi: 10.1007/s00103-018-2741-z.

Daellenbach, K. R. *et al.* (2020) ‘Sources of particulate-matter air pollution and its oxidative potential in Europe’, *Nature*, 587(7834), pp. 414–419. doi: 10.1038/s41586-020-2902-8.

Dall’Osto, M. *et al.* (2011) ‘Remarkable dynamics of nanoparticles in the urban atmosphere’,

Atmospheric Chemistry and Physics, 11(13), pp. 6623–6637. doi: 10.5194/acp-11-6623-2011.

Daly, A. & Zannetti, P. (2007) 'Air Pollution Modeling – An Overview. Chapter 2 of AMBIENT AIR POLLUTION, *The Arab School for Science and Technology (ASST) and The EnviroComp Institute*. Retrieved from: home.iitk.ac.in/~anubha/Modeling.pdf (last accessed on 6 August 2021)

Dallmann, T. R. & Harley, R. A. (2010) 'Evaluation of mobile source emission trends in the United States', *Journal of Geophysical Research Atmospheres*, 115(14), pp. 1–12. doi: 10.1029/2010JD013862.

Deng, W. *et al.* (2017) 'Primary particulate emissions and secondary organic aerosol (SOA) formation from idling diesel vehicle exhaust in China', *Science of the Total Environment*, 593–594, pp. 462–469. doi: 10.1016/j.scitotenv.2017.03.088.

Di, Q. *et al.* (2017) 'Air pollution and mortality in the medicare population', *New England Journal of Medicine*, 376(26), pp. 2513–2522. doi: 10.1056/NEJMoa1702747.

Dias, D. *et al.* (2018) 'Spatial and Temporal Dynamics in Air Pollution Exposure Assessment' *International Journal of Environmental Research and Public Health*, 15(3), p. 558. doi: 10.3390/ijerph15030558.

Dominici, F. *et al.* (2002) ' On the Use of Generalized Additive Models in Time-Series Studies of Air Pollution and Health', *American Journal of Epidemiology,* 156 (3), p. 193-203. doi: 10.1093/aje/kwf062.

Dominici, F. (2004) ' Time-Series Analysis of Air Pollution and Mortality: A Statistical Review', *Health Effects Institute Research Report*, 123. Retrieved from: www.healtheffects.org/publication/time-series-analysis-air-pollution-and-mortality-statistical-review (last accessed on 6 August 2021).

Downward, G. S. *et al.* (2018) 'Long-Term Exposure to Ultrafine Particles and Incidence of Cardiovascular and Cerebrovascular Disease in a Prospective Study of a Dutch Cohort', Environmental Health Perspectives, 126 (12). doi: 10.1289/EHP3047.

EEA (European Environment Agency) (2020a) 'Air quality in Europe - 2020 report'. ISSN 1977-8449. Retrieved from: www.eea.europa.eu/publications/air-quality-in-europe-2020-report (last accessed on 6 August 2021).

EEA (2020b) 'Air pollution country factsheet for Germany'. Retrieved from: www.eea.europa.eu/themes/air/country-fact-sheets/2020-country-fact-sheets/germany (last accessed on 6 August 2021).

EEC (European Economic Community) (1970): 'Council Directive 70/220/EEC of 20 March 1970 on the approximation of the laws of the Member States relating to measures to be taken against air pollution by gases from positive-ignition engines of motor vehicles'. Retrieved from: eur-lex.europa.eu/legal-content/EN/TXT/HTML/?uri=CELEX:31970L0220&from=DE (last accessed on 6 August 2021).

EEC (1991): 'Council Directive 91/441/EEC of 26 June 1991 amending Directive 70/220/EEC on the approximation of the laws of the Member States relating to measures to be taken against air pollution by emissions from motor vehicles '. Retrieved from: eur-lex.europa.eu/legal-content/EN/TXT/HTML/?uri=CELEX:31991L0441&from=en (last accessed on 6 August 2021).

Farina, F. *et al.* (2019) 'In Vivo Comparative Study on Acute and Sub-acute Biological Effects Induced by Ultrafine Particles of Different Anthropogenic Sources in BALB/c Mice', *International Journal of Molecular Sciences*, 20(11), p. 2805. doi: 10.3390/ijms20112805.

Fiordelisi, A. *et al.* (2017) 'The mechanisms of air pollution and particulate matter in cardiovascular diseases', *Heart Failure Reviews*, 22(3), pp. 337–347. doi: 10.1007/s10741-017-9606-7.

Fontaras, G. *et al.* (2014) 'Development and review of Euro 5 passenger car emission factors based on experimental results over various driving cycles', *Science of the Total Environment*. The Authors, 468–469(2014), pp. 1034–1042. doi: 10.1016/j.scitotenv.2013.09.043.

Fujitani, Y. *et al.* (2020) 'Particle number emission factors from diesel trucks at a traffic intersection: Long-term trend and relation to particle mass-based emission regulation', *Atmospheric Environment: X*. Elsevier Ltd, 5, p. 100055. doi: 10.1016/j.aeaoa.2019.100055.

Global Health Metrics (2018) 'Global, regional, and national comparative risk assessment of 84 behavioural, environmental and occupational, and metabolic risks or clusters of risks for 195 countries and territories, 1990 – 2017: a systematic analysis for the Global Burden of Disease', *Lancet*, pp. 1990–2017. doi: 10.1016/S0140-6736(18)32225-6.

Giechaskiel, B. *et al*. (2013) 'Review of motor vehicle particulate emissions sampling and measurement: From smoke and filter mass to particle number', *Journal of Aerosol Science*, 67, p. 48-86. doi: 10.1016/j.jaerosci.2013.09.003.

Giechaskiel, B. *et al.* (2019) 'European regulatory framework and particulate matter emissions of gasoline light-duty vehicles: A review', *Catalysts*, 9(7). doi: 10.3390/catal9070586.

Giemsa, E. *et al.* (2021) 'Influence of Local Sources and Meteorological Parameters on the Spatial and Temporal Distribution of Ultrafine Particles in Augsburg, Germany', *Front. Environ. Sci*, 8:609846. doi: 10.3389/fenvs.2020.609846.

Giles, L. V. et al. (2011) 'From Good Intentions to Proven Interventions: Effectiveness of Actions to Reduce the Health Impacts of Air Pollution', *Environmental Health Perspectives*, 199/1. doi: 10.1289/ehp.1002246.

Grant and Booth (2009) 'A typology of reviews: an analysis of 14 review types and associated methodologies', *Health Information and Libraries Journal*, 26(2). doi: 10.1111/j.1471-1842.2009.00848.x.

Gross, M. & Sonnberger, M. (2020) 'How the diesel engine became a "dirty" actant: Compression ignitions and actor networks of blame', *Energy Research & Social Science*, 61, p. 101359. doi: 10.1016/j.erss.2019.101359.

Guo, Y. *et al.* (2019) 'An experimental study of the role of biodiesel on the performance of diesel particulate filters', *Fuel*. Elsevier, 247(March), pp. 67–76. doi: 10.1016/j.fuel.2019.03.042.

Habre, R. *et al.* (2018) 'Short-term effects of airport-associated ultrafine particle exposure on lung function and inflammation in adults with asthma', *Environment International*, 118(May), pp. 48–59. doi: 10.1016/j.envint.2018.05.031.

Hachem, M. *et al.* (2020) 'Short-term association of in-vehicle ultrafine particles and black carbon concentrations with respiratory health in Parisian taxi drivers', *Environmentl International*, 147. doi: 10.1016/j.envint.2020.106346.

Hadrup, N. *et al.* (2020) 'Acute Phase Response as a Biological Mechanism-of-Action of (Nano)particle-Induced Cardiovascular Disease', *Small*, 16(21), p. 1907476. doi: 10.1002/smll.201907476.

Hamanaka, R. B. & Mutlu, G. M. (2018) 'Particulate Matter Air Pollution: Effects on the Cardiovascular System', *Frontiers in Endocrinology*, 9. doi: 10.3389/fendo.2018.00680.

Harrison, R. M. *et al.* (2018) 'Diesel exhaust nanoparticles and their behaviour in the atmosphere', *Proceedings of the Royal Society A: Mathematical, Physical and Engineering Sciences*, 474(2220). doi: 10.1098/rspa.2018.0492.

HEI (Health Effects Institute) (2003) 'Assessing Health Impact of Air Quality Regulations: Concepts and Methods for Accountability Research', *Health Effect Institute*. Retrieved from: www.healtheffects.org/system/files/Comm11ExecSumm.pdf

HEI Review Panel (2013) 'Understanding the Health Effects of Ambient Ultrafine Particles', *Health Effect Institute*. Retrieved from: pubs.healtheffects.org/view.php?id=394 (last accessed on 6 August 2021).

Hennig, F. *et al.* (2018) 'Ultrafine and fine particle number and surface area concentrations and daily cause-specific mortality in the Ruhr area, Germany, 2009–2014', *Environmental Health Perspectives*, 126(2). doi: 10.1289/EHP2054.

Héroux, ME. *et al.* (2015) 'Quantifying the health impacts of ambient air pollutants: recommendations of a WHO/Europe project', *International Journal of Public Health,* 60, 619–627. doi: 10.1007/s00038-015-0690-y.

Hilker, N. *et al.* (2021) 'Elucidating long-term trends, seasonal variability, and local impacts from thirteen years of near-road particle size data (2006–2019)', *Science of the Total Environment*, 774. doi: 10.1016/j.scitotenv.2021.145028.

Hime, N. *et al.* (2018) 'A Comparison of the Health Effects of Ambient Particulate Matter Air Pollution from Five Emission Sources', *International Journal of Environmental Research and Public Health*, 15(6), p. 1206. doi: 10.3390/ijerph15061206.

Hoffmann, B. *et al.* (2020) ' Air pollution and health: recent advances in air pollution epidemiology to inform the European Green Deal: a joint workshop report of ERS, WHO, ISEE and HEI', *European Respiratory Journal*, 56 (5). doi: 10.1183/13993003.02575-2020.

Huang, C. *et al.* (2013) 'A PEMS study of the emissions of gaseous pollutants and ultrafine particles from gasoline- and diesel-fueled vehicles', *Atmospheric Environment*. Elsevier Ltd, 77, pp. 703–710. doi: 10.1016/j.atmosenv.2013.05.059.

Hulkonnen, M. *et al*. (2020) ' The atmospheric impacts of initiatives advancing shifts towards low-emission mobility: A scoping review', *Science of the Total Environment,* 713. doi: 10.1016/j.scitotenv.2019.136133.

Ikenna, C. E. *et al*. (2015) ' Association between Ambient Air Pollution and Diabetes Mellitus in Europe and North America: Systematic Review and Meta-Analysis', Environmental Health Perspectives, 123:5. doi: 10.1289/ehp.1307823.

Institute for Health Metrics and Evaluation (IHME) (2019) 'Global Burden of Disease'. Retrieved from: ghdx.healthdata.org/gbd-results-tool?params=gbd-api-2019-permalink/45cdfe7d64a57471af4ba2c96dbf5617 (last accessed on 6 August 2021).

Jacobs, M. *et al.* (2017) 'The association between ambient air pollution and selected adverse pregnancy outcomes in China: A systematic review', *Science of The Total Environment*, 579, pp. 1179–1192. doi: 10.1016/j.scitotenv.2016.11.100.

Jathar, S. H. *et al.* (2017) 'Linking Load, Fuel, and Emission Controls to Photochemical Production of Secondary Organic Aerosol from a Diesel Engine', *Environmental Science and Technology*, 51(3), pp. 1377–1386. doi: 10.1021/acs.est.6b04602.

Jeong, C. H. *et al.* (2019) 'Temporal and spatial variability of traffic-related PM2.5 sources: Comparison of exhaust and non-exhaust emissions', *Atmospheric Environment*. Elsevier, 198(October 2018), pp. 55–69. doi: 10.1016/j.atmosenv.2018.10.038.

Jerrett, M. *et al.* (2005) 'A review and evaluation of intraurban air pollution exposure models', *Journal of Exposure Science & Environmental Epidemiology*, 15(2), pp. 185–204. doi: 10.1038/sj.jea.7500388.

de Jesus, A. L. *et al*. (2020) ' Long-term trends in PM2.5 mass and particle number concentrations in urban air: The impacts of mitigation measures and extreme events due to changing climates', Environmental Pollution, 263:A. doi: 10.1016/j.envpol.2020.114500.

Karagulian, F. *et al.* (2015) 'Contributions to cities' ambient particulate matter (PM): A systematic review of local source contributions at global level', *Atmospheric Environment*. Elsevier Ltd, 120, pp. 475–483. doi: 10.1016/j.atmosenv.2015.08.087.

Karagulian, F. *et al.* (2019) 'Review of the Performance of Low-Cost Sensors for Air Quality Monitoring', *Atmosphere*, 10(9), p. 506. doi: 10.3390/atmos10090506.

Karjalainen, P. *et al.* (2019) 'Strategies to Diminish the Emissions of Particles and Secondary Aerosol Formation from Diesel Engines', *Environmental Science and Technology*, 53(17), pp. 10408–10416. doi: 10.1021/acs.est.9b04073.

Kelly, F. J. & Fussell, J. C. (2020) 'Toxicity of airborne particles—established evidence, knowledge gaps and emerging areas of importance', *Philosophical Transactions of the Royal Society A: Mathematical, Physical and Engineering Sciences*, 378(2183), p. 20190322. doi: 10.1098/rsta.2019.0322.

Keskinen, J. & Rönkkö, T. (2010) 'Can real-world diesel exhaust particle size distribution be reproduced in the laboratory? A critical review', *Journal of the Air and Waste Management Association*, 60(10), pp. 1245–1255. doi: 10.3155/1047-3289.60.10.1245.

Khan, J. *et al.* (2018) 'Road traffic air and noise pollution exposure assessment – A review of tools and techniques', *Science of the Total Environment*. Elsevier, 634, pp. 661–676. doi: 10.1016/j.scitotenv.2018.03.374.

de Kok, T. M. C. M. *et al.* (2006) 'Toxicological assessment of ambient and traffic-related particulate matter: A review of recent studies', *Mutation Research/Reviews in Mutation Research*, 613(2–3), pp. 103–122. doi: 10.1016/j.mrrev.2006.07.001.

Kim, H. *et al.* (2021) 'Alternative adjustment for seasonality and long-term time-trend in time-series analysis for long-term environmental exposures and disease counts', *BMC Medical Research Methodology*, 21:2. doi: 10.1186/s12874-020-01199-1.

Kontses, A. *et al*. (2019) ' Effects of fuel properties on particulate emissions of diesel cars equipped with diesel particulate filters', *Fuel*, 255. doi: 10.1016/j.fuel.2019.115879.

Koolen, C. D. & Rothenberg, G. (2019) 'Air Pollution in Europe', *ChemSusChem*, 12(1), pp. 164–172. doi: 10.1002/cssc.201802292.

Kraftfahrt-Bundesamt (KBA) (2021) 'Motor vehicle statistics'. Retrieved from: www.kba.de/DE/Statistik/Fahrzeuge/fahrzeuge_node.html;jsessionid=2850A377AE08CA32A60D4E15506B5B2A.live21322 (last accessed on 6 August 2021).

Krecl, P. *et al.* (2020) 'Cyclists' exposure to air pollution under different traffic management strategies', *Science of the Total Environment*,723:138043. doi: 10.1016/j.scitotenv.2020.138043.

Krivoshto, I. N. *et al.* (2008) 'The toxicity of diesel exhaust: Implications for primary care', *Journal of the American Board of Family Medicine*, 21(1), pp. 55–62. doi: 10.3122/jabfm.2008.01.070139.

Kumar, P. *et al.* (2013b) 'Nanoparticle emissions from 11 non-vehicle exhaust sourcese - A review', Atmospheric Environment, 67:252-277, doi: 10.1016/j.atmosenv.2012.11.011.

Kumar, P. *et al.* (2014) 'Ultrafine particles in cities', *Environment International*, 66, pp. 1–10. doi: 10.1016/j.envint.2014.01.013.

Kumar, S. *et al*. (2013a) 'Ultrafine particles in urban ambient air and their health perspectives', *Reviews on Environmental Health*, 28(2–3), pp. 117–128. doi: 10.1515/reveh-2013-0008.

Kwak, J. H. *et al.* (2013) 'Characterization of non-exhaust coarse and fine particles from on-road driving and laboratory measurements', *Science of the Total Environment*. Elsevier B.V., 458–460, pp. 273–282. doi: 10.1016/j.scitotenv.2013.04.040.

Kwon, H. S. *et al.* (2020) 'Ultrafine particles: unique physicochemical properties relevant to health and disease', *Experimental and Molecular Medicine*. Springer US, 52(3), pp. 318–328. doi: 10.1038/s12276-020-0405-1.

Kyung, S. Y. *et al.* (2020) 'Particular-matter related respiratory diseases', *Tubercolosis and Respiratory Diseases*, 83(2), p. 116-121. doi: 10.4046/trd.2019.0025.

Lammers, A. *et al.* (2020) 'Effects of short-term exposures to ultrafine particles near an airport in healthy subjects', *Environment International*, 141, p. 105779. doi: 10.1016/j.envint.2020.105779.

Lanzinger, S. *et al.* (2015) ' Associations between ultrafine and fine particles and mortality in five central European cities - Results from the UFIREG study', *Environment International,* 88, p. 44-52. doi: 10.1016/j.envint.2015.12.006.

Lanzinger, S. *et al.* (2016) ' Ultrafine and Fine Particles and Hospital Admissions in Central Europe, Results from the UFIREG Study', *American Journal of Respiratory and Critical Care Medicine*, 194(10). doi: 10.1164/rccm.201510-2042OC.

Lee, K. K. *et al.* (2018) 'Air Pollution and Stroke', *Journal of Stroke*, 20(1), pp. 2–11. doi: 10.5853/jos.2017.02894.

Leikauf, G. D. *et al.* (2020) 'Mechanisms of ultrafine particle-induced respiratory health effects', *Experimental & Molecular Medicine*, 52(3), pp. 329–337. doi: 10.1038/s12276-020-0394-0.

Lelieveld, J. *et al.* (2019) 'Cardiovascular disease burden from ambient air pollution in Europe reassessed using novel hazard ratio functions', *European Heart Journal*, 40(20), pp. 1590–1596. doi: 10.1093/eurheartj/ehz135.

Li, F. *et al.* (2018a) 'Organic speciation of ambient quasi-ultrafine particulate matter (PM0.36) in Augsburg, Germany: Seasonal variability and source apportionment', *Science of the Total Environment*. Elsevier B.V., 615, pp. 828–837. doi: 10.1016/j.scitotenv.2017.09.158.

Li, F. *et al.* (2018b) 'Spatial and temporal variation of sources contributing to quasi-ultrafine particulate matter PM0.36 in Augsburg, Germany', *Science of the Total Environment*. Elsevier B.V., 631–632, pp. 191–200. doi: 10.1016/j.scitotenv.2018.03.041.

Liu, C. *et al.* (2019) 'Ambient Particulate Air Pollution and Daily Mortality in 652 Cities', The New England Journal of Medicine', 381:8, p. 705-715. doi: 10.1056/NEJMoa1817364.

Liu, F. *et al.* (2019) 'Associations between long-term exposure to ambient air pollution and risk of

type 2 diabetes mellitus: A systematic review and meta-analysis', *Environmental Pollution*, 252, pp. 1235–1245. doi: 10.1016/j.envpol.2019.06.033.

Longhin, E. *et al.* (2016) 'Physico-chemical properties and biological effects of diesel and biomass particles', *Environmental Pollution*, 215, pp. 366–375. doi: 10.1016/j.envpol.2016.05.015.

Longhin, E. M. *et al.* (2020) 'Fifteen Years of Airborne Particulates in Vitro Toxicology in Milano: Lessons and Perspectives Learned', *International Journal of Molecular Sciences*, 21(7), p. 2489. doi: 10.3390/ijms21072489.

Ma, N. and Birmili, W. (2015) 'Estimating the contribution of photochemical particle formation to ultrafine particle number averages in an urban atmosphere', *Science of the Total Environment*, 512–513, pp. 154–166. doi: 10.1016/j.scitotenv.2015.01.009.

Maag, B. *et al.* (2018) 'A Survey on Sensor Calibration in Air Pollution Monitoring Deployments', *IEEE Internet of Things Journal*, 5(6), pp. 4857–4870. doi: 10.1109/JIOT.2018.2853660.

Manoli, E. *et al.* (2016) 'Polycyclic aromatic hydrocarbons (PAHs) at traffic and urban background sites of northern Greece: source apportionment of ambient PAH levels and PAH-induced lung cancer risk', *Environmental Science and Pollution Research*, 23(4), pp. 3556–3568. doi: 10.1007/s11356-015-5573-5.

Markham, A. C. (1994) 'A Brief History of Pollution', *Routledge*, 1st edition. doi: 10.4324/9780429344879.

Martos, F. J. *et al.* (2020) 'Modelling of particle size distributions produced by a Diesel engine fueled with different fossil and renewable fuels under like urban and extra-urban operating conditions', *Fuel*. Elsevier, 263(September 2019), p. 116730. doi: 10.1016/j.fuel.2019.116730.

Mathissen, M. *et al.* (2011) 'Investigation on the potential generation of ultrafine particles from the tire-road interface', *Atmospheric Environment*. Elsevier Ltd, 45(34), pp. 6172–6179. doi: 10.1016/j.atmosenv.2011.08.032.

Mehus, A. A. *et al.* (2015) 'Comparison of Acute Health Effects from Exposures to Diesel and Biodiesel Fuel Emissions', *Journal of Occupational and Environmental Medicine*, 57(7), pp. 705–712. doi: 10.1097/JOM.0000000000000473.

Meng, X. *et al*. (2013) 'Size-fractionated particle number concentrations and daily mortality in a Chinese city', *Environmental Health Perspective*s, 121:1174–1178. doi: 10.1289/ehp.1206398.

Mills, N. L. *et al.* (2011) 'Combustion-derived nanoparticulate induces the adverse vascular effects of diesel exhaust inhalation', *European Heart Journal*, 32(21), pp. 2660–2671. doi: 10.1093/eurheartj/ehr195.

Mohankumar, S. & Senthilkumar, P. (2017) 'Particulate matter formation and its control methodologies for diesel engine: A comprehensive review', *Renewable and Sustainable Energy Reviews*. Elsevier Ltd, 80(May), pp. 1227–1238. doi: 10.1016/j.rser.2017.05.133.

Moldonová, J. *et al.* (2009) 'Characterisation of particulate matter and gaseous emissions froma large ship diesel engine', *Atmospheric Environment*, 43, p. 2632-2641. doi: 10.1016/j.atmosenv.2009.02.008.

Morwaska, L. *et al.* (2017) 'Airborne particles in indoor environment of homes, schools, offices and aged care facilities: The main routes of exposure', *Environment International*, 108: 75–83. doi: 10.1016/j.envint.2017.07.025.

IARC (International Agency for Research on Cancer) (2014) 'Diesel and Gasoline Engine Exhausts and Some Nitroarenes. Iarc Monographs on the Evaluation of Carcinogenic Risks To Humans', *IARC monographs on the evaluation of carcinogenic risks to humans / World Health Organization, International Agency for Research on Cancer*, 105, pp. 9–699.

Mosley S. (2014) Environmental History of Air Pollution and Protection. In: Agnoletti M., Neri Serneri S. (eds) The Basic Environmental History. Environmental History, vol 4. Springer, Cham. doi: 10.1007/978-3-319-09180-8_5.

Moreno-Rios, A. *et al.* (2021) 'Sources, characteristics, toxicity, and control of ultrafine particles: An overview', *Geoscience Frontiers*. doi: 10.1016/j.gsf.2021.101147

Mudway, *et al.* (2020) 'Oxidative stress in air pollution research', *Free Radical Biology and Medicine*, 151, pp. 2–6. doi: 10.1016/j.freeradbiomed.2020.04.031.

Müller, J. O. *et al.* (2006) 'Diesel engine exhaust emission: Oxidative behavior and microstructure of black smoke soot particulate', *Environmental Science and Technology*, 40(4), pp. 1231–1236. doi: 10.1021/es0512069.

Nikolova, I. *et al.* (2018) 'The influence of particle composition upon the evolution of urban ultrafine diesel particles on the neighbourhood scale', *Atmospheric Chemistry and Physics*, 18(23), pp. 17143–17155. doi: 10.5194/acp-18-17143-2018.

Nováková, Z. *et al.* (2020) 'Toxic potentials of particulate and gaseous air pollutant mixtures and the role of PAHs and their derivatives', *Environment International*, 139, p. 105634. doi: 10.1016/j.envint.2020.105634.

Núria, S. *et al.* (2020) 'How do ultrafine particles in urban air affect ambulatory blood pressure?', *Journal of Hypertension*, 38:5, p. 845-849. doi: 10.1097/HJH.0000000000002343.

Ohlwein, S. *et al.* (2019) 'Health effects of ultrafine particles: a systematic literature review update of epidemiological evidence', *International Journal of Public Health*, 64(4), pp. 547–559. doi: 10.1007/s00038-019-01202-7.

Orellano, P. *et al.* (2017) 'Effect of outdoor air pollution on asthma exacerbations in children and adults: Systematic review and multilevel meta-analysis', *PLOS ONE*. Edited by Q. Sun, 12(3), p. e0174050. doi: 10.1371/journal.pone.0174050.

Øvrevik, J. (2019) 'Oxidative potential versus biological effects: A review on the relevance of cell-free/abiotic assays as predictors of toxicity from airborne particulate matter', *International Journal of Molecular Sciences*. MDPI AG, 20(19). doi: 10.3390/ijms20194772.

Pan, A. *et al*. (2018) 'Time-Series Analysis of Air Pollution and Health Accounting for Covariate-Dependent Overdispersion', *American Journal of Epidemiology*, 187:12, p. 2698–2704. doi: 10.1093/aje/kwy170.

Pant, P. & Harrison, R. M. (2013) 'Estimation of the contribution of road traffic emissions to particulate matter concentrations from field measurements: A review', *Atmospheric Environment*. Elsevier Ltd, 77, pp. 78–97. doi: 10.1016/j.atmosenv.2013.04.028.

Park, M. *et al.* (2018) 'Differential toxicities of fine particulate matters from various sources', *Scientific Reports*, 8(1), pp. 1–11. doi: 10.1038/s41598-018-35398-0.

Peters, R. *et al.* (2019) 'Air Pollution and Dementia: A Systematic Review', *Journal of Alzheimer's Disease*. Edited by K. Anstey and R. Peters, 70(s1), pp. S145–S163. doi: 10.3233/JAD-180631.

Platt, S. M. *et al.* (2017) ‘Gasoline cars produce more carbonaceous particulate matter than modern filter-equipped diesel cars’, *Scientific Reports*, 7(1), pp. 1–9. doi: 10.1038/s41598-017-03714-9.

de Prado Bert, P. *et al.* (2018) ‘The Effects of Air Pollution on the Brain: a Review of Studies Interfacing Environmental Epidemiology and Neuroimaging’, *Current Environmental Health Reports*, 5(3), pp. 351–364. doi: 10.1007/s40572-018-0209-9.

Pries, L. & Wäcken, N. (2020) ‘The 2015 Volkswagen “Diesel-Gate” and Its Impact on German Carmakers’, *New Frontiers of the Automobile Industry*, pp. 89–111. doi: 10.1007/978-3-030-18881-8_4.

Quadir, R. M. *et al.* (2013) 'Concentrations and source contributions of particulate organic matter before and after implementation of a low emission zone in Munich, Germany', *Environmental Pollution*, 175, p.158-167. doi: 10.1016/j.envpol.2013.01.002.

Rajagopalan, S. *et al.* (2018) 'Air Pollution and Cardiovascular Disease: JACC State-of-the-Art Review', *Journal of the American College of Cariology*, 72(17) p. 2054-2070. doi: 10.1016/j.jacc.2018.07.099.

Rakowska, A. *et al*. (2014) 'Impact of traffic volume and composition on the air quality and pedestrian exposure in urban street canyon', *Atmospheric Environment*, 98, p. 260-270. doi: 10.1016/j.atmosenv.2014.08.073.

Rankin, G. D. *et al.* (2021) ‘Acute Exposure to Diesel Exhaust Increases Muscle Sympathetic Nerve Activity in Humans’, *Journal of the American Heart Association*, 10(10). doi: 10.1161/JAHA.120.018448.

Ravindra, K. *et al.* (2019) ‘Generalized additive models: Building evidence of air pollution, climate change and human health’, *Environment International*, 132, p. 104987. doi: 10.1016/j.envint.2019.104987.

Reijnders, J. *et al.* (2018) ‘Particle nucleation-accumulation mode trade-off: A second diesel dilemma?’, *Journal of Aerosol Science*. Elsevier Ltd, 124(June), pp. 95–111. doi: 10.1016/j.jaerosci.2018.06.013.

Readelli, M *et al*. (2019) 'Health effects of ambient black carbon and ultrafine particles: review and integration of the epidemiological evidence', Environmental Epidemiology, 3, p. 347-348. doi: 10.1097/01.EE9.0000609832.55044.74.

Renzi, M. *et al.* (2017) 'Analysis of Temporal Variability in the Short-term Effects of Ambient Air Pollutants on Nonaccidental Mortality in Rome, Italy (1998–2014)', *Environmental Health Perspectives*, 125:6. doi: 10.1289/EHP19.

Reşitoɪlu, I. A. *et al.* (2015) ‘The pollutant emissions from diesel-engine vehicles and exhaust aftertreatment systems’, *Clean Technologies and Environmental Policy*, 17(1), pp. 15–27. doi: 10.1007/s10098-014-0793-9.

Riedl, M. & Diaz-Sanchez, D. (2005) ‘Biology of diesel exhaust effects on respiratory function’, *Journal of Allergy and Clinical Immunology*, 115(2), pp. 221–228. doi: 10.1016/j.jaci.2004.11.047.

Ris, C. (2007) ‘U.S. EPA Health assessment for diesel engine exhaust: A review’, *Inhalation Toxicology*, 19(SUPPL. 1), pp. 229–239. doi: 10.1080/08958370701497960.

Rivas, I. *et al.* (2020) ‘Source apportionment of particle number size distribution in urban background and traffic stations in four European cities’, *Environment international*. Elsevier, 135(November 2019), p. 105345. doi: 10.1016/j.envint.2019.105345.

Rizza, V. *et al.* (2019) 'Effects of the exposure to ultrafine particles on heart rate in a healthy population', *Science of the Total Environment*. Elsevier B.V., 650, pp. 2403–2410. doi: 10.1016/j.scitotenv.2018.09.385.

RKI (Robert-Koch Institute) (2020) 'Infektionsepidemiologische Jahrbücher meldepflichtiger Krankheiten'. Retrieved from: www.rki.de/jahrbuch (last accessed on: 6 August 2021).

Robertson, S. & Miller, M. R. (2018) 'Ambient air pollution and thrombosis', *Particle and Fibre Toxicology*, 15(1), p. 1. doi: 10.1186/s12989-017-0237-x.

Rönkkö, T. & Timonen, H. (2019) 'Overview of Sources and Characteristics of Nanoparticles in Urban Traffic-Influenced Areas', *Journal of Alzheimer's Disease*, 72(1), pp. 15–28. doi: 10.3233/JAD-190170.

Rückerl, R. *et al*. (2011) 'Health effects of particulate air pollution: a review of epidemiological evidence', Inhalation Toxicology, 23:555-92. doi: 10.3109/08958378.2011.593587.

Sagai, M. *et al*. (1993) 'Biological effects of diesel exhaust particles. I. in vitro production of superoxide and in vivo toxicity in mouse', Free Radical Biology and Medicine, 14:1, p. 37-47. doi: 10.1016/0891-5849(93)90507-Q.

Saha, P. K. *et al.* (2019) 'Quantifying high-resolution spatial variations and local source impacts of urban ultrafine particle concentrations', *Science of the Total Environment*. Elsevier B.V., 655, pp. 473–481. doi: 10.1016/j.scitotenv.2018.11.197.

Salvi, S. *et al.* (1997) 'Acute Inflammatory Responses in the Airways and Peripheral Blood After Short-Term Exposure to Diesel Exhaust in Healthy Human Volunteers', *American Journal of Respiratory and Critical Care Medicine*, 159(3). doi: 10.1164/ajrccm.159.3.9709083

Samoli, E. *et al.* (2016) 'Exposure to ultrafine particles and respiratory hospitalisations in five European cities', *European Respiratory Journal*, 48(3), pp. 674–682. doi: 10.1183/13993003.02108-2015.

Samoli, E. *et al.* (2020) 'Meta-analysis on short-term exposure to ambient ultrafine particles and respiratory morbidity', *European Respiratory Review*, 29(158), p. 200116. doi: 10.1183/16000617.0116-2020.

Sanchez, K.A. *et al.* (2020) 'Urban policy interventions to reduce traffic emissions and traffic-related air pollution: Protocol for a systematic evidence map', *Environment International*, 142:105826. doi: 10.1016/j.envint.2020.105826.

Schraufnagel, D. E. (2020) 'The health effects of ultrafine particles', *Experimental & Molecular Medicine*, 52(3), pp. 311–317. doi: 10.1038/s12276-020-0403-3.

Shin, J. *et al.* (2021) 'Effect of Short-Term Exposure to Fine Particulate Matter and Temperature on Acute Myocardial Infarction in Korea', *International Journal of Environmental Research and Public Health*, 18(9), p. 4822. doi: 10.3390/ijerph18094822.

Shirmohammadi, F. *et al.* (2016) 'Fine and ultrafine particulate organic carbon in the Los Angeles basin: Trends in sources and composition', *Science of the Total Environment*, 541, pp. 1083–1096. doi: 10.1016/j.scitotenv.2015.09.133.

Sicard, P. *et al.* (2021) 'Urban population exposure to air pollution in Europe over the last decades', *Environmental Sciences Europe*, 33(1), p. 28. doi: 10.1186/s12302-020-00450-2.

da Silveira Fleck, A. *et al.* (2020) 'Characterization and Quantification of Ultrafine Particles and Carbonaceous Components from Occupational Exposures to Diesel Particulate Matter in Selected

Workplaces', *Annals of Work Exposures and Health*, 64(5), pp. 490–502. doi: 10.1093/annweh/wxaa027.

Silverman, D. T. *et al.* (2012) 'The Diesel Exhaust in Miners Study: A Nested Case-Control Study of Lung Cancer and Diesel Exhaust', *JNCI Journal of the National Cancer Institute*, 104(11), pp. 855–868. doi: 10.1093/jnci/djs034.

Soldevila, N. *et al.* (2020) 'How do ultrafine particles in urban air affect ambulatory blood pressure?', Journal of Hypertension, 38:5, p. 845-849. doi: 10.1097/HJH.0000000000002343.

Soppa, V. J. *et al*. (2019) ' Effects of short-term exposure to fine and ultrafine particles from indoor sources on arterial stiffness - A randomized sham-controlled exposure study', *Int. K. Hyg. Environ. Health*, 228(8), p. 1115-1132. doi: 10.1016/j.ijheh.2019.08.002

Stafoggia, M. *et al.* (2017) ' Association Between Short-term Exposure to Ultrafine Particles and Mortality in Eight European Urban Areas', *Epidemiology*, 28 (2). doi: 10.1097/EDE.0000000000000599.

Steiner, S. *et al.* (2016) 'Diesel exhaust: current knowledge of adverse effects and underlying cellular mechanisms', *Archives of Toxicology*. Springer Berlin Heidelberg, 90(7), pp. 1541–1553. doi: 10.1007/s00204-016-1736-5.

Stölzel, M. *et al*. (2006) ' Daily mortality and particulate matter in different size classes in Erfurt, Germany', *Journal of Exposure Science & Environmental Epidemiology,* 17, p. 458–467. doi: 10.1038/sj.jes.7500538.

Su, D. S. *et al.* (2004) 'Fullerene-like soot from EuroIV diesel engine: Consequences for catalytic automotive pollution control', *Topics in Catalysis*, 30–31(July), pp. 241–246. doi: 10.1023/b:toca.0000029756.50941.02.

Su, C. *et al*. (2015) ' Assessing responses of cardiovascular mortality to particulate matter air pollution for pre-, during- and post-2008 Olympics period', Environmental Research, 142, p. 112-122. doi: 1 0.1016/j.envres.2015.06.025.

Sun, J. *et al.* (2020) ' Decreasing trends of particle number and black carbon mass concentrations at 16 observational sites in Germany from 2009 to 2018', Atmospheric Chemistry and Physics, 20, p. 7049-7068. doi: 10.5194/acp-20-7049-2020.

Sun, Z. & Zhu, D. (2019a) 'Exposure to outdoor air pollution and its human-related health outcomes: An evidence gap map', *BMJ Open*, 9(12), pp. 1–18. doi: 10.1136/bmjopen-2019-031312.

Sun, Z. & Zhu, D. (2019b) 'Exposure to outdoor air pollution and its human health outcomes: A scoping review', *PLOS ONE*. Edited by M. Body-Malapel, 14(5), p. e0216550. doi: 10.1371/journal.pone.0216550.

Taiwo, A. M. *et al.* (2014) 'Mass and number size distributions of particulate matter components: Comparison of an industrial site and an urban background site', *Science of the Total Environment*. Elsevier B.V., 475, pp. 29–38. doi: 10.1016/j.scitotenv.2013.12.076.

Thurston, G. D. *et al.* (2017) 'A joint ERS/ATS policy statement: what constitutes an adverse health effect of air pollution? An analytical framework', *European Respiratory Journal*, 49(1), p. 1600419. doi: 10.1183/13993003.00419-2016.

Tobías, A. *et al.* (2018) 'Short-term effects of ultrafine particles on daily mortality by primary vehicle exhaust versus secondary origin in three Spanish cities', *Environment International*. Elsevier, 111(December 2017), pp. 144–151. doi: 10.1016/j.envint.2017.11.015.

Tousoulis, D. *et al.* (2020) ‘Acute exposure to diesel affects inflammation and vascular function’, *European Journal of Preventive Cardiology*, p. 204748731989802. doi: 10.1177/2047487319898020.

Tsai, T.-L. *et al.* (2019) ‘Fine particulate matter is a potential determinant of Alzheimer’s disease: A systemic review and meta-analysis’, *Environmental Research*, 177, p. 108638. doi: 10.1016/j.envres.2019.108638.

Tseng, C.-Y. *et al.* (2017) ‘Causation by Diesel Exhaust Particles of Endothelial Dysfunctions in Cytotoxicity, Pro-inflammation, Permeability, and Apoptosis Induced by ROS Generation’, *Cardiovascular Toxicology*, 17(4), pp. 384–392. doi: 10.1007/s12012-016-9364-0.

UBA (Umweltbundesamt) (2015) 'Auswertung der Wirkung von Umweltzonen auf die Erneuerung der Fahrzeugflotten in deutschen Städten. Sachverständigengutachten', ISSN 1862-4804. Retrieved from in German language: www.umweltbundesamt.de/publikationen/auswertung-der-wirkung-von-umweltzonen-auf-die (last accessed on 6 August 2021).

UBA (2020a) 'Low emission zones in Germany'. Retrieved from: www.umweltbundesamt.de/en/topics/air/particulate-matter-pm10/low-emission-zones-in-germany (last accessed on 6 August 2021).

UBA (2020b) ' Air Quality 2019. Preliminary Evaluation'. Retrieved from: www.umweltbundesamt.de/sites/default/files/medien/1410/publikationen/2020-03-20_hgp_air-quality-2019_bf.pdf (last accessed on 6 August 2021).

USEPA (United States Environmental Protection Agency) (2019) ' Integrated Science Assessment (ISA) for Particulate Matter (Final Report, Dec 2019)'. Retrieved from: cfpub.epa.gov/ncea/isa/recordisplay.cfm?deid=347534 (last accessed: 6 August 2021).

Valverde, V. & Giechaskiel, B. (2020) ‘Assessment of gaseous and particulate emissions of a euro 6d-temp diesel vehicle driven >1300 km including six diesel particulate filter regenerations’, *Atmosphere*, 11(6). doi: 10.3390/atmos11060645.

Viana, M. *et al.* (2020) 'Air quality mitigation in European cities: Status and challenges ahead', *Environment International*, 143. doi: 10.1016/j.envint.2020.105907.

Wang, X. *et al.* (2019) ‘An overview of physical and chemical features of diesel exhaust particles’, *Journal of the Energy Institute*. Elsevier Ltd, 92(6), pp. 1864–1888. doi: 10.1016/j.joei.2018.11.006.

Watson, A. Y. & Valberg, P. A. (2001) ‘Carbon black and soot: two different substances.’, *AIHAJ : a journal for the science of occupational and environmental health and safety*. United States, 62(2), pp. 218–228. doi: 10.1080/15298660108984625.

Wehner, B. *et al.* (2009) ‘Aerosol number size distributions within the exhaust plume of a diesel and a gasoline passenger car under on-road conditions and determination of emission factors’, *Atmospheric Environment*, 43(6), pp. 1235–1245. doi: 10.1016/j.atmosenv.2008.11.023.

Weitekamp, C. A. *et al.* (2020) ‘A systematic review of the health effects associated with the inhalation of particle-filtered and whole diesel exhaust’, *Inhalation Toxicology*, 32(1), pp. 1–13. doi: 10.1080/08958378.2020.1725187.

Wichmann-Fiebig, M. (2020) 'Considerations on a legal framework for UFP in ambient air', *Gefahrstoffe*, 80(01-02), p. 44-46. doi: 10.37544/0949-8036-2020-01-02-46.

Wiedensohler, A. *et al*. (2012) 'Mobility particle size spectrometers: harmonization of technical standards and data structure to facilitate high quality long-term observations of atmospheric particle number size distributions', *Atmos. Meas. Tech*., 5, p.657-685. doi: 10.5194/amt-5-657-2012

WHO (World Health Organization) (2006) 'Air Quality Guidelines. Global update 2005', *World Health Organization*. doi: 10.1007/BF02986808.

WHO EURO (World Health Organization Regional Office for Europe) (2013). 'Review of Evidence on Health Aspects of Air Pollution – REVIHAAP Project'. Retrieved from: www. euro.who.int/__data/ assets/pdf_file/0004/193108/REVIHAAP-Final-technical-report-final-version.pdf?ua=1 (last accessed on 6 August 2021)

WHO (2015) 'International statistical classification of diseases and related health problems, 10th revision, Fifth edition', *World Health Organization*. Retrieved from: apps.who.int/iris/handle/10665/246208 (last accessed on 6 August 2021).

WHO (2016) 'Ambient air pollution: a global assessment of exposure and burden of disease', *WHO Press*, Retrieved from: apps.who.int/iris/handle/10665/250141 (last accessed on 6 August 2021).

Winquist, A. *et al.* (2012). 'Power estimation using simulations for air pollution time-series studies', *Environmental Health*, 11:68. doi: 10.1186/1476-069X-11-68.

Xie, X. *et al.* (2017) 'A Review of Urban Air Pollution Monitoring and Exposure Assessment Methods', *ISPRS International Journal of Geo-Information*, 6(12), p. 389. doi: 10.3390/ijgi6120389.

Yang, B.-Y. *et al.* (2018) 'Global association between ambient air pollution and blood pressure: A systematic review and meta-analysis', *Environmental Pollution*, 235, pp. 576–588. doi: 10.1016/j.envpol.2018.01.001.

Yang, B.-Y. *et al.* (2020) 'Ambient air pollution and diabetes: A systematic review and meta-analysis', *Environmental Research*, 180, p. 108817. doi: 10.1016/j.envres.2019.108817.

Yang, Y. *et al.* (2019) 'Short-term and long-term exposures to fine particulate matter constituents and health: A systematic review and meta-analysis', *Environmental Pollution*, 247, pp. 874–882. doi: 10.1016/j.envpol.2018.12.060.

Yin, G. *et al*. (2019) 'Associations between size-fractionated particle number concentrations and COPD mortality in Shanghai, China', Atmospheric Environment, 214. doi: 10.1016/j.atmosenv.2019.116875.

Yorifuji, T. *et al.* (2016) 'Fine-particulate air pollution from diesel emission control and mortality rates in Tokyo: A quasi-experimental study', *Epidemiology*, 27(6), pp. 769–778. doi: 10.1097/EDE.0000000000000546.

Young, L. H. *et al.* (2012) 'Effects of biodiesel, engine load and diesel particulate filter on nonvolatile particle number size distributions in heavy-duty diesel engine exhaust', *Journal of Hazardous Materials*. Elsevier B.V., 199–200, pp. 282–289. doi: 10.1016/j.jhazmat.2011.11.014.

Zeraati-Rezaei, S. *et al.* (2020) 'Size-resolved physico-chemical characterization of diesel exhaust particles and efficiency of exhaust aftertreatment', *Atmospheric Environment*. Pergamon, 222, p. 117021. doi: 10.1016/j.atmosenv.2019.117021.

Zebroni, A. *et al.* (2019) 'Mixture Effects of Diesel Exhaust and Metal Oxide Nanoparticles in Human Lung A549 Cells', nanomaterials, 9:9. doi: 10.3390/nano9091302.

Zerboni, A. *et al.* (2021) 'Cellular Mechanisms Involved in the Combined Toxic Effects of Diesel Exhaust and Metal Oxide Nanoparticles', *Nanomaterials*, 11(6), p. 1437. doi: 10.3390/nano11061437.

Zhang, J. J. *et al.* (2009) 'Health effects of real-world exposure to diesel exhaust in persons with asthma', *Research report (Health Effects Institute)*, (138), pp. 5–109; discussion 111-23. Available at:

www.ncbi.nlm.nih.gov/pubmed/19449765.

Zhang, R. *et al.* (2015) 'Formation of Urban Fina Particulate Matter', Chemical Reviews, 115: 3803-3855. doi: 10.1021/acs.chemrev.5b00067

Zhang, R. *et al.* (2018) 'Morphology and property investigation of primary particulate matter particles from different sources', *Nano Research*, 11(6). doi: 10.1007/s12274-017-1724-y.

Zhao, J. *et al.* (2020) 'Particle Mass Concentrations and Number Size Distributions in 40 Homes in Germany: Indoor-to-outdoor Relationships, Diurnal and Seasonal Variation', Aerosol and Air Quality Research, 20: p. 576-589. doi: doi: 10.4209/aaqr.2019.09.0444.

6. Annex

6.1 Sensitivity results for full model validation

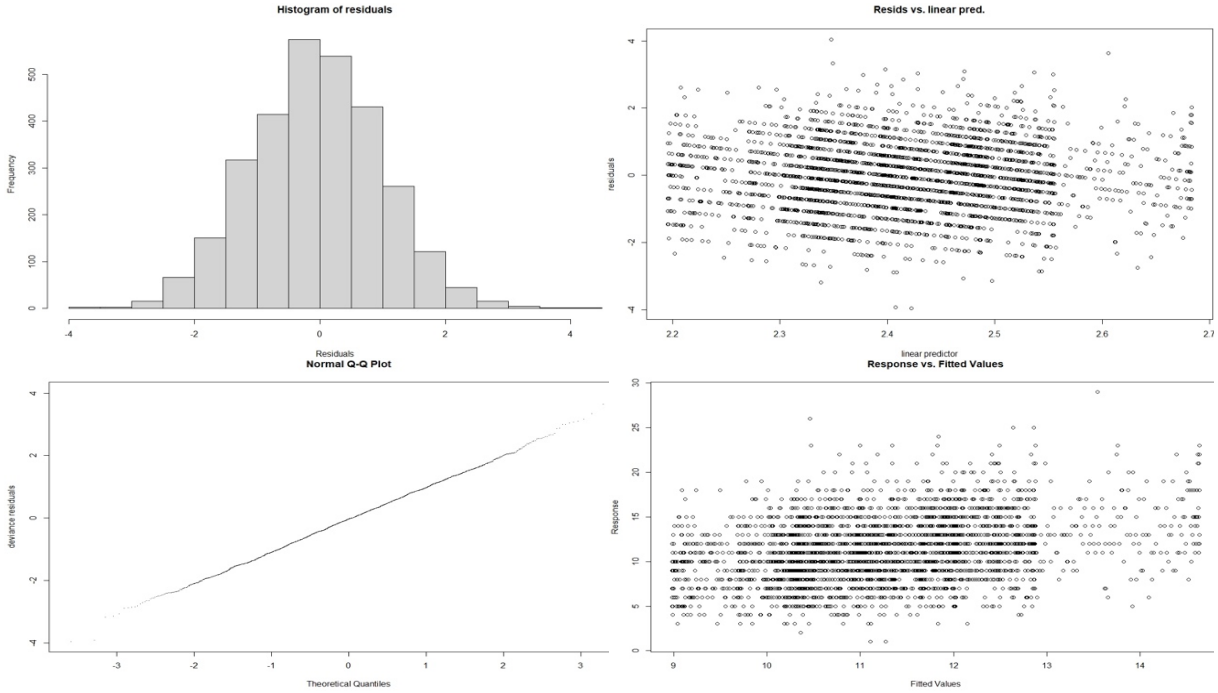

Fig. 25: Model validation plots for cardiovascular mortality for the full model (modelled exposure: $PNC_{30\text{-}120}$; outcome: cardio-vascular mortality). Four graphics from top left to bottom right: residuals, residuals vs linear predictor, Q-Q plot, response vs fitted values. Full model adjusted for time trend, day of the week, holidays and summer population decrease, influenza, temperature and humidity.

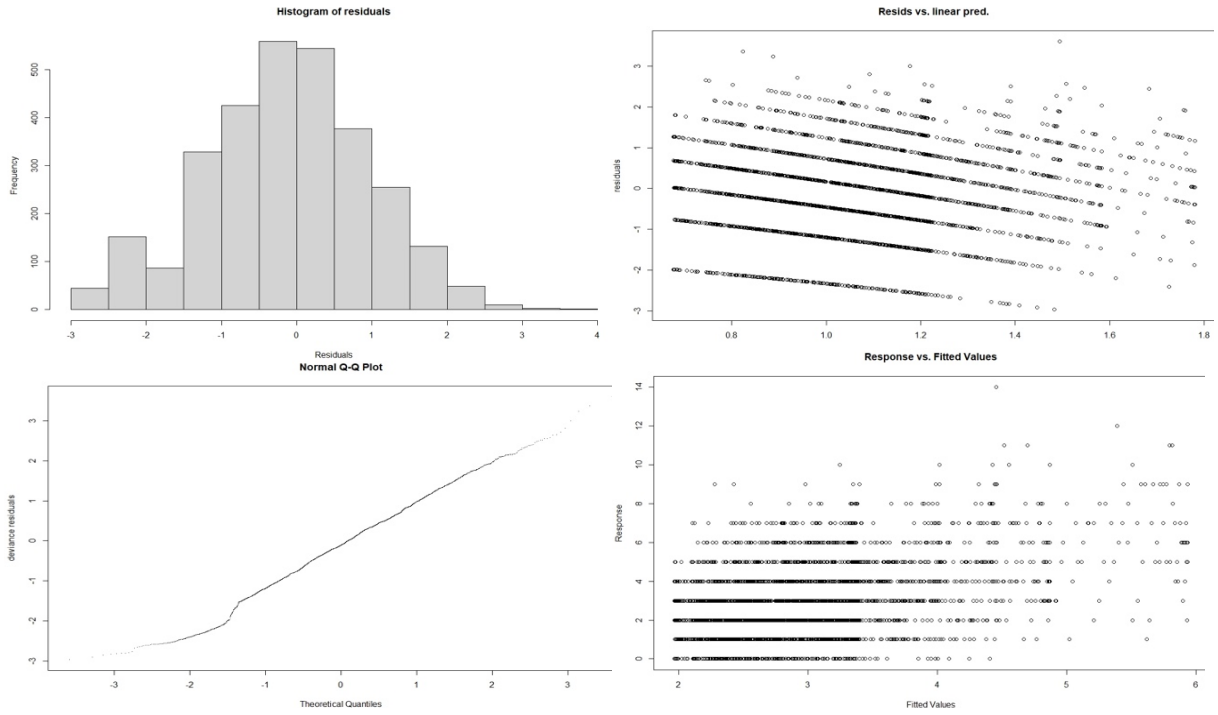

Fig. 26: Model validation plots for respiratory mortality for the full model (modelled exposure: $PNC_{30\text{-}120}$; outcome: respiratory mortality). Four graphics from top left to bottom right: residuals, residuals vs linear predictor, Q-Q plot, response vs fitted values. Full model adjusted for time trend, day of the week, holidays and summer population decrease, influenza, temperature and humidity.

6.2 Sensitivity results for full model estimates

6.2.1 Full model with single lags

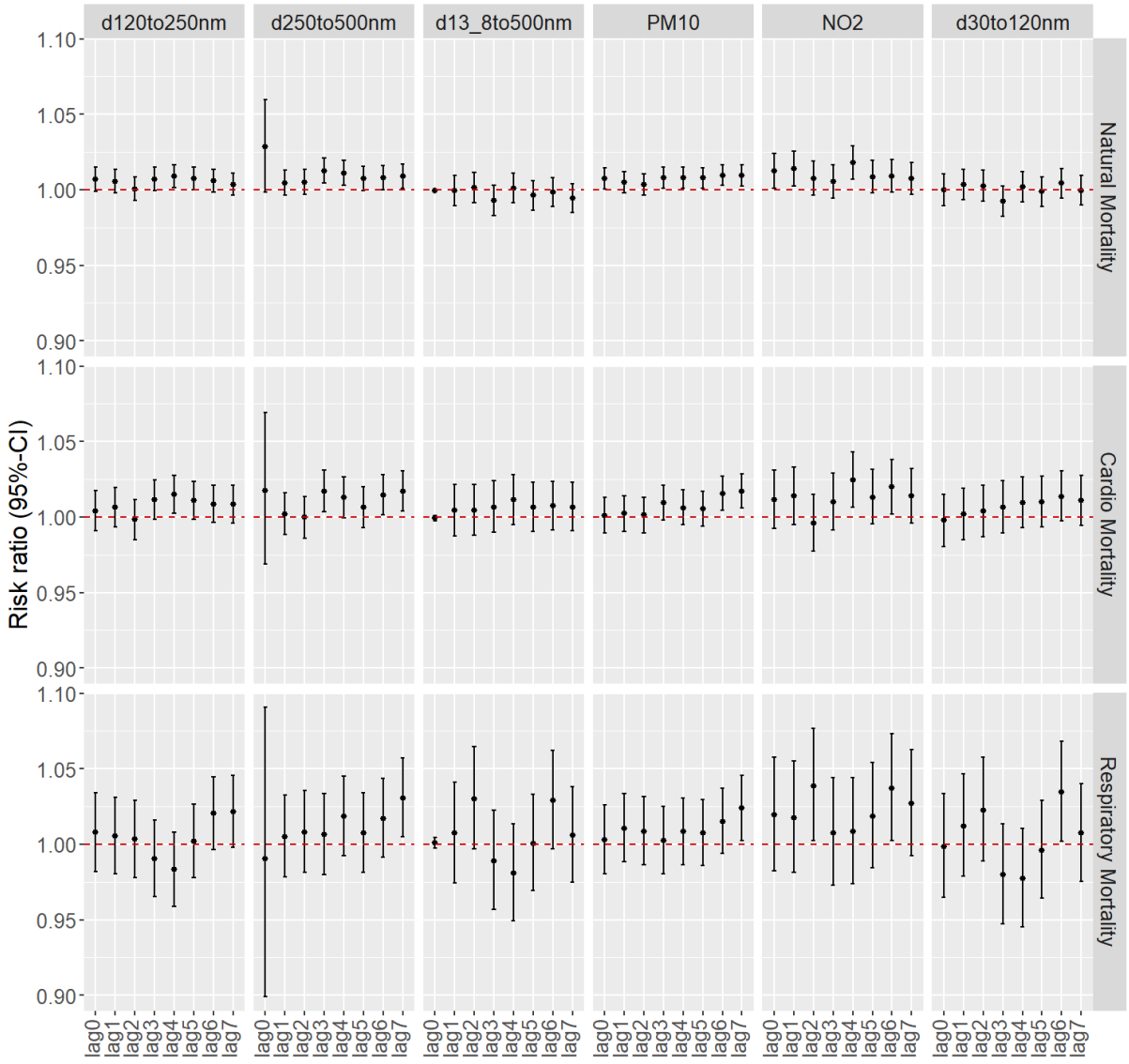

Fig. 27: Risk ratios with 95% CI based on the full model for PNC_{30-120} in comparison with larger particles ($PNC_{120-250}$, $PNC_{250-500}$), with total PNC as PNC_{13-500}, and with PM_{10} and NO_2 for single lags over one week. Full model adjusted for time trend, day of the week, holidays and summer population decrease, influenza, temperature and humidity.

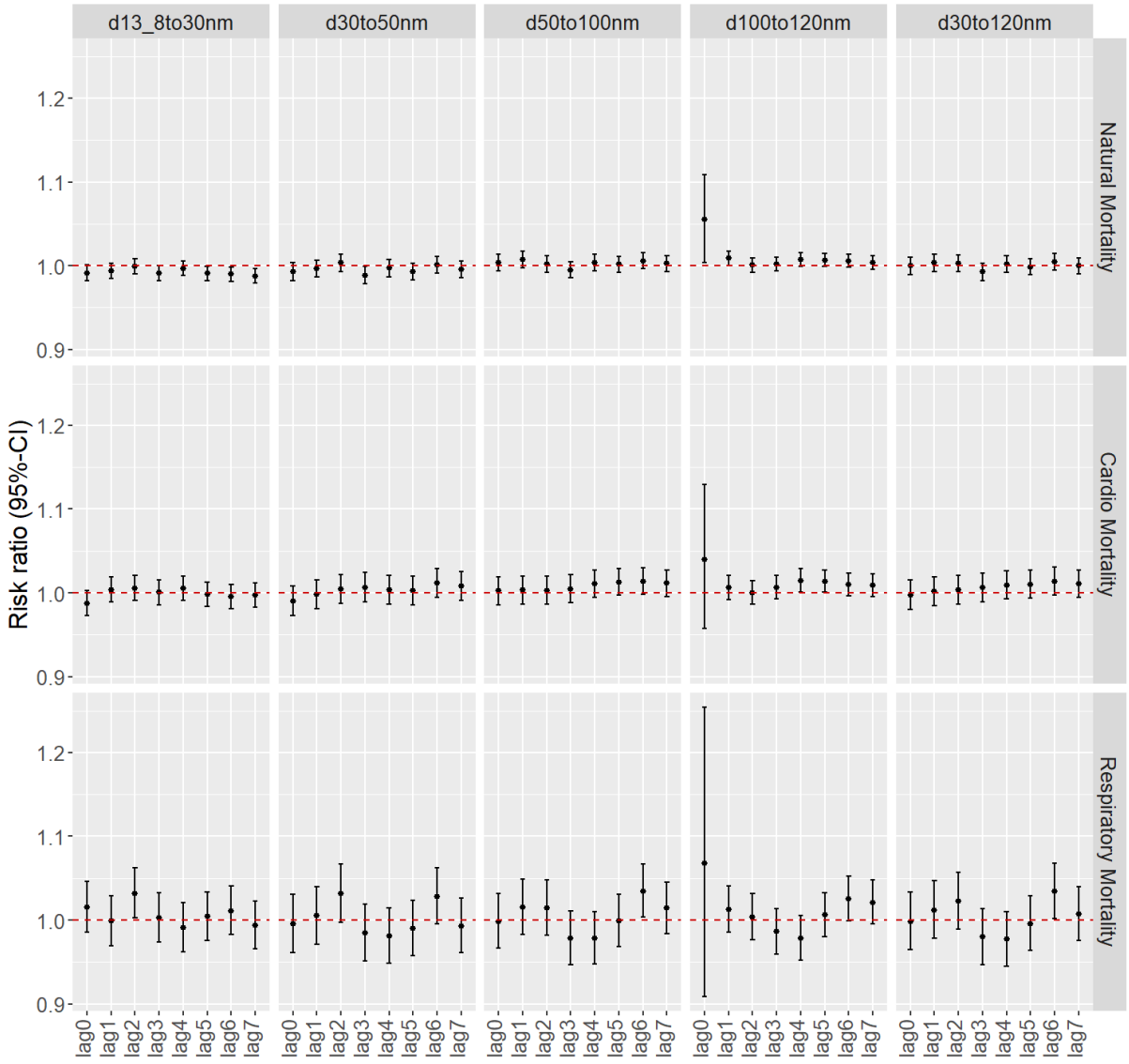

Fig. 28: Risk ratios with 95% CI based on the full model for $PNC_{30\text{-}120}$ in comparison with its sub ranges ($PNC_{30\text{-}50}$, $PNC_{50\text{-}100}$ and $PNC_{100\text{-}120}$) and smaller particles ($PNC_{13\text{-}30}$) for single lags over one week. Full model adjusted for time trend, day of the week, holidays and summer population decrease, influenza, temperature and humidity.

6.2.2 Full model - adjusted for PM_{10}

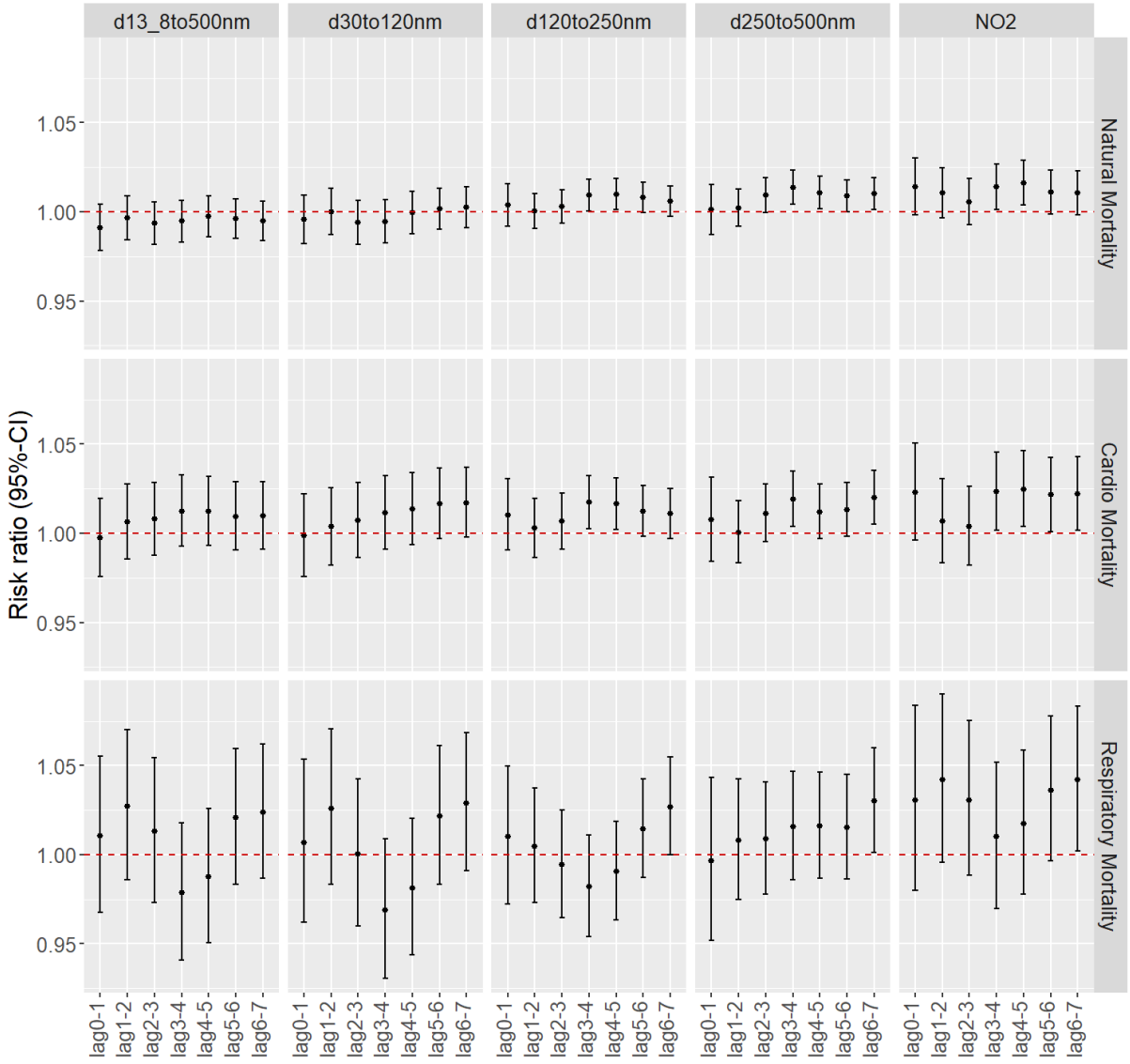

Fig. 29: Risk ratios with 95% CI based on the full model adjusted for PM_{10} for PNC_{30-120} in comparison with larger particles ($PNC_{120-250}$, $PNC_{250-500}$), with total PNC as PNC_{13-500}, and with NO_2 for two-day aggregate lags over one week. Extended full model adjusted also for PM_{10} besides for time trend, day of the week, holidays and summer population decrease, influenza, temperature and humidity.

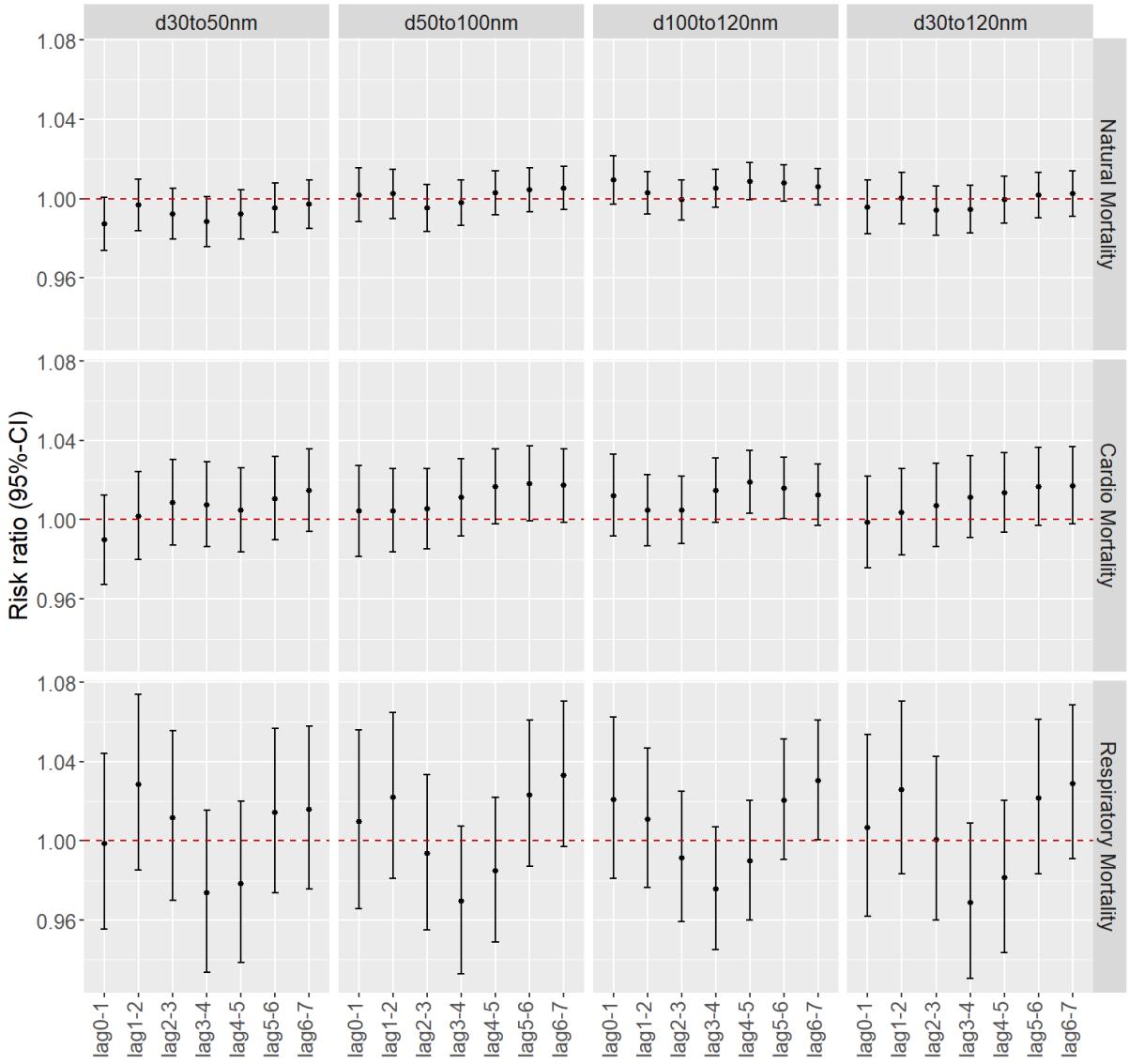

Fig. 30: Risk ratios with 95% CI based on the full model adjusted for PM_{10} for PNC_{30-120} in comparison with its sub ranges (PNC_{30-50}, PNC_{50-100} and $PNC_{100-120}$) and smaller particles (PNC_{13-30}) for two-day aggregate lags over one week. Extended full model adjusted also for PM_{10} besides for time trend, day of the week, holidays and summer population decrease, influenza, temperature and humidity.

6.2.3 Full model - adjusted for NO_2

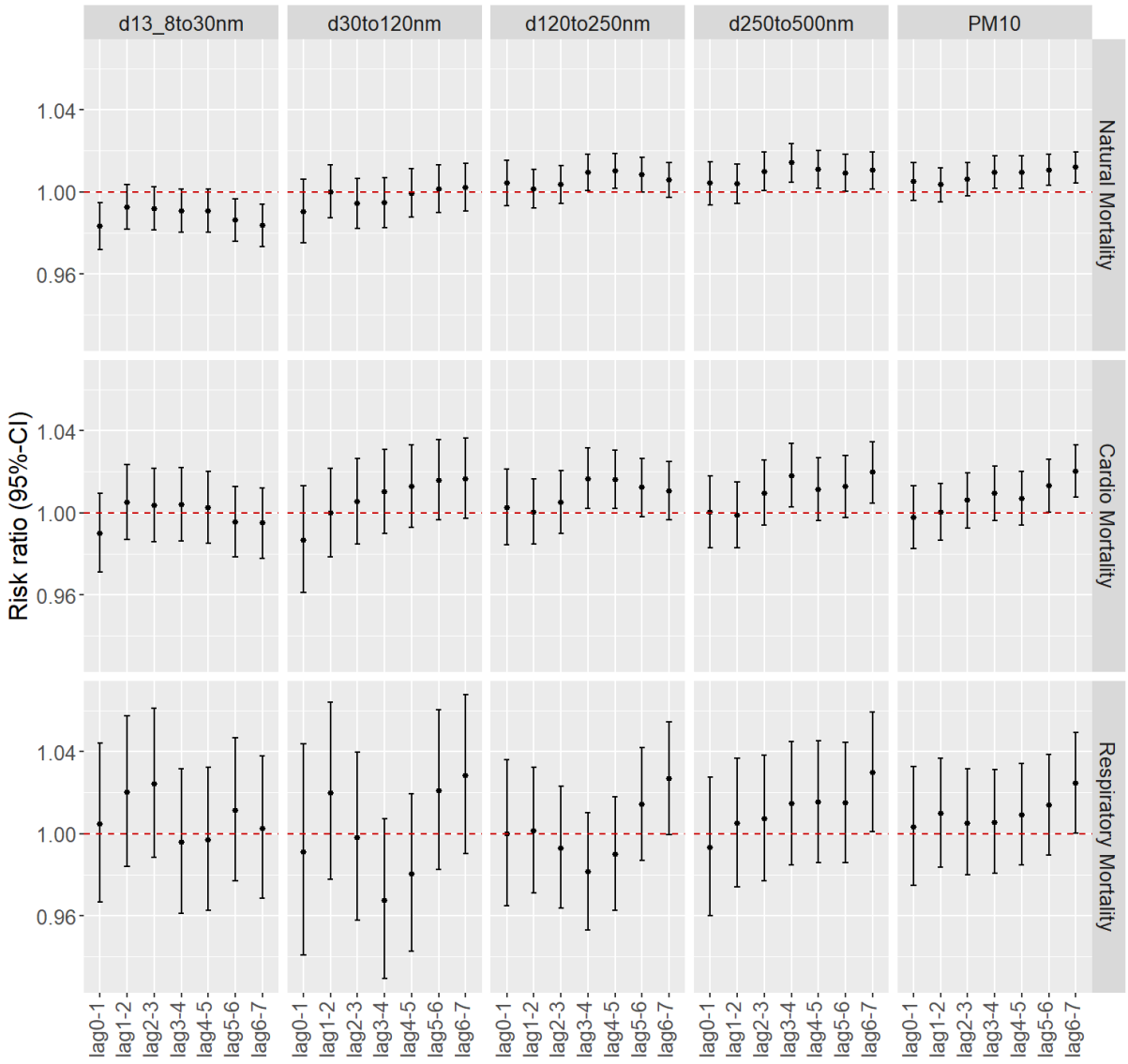

Fig. 31: Risk ratios with 95% CI based on the full model adjusted for NO_2 for $PNC_{30\text{-}120}$ in comparison with larger particles ($PNC_{120\text{-}250}$, $PNC_{250\text{-}500}$), with total PNC as $PNC_{13\text{-}500}$, and with PM_{10} for two-day aggregate lags over one week. Extended full model adjusted also for NO_2 besides for time trend, day of the week, holidays and summer population decrease, influenza, temperature and humidity.

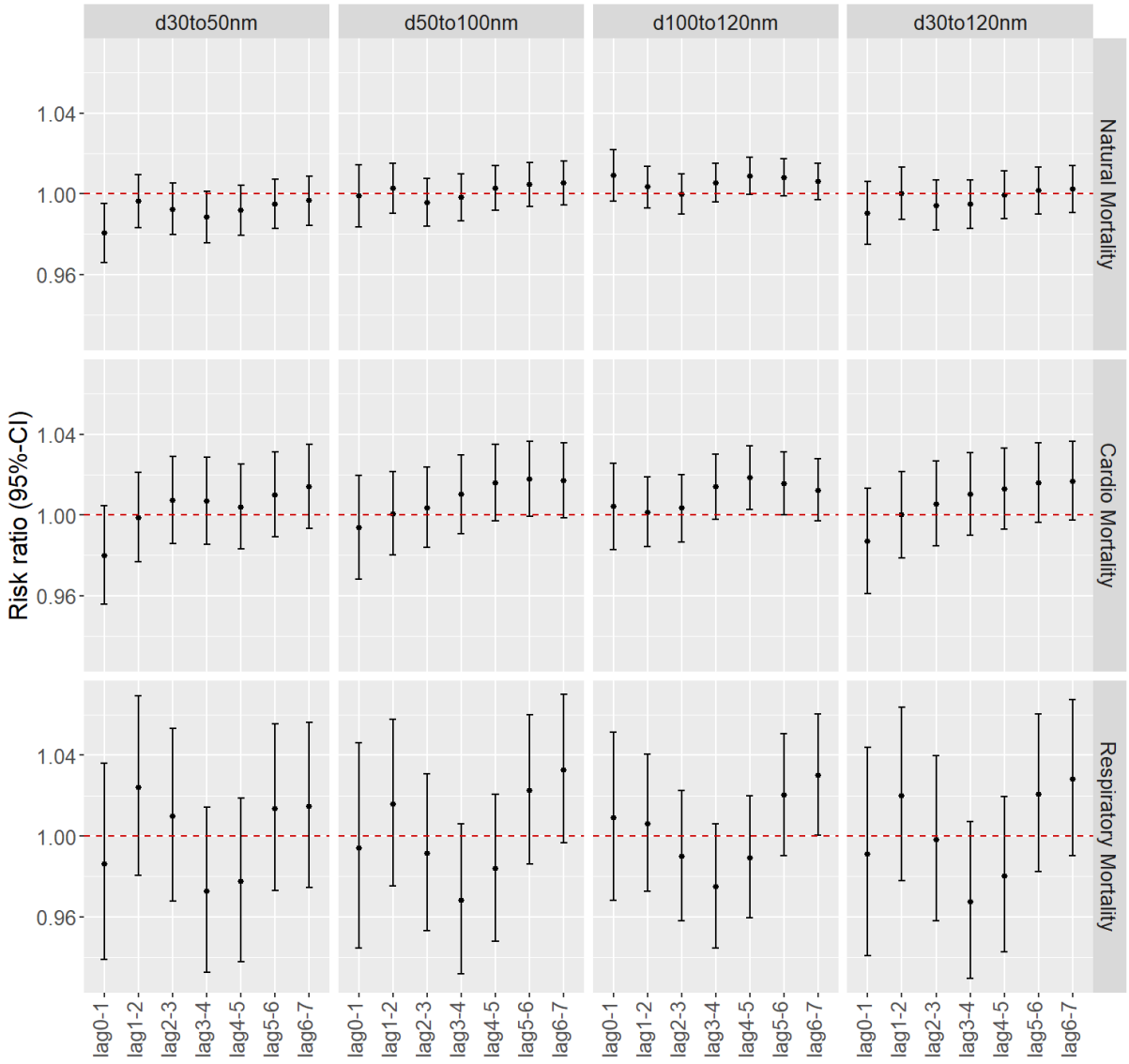

Fig. 32: Risk ratios with 95% CI based on the full model adjusted for NO_2 for PNC_{30-120} in comparison with its sub ranges (PNC_{30-50}, PNC_{50-100} and $PNC_{100-120}$) and smaller particles (PNC_{13-30}) for two-day aggregate lags over one week. Extended full model adjusted also for NO_2 besides for time trend, day of the week, holidays and summer population decrease, influenza, temperature and humidity.

6.3 Sensitivity results for effect modification by UEZ regulation

6.3.1 Full model with alternative dichotomous interaction term for before/after the year 2013

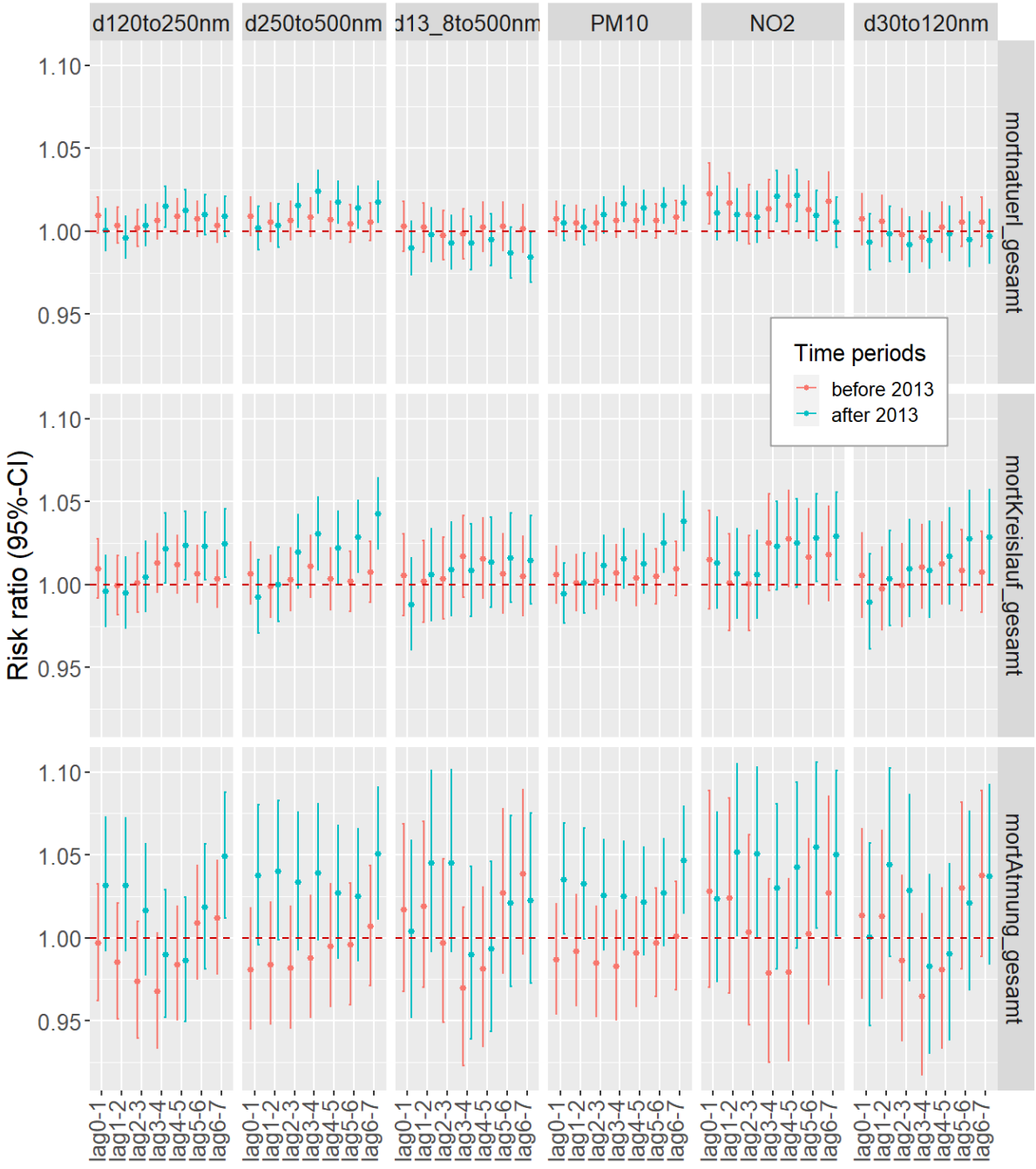

Fig. 33: Risk ratios with 95% CI based on the full model with the dichotomous interaction term before and after 2013 for PNC_{30-120} in comparison with larger particles ($PNC_{120-250}$, $PNC_{250-500}$), with total PNC as PNC_{13-500}, and with PM_{10} and NO_2 for two-day moving average aggregate lags over one week. Full model adjusted for time trend, day of the week, holidays and summer population decrease, influenza, temperature and humidity.

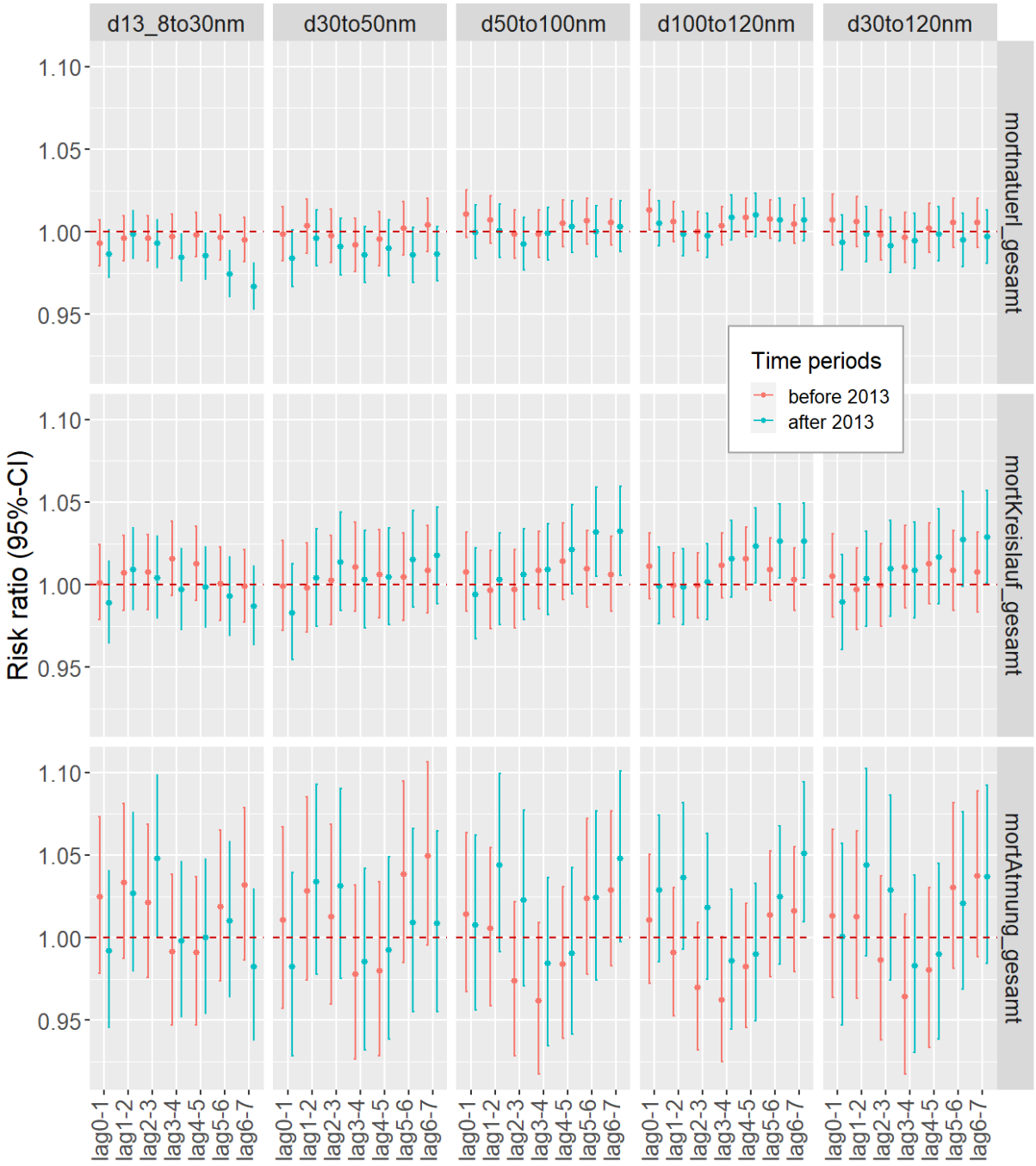

Fig. 34: Risk ratios with 95% CI based on the full model with the dichotomous interaction term before and after 2013 for PNC_{30-120} in comparison with its sub ranges (PNC_{30-50}, PNC_{50-100} and $PNC_{100-120}$) and smaller particles (PN_{C13-30}) for two-day moving average aggregate lags over one week. Full model adjusted for time trend, day of the week, holidays and summer population decrease, influenza, temperature and humidity.

6.3.2 Full model with dichotomous interaction term - adjusted for PM_{10}

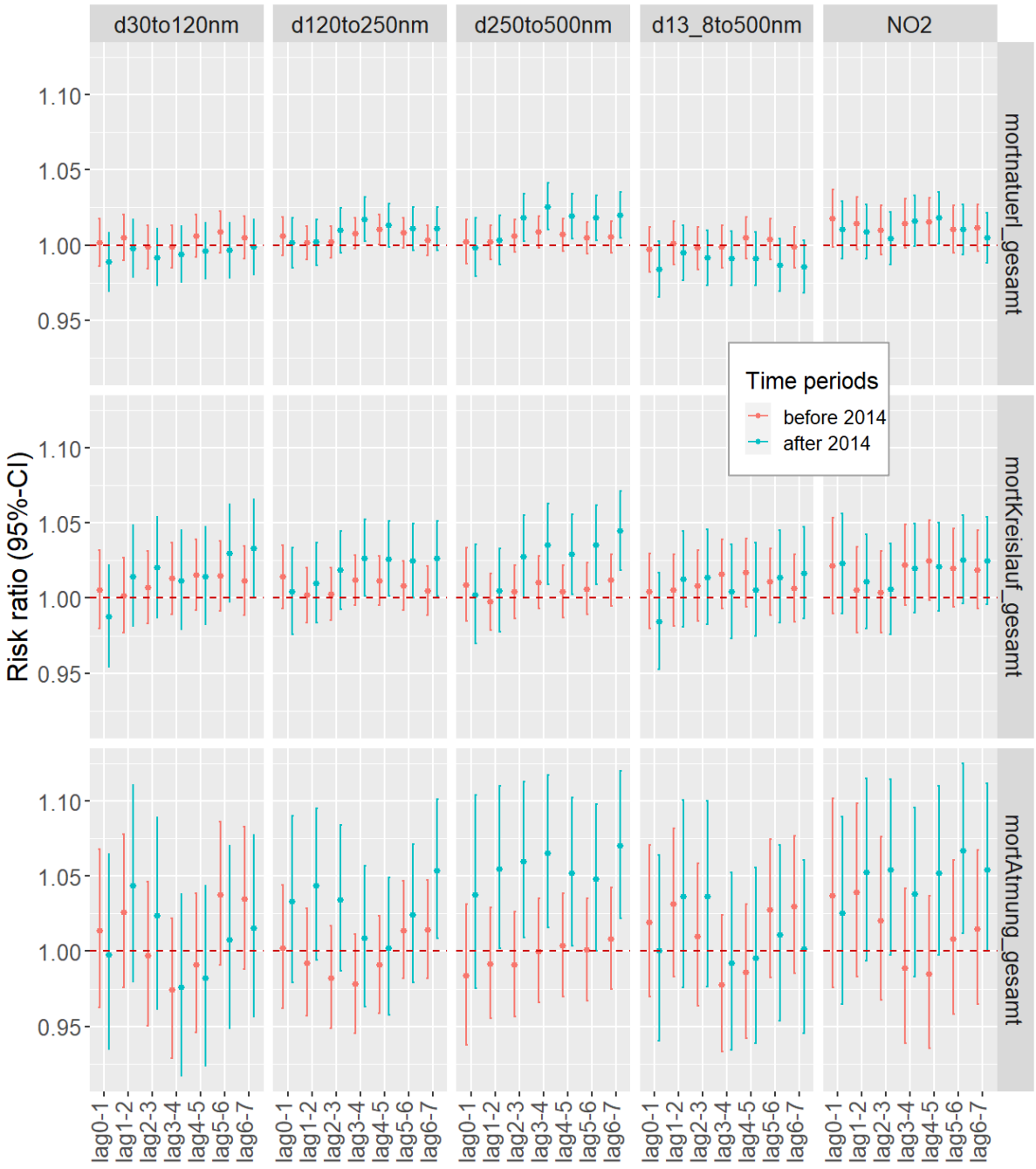

Fig. 35: Risk ratios with 95% CI based on the full model with the dichotomous interaction term adjusted for PM_{10} for before and after 2014 for PNC_{30-120} in comparison with larger particles ($PNC_{120-250}$, $PNC_{250-500}$), with total PNC as PNC_{13-500}, and with NO_2 for two-day moving average aggregate lags over one week. Extended full model adjusted also for PM_{10} besides for time trend, day of the week, holidays and summer population decrease, influenza, temperature and humidity.

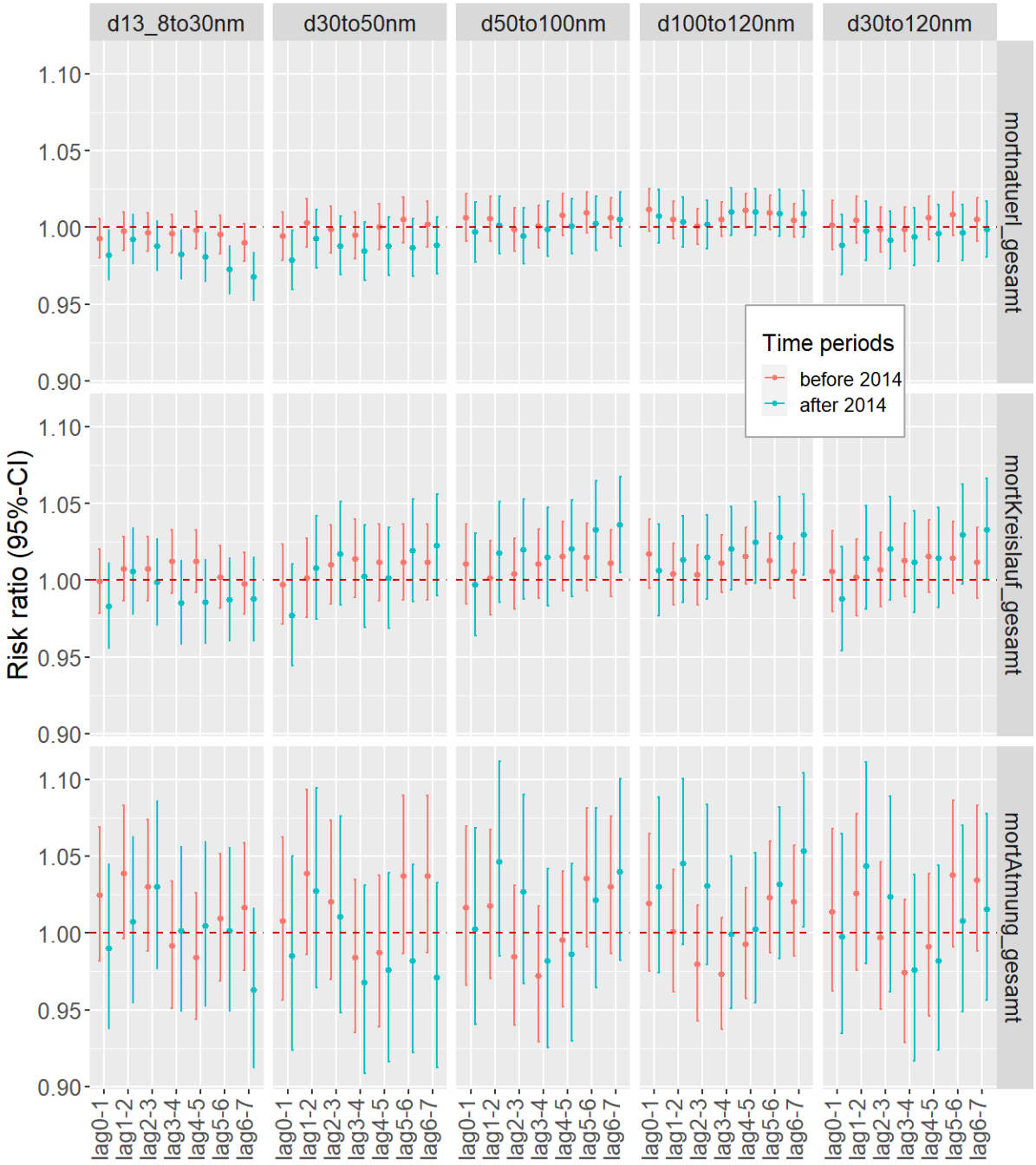

Fig. 36: Risk ratios with 95% CI based on the full model with the dichotomous interaction term adjusted for PM_{10} for before and after 2014 for PNC_{30-120} in comparison with its sub ranges (PNC_{30-50}, PNC_{50-100} and $PNC_{100-120}$) and smaller particles (PNC_{13-30}) for two-day moving average aggregate lags over one week. Extended full model adjusted also for PM_{10} besides for time trend, day of the week, holidays and summer population decrease, influenza, temperature and humidity.

6.3.3 Full model with dichotomous interaction term - adjusted for NO_2

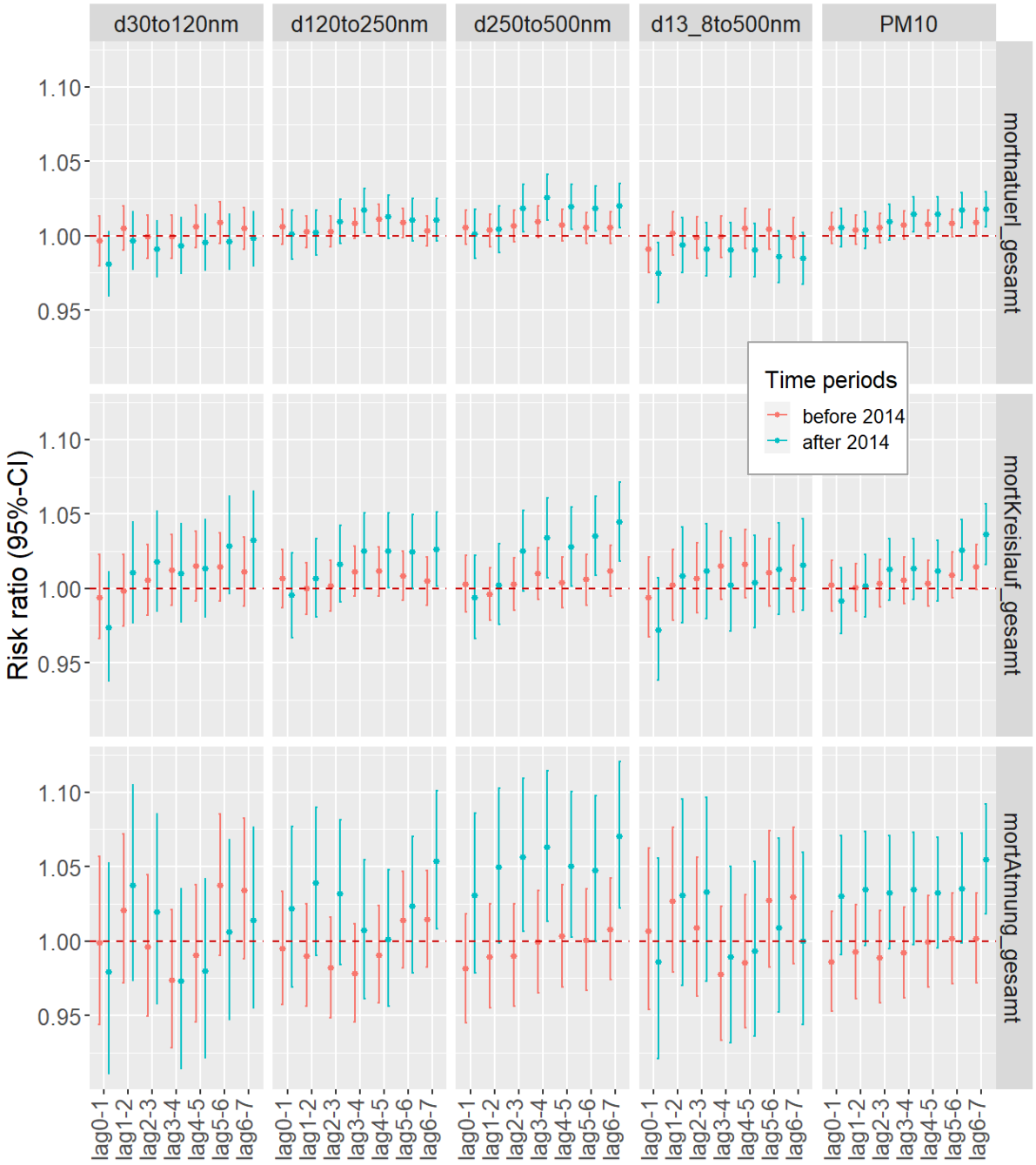

Fig. 37: Risk ratios with 95% CI based on the full model with the dichotomous interaction term adjusted for NO_2 for before and after 2014 for PNC_{30-120} in comparison with larger particles ($PNC_{120-250}$, $PNC_{250-500}$), with total PNC as PNC_{13-500}, and with PM_{10} for two-day moving average aggregate lags over one week. Extended full model adjusted also for NO_2 besides for time trend, day of the week, holidays and summer population decrease, influenza, temperature and humidity.

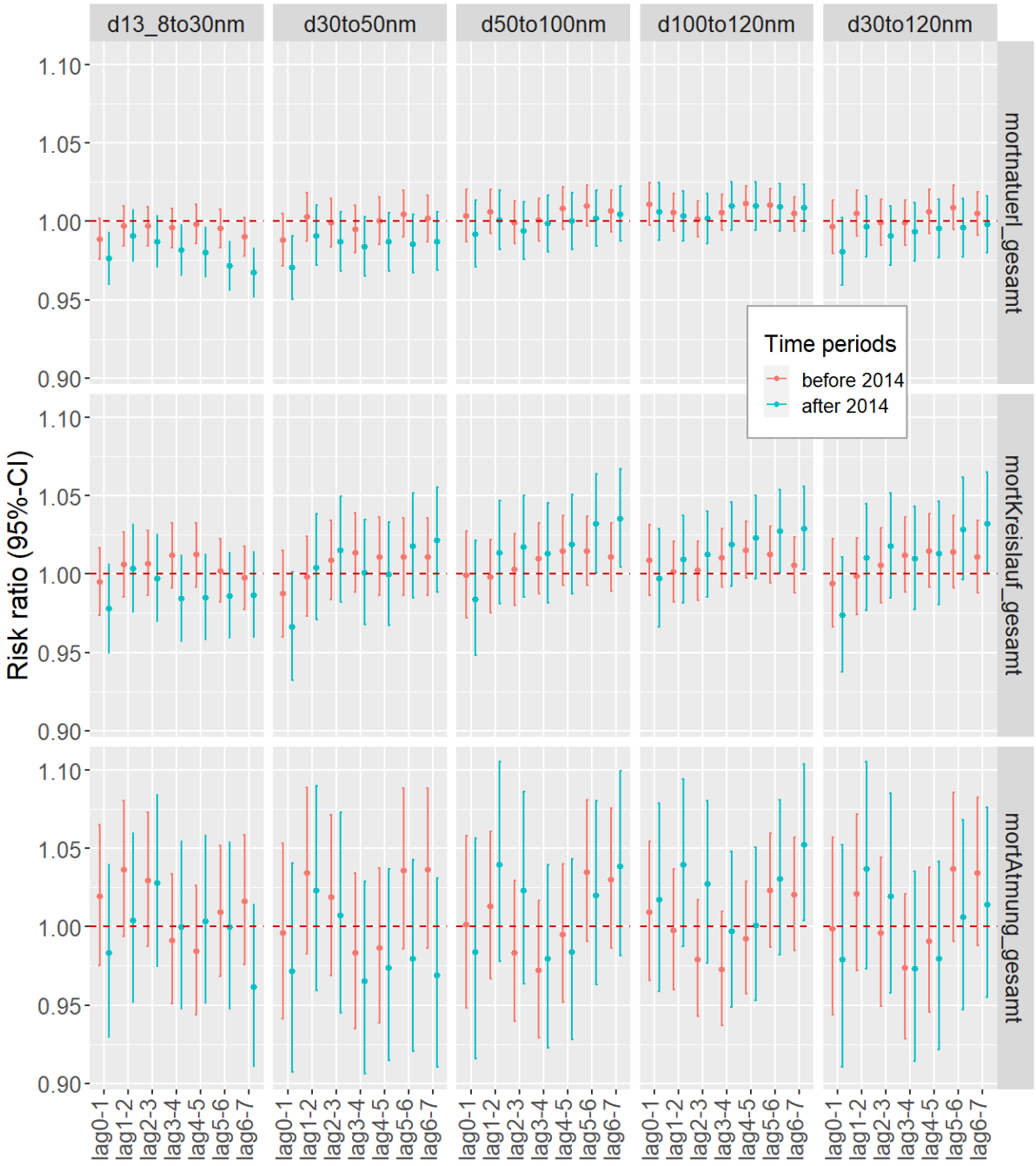

Fig. 38: Risk ratios with 95% CI based on the full model with the dichotomous interaction term adjusted for NO_2 for before and after 2014 for PNC_{30-120} in comparison with its sub ranges (PNC_{30-50}, PNC_{50-100} and $PNC_{100-120}$) and smaller particles (PNC_{13-30}) for two-day moving average aggregate lags over one week. Extended full model adjusted also for NO_2 besides for time trend, day of the week, holidays and summer population decrease, influenza, temperature and humidity.

6.4 Sensitivity results for effect modification by DPF prevalence

6.4.1 Full model with ordinal interaction term - adjusted for PM_{10}

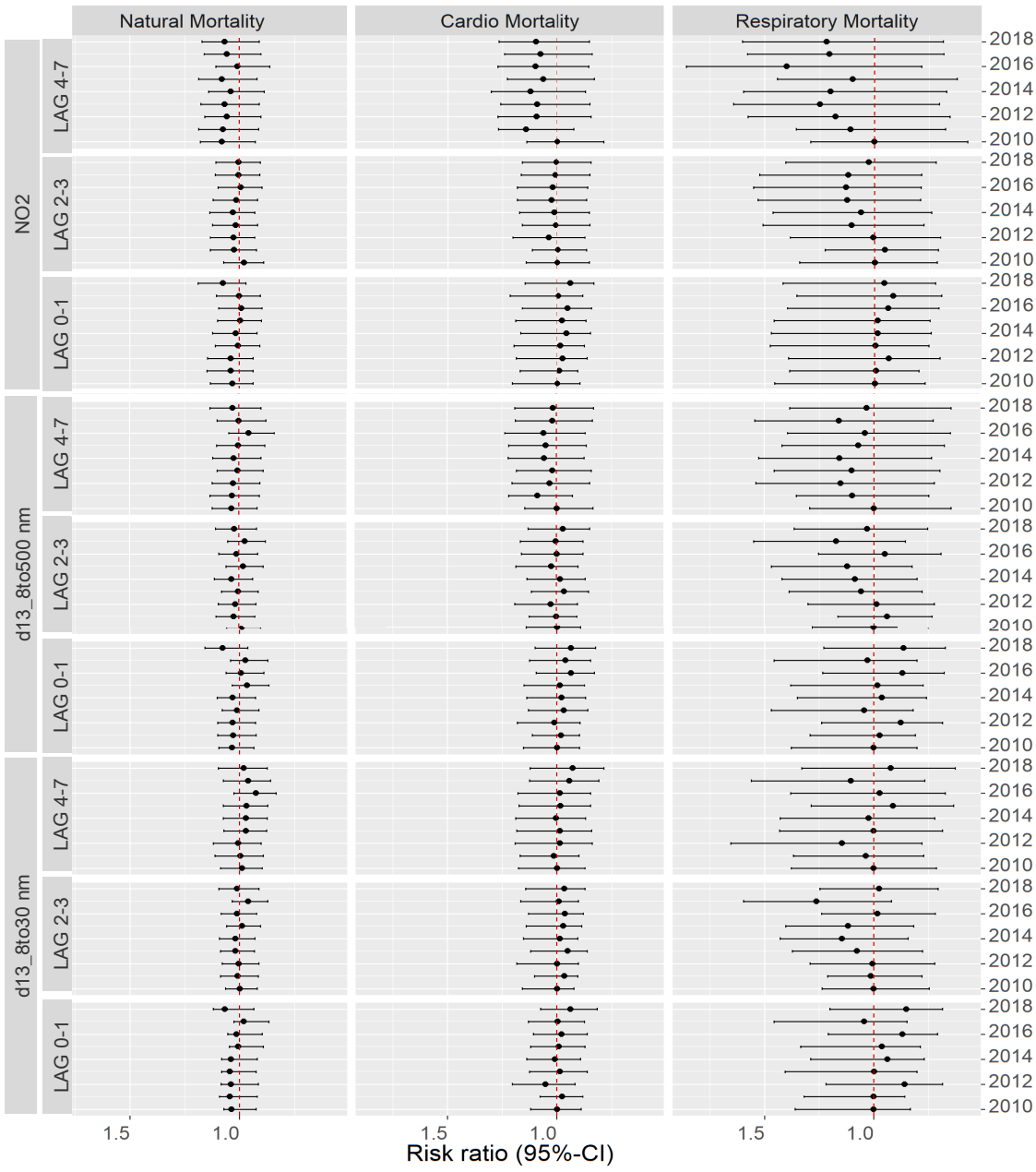

Fig. 39: Risk ratios compared with the base-year 2009 with 95% CI based on the full model with the ordinal (annual) interaction term adjusted for PM_{10} for smaller particles (PNC_{13-30}), total PNC as PNC_{13-500}, and for NO_2 for immediate (lag0-1), slightly lagged (lag2-3) and lagged (lag4-7) associations. Extended full model adjusted also for PM_{10} besides for time trend, day of the week, holidays and summer population decrease, influenza, temperature and humidity.

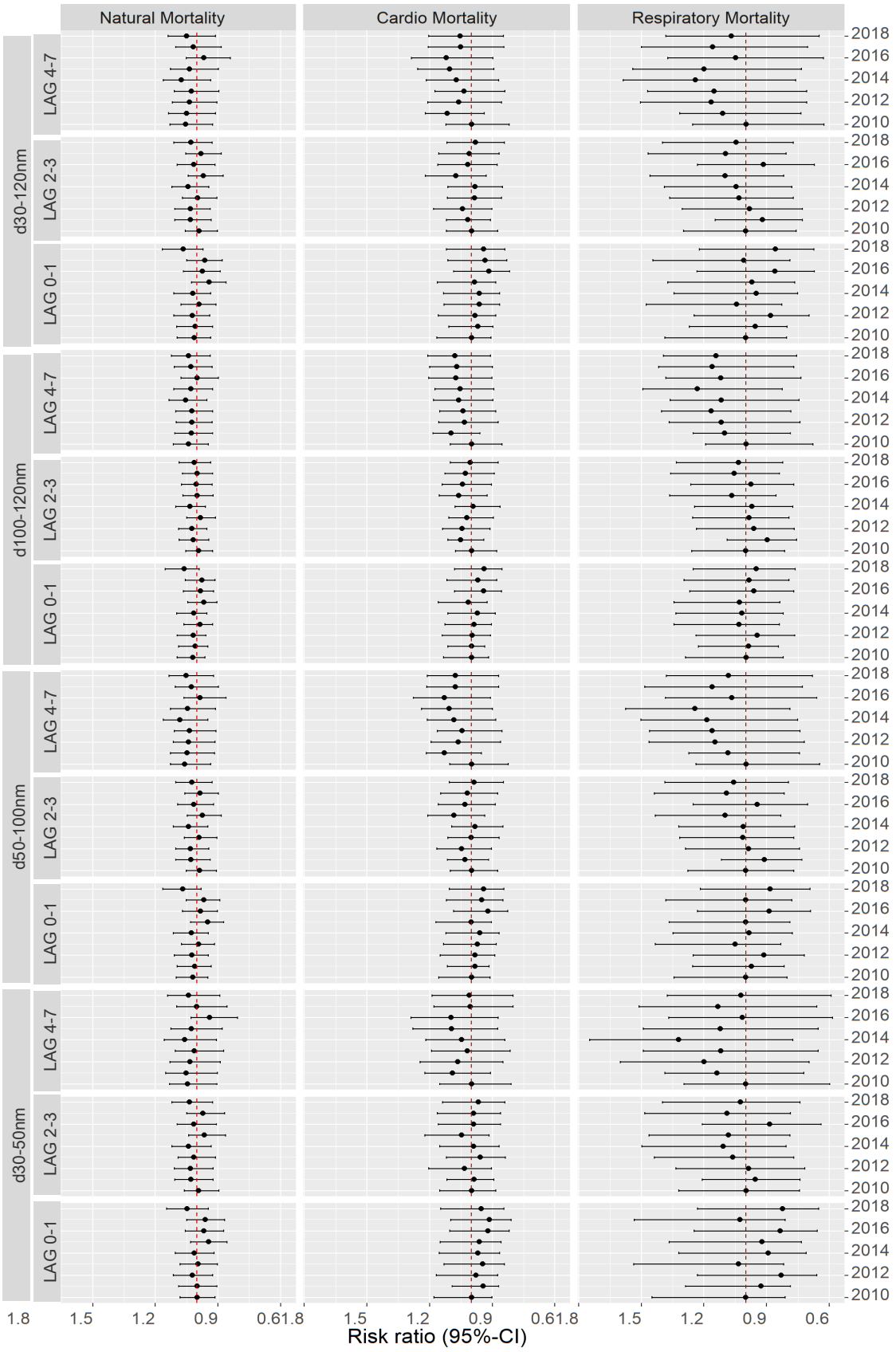

Fig. 40: Risk ratios compared with the base-year 2009 with 95% CI based on the full model with the ordinal (annual) interaction term adjusted for PM_{10} for PNC_{30-120} in comparison with its sub ranges (PNC_{30-50}, PNC_{50-100} and $PNC_{100-120}$) for immediate (lag0-1), slightly lagged (lag2-3) and lagged (lag4-7) associations. Extended full model adjusted also for PM_{10} besides for time trend, day of the week, holidays and summer population decrease, influenza, temperature and humidity.

6.4.2 Full model with ordinal interaction term - adjusted for NO_2

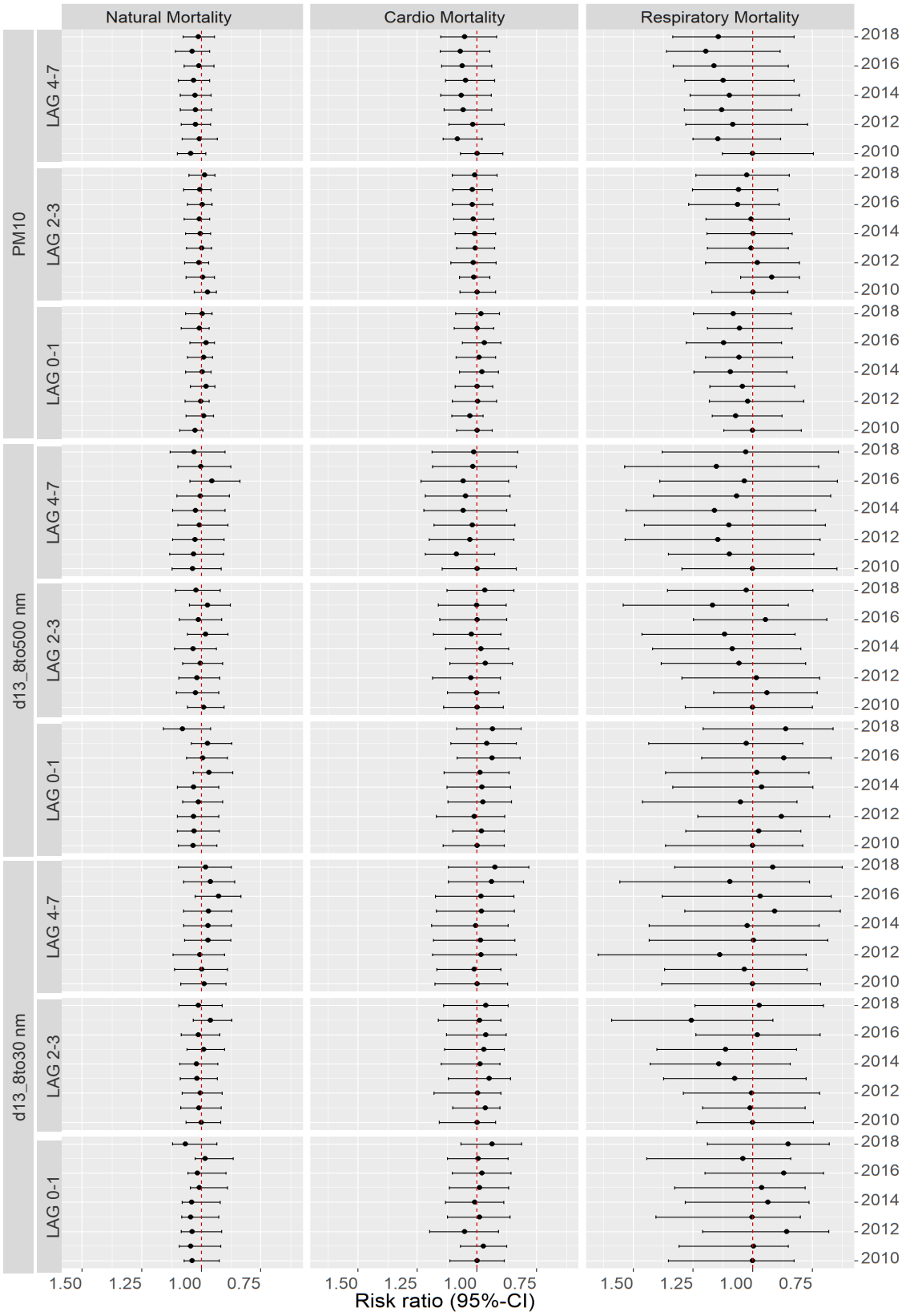

Fig. 41: Risk ratios compared with the base-year 2009 with 95% CI based on the full model with the ordinal (annual) interaction term adjusted for NO_2 for smaller particles (PNC_{13-30}), total PNC as PNC_{13-500}, and for PM_{10} for immediate (lag0-1), slightly lagged (lag2-3) and lagged (lag4-7) associations. Extended full model adjusted also for NO_2 besides for time trend, day of the week, holidays and summer population decrease, influenza, temperature and humidity.

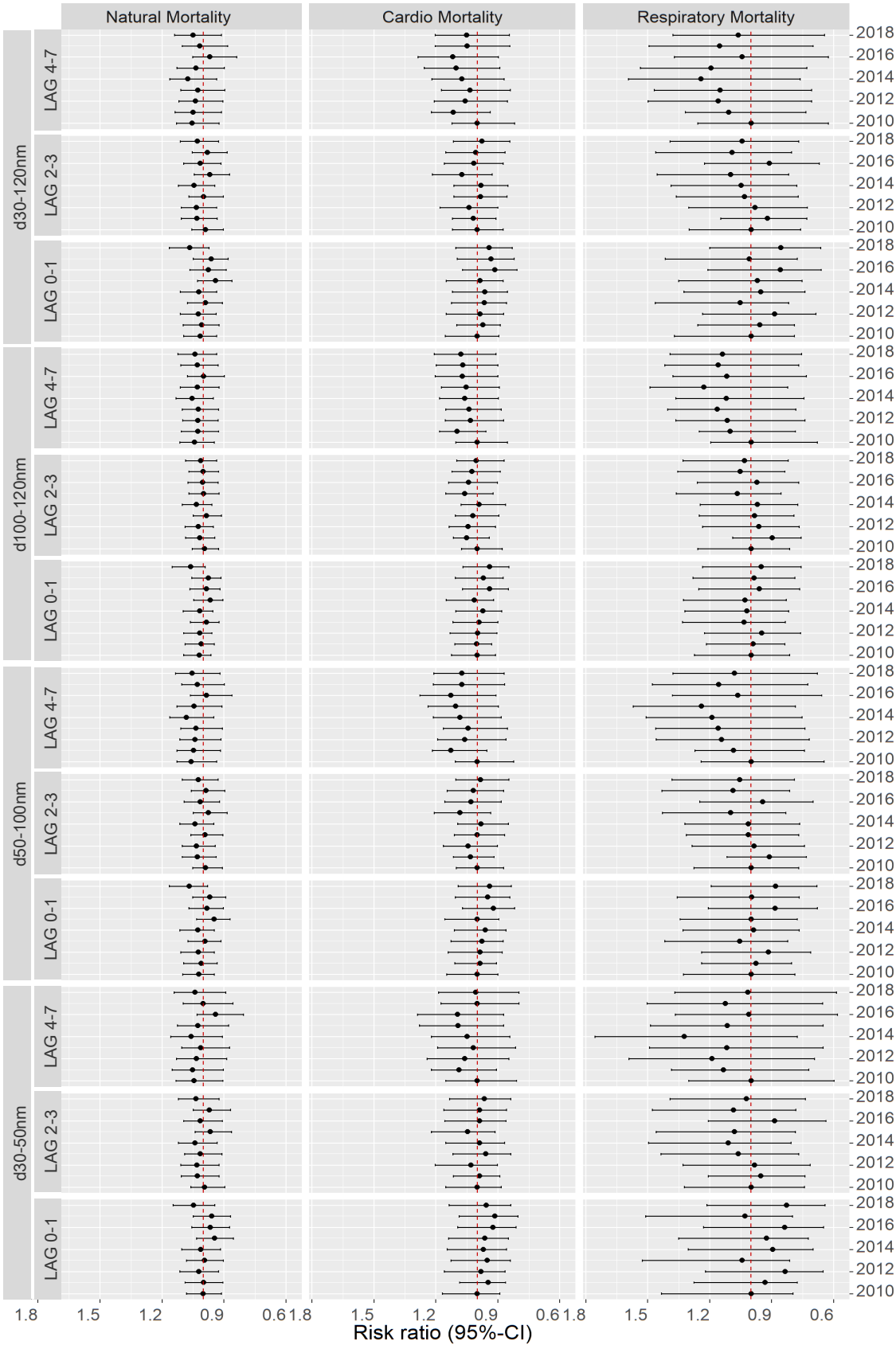

Fig. 42: Risk ratios compared with the base-year 2009 with 95% CI based on the full model with the ordinal (annual) interaction term adjusted for NO_2 for PNC30-120 in comparison with its sub ranges (PNC_{30-50}, PNC_{50-100} and $PNC_{100-120}$) for immediate (lag0-1), slightly lagged (lag2-3) and lagged (lag4-7) associations. Extended full model adjusted also for NO_2 besides for time trend, day of the week, holidays and summer population decrease, influenza, temperature and humidity.

Acknowledgements

I would like to sincerely thank my doctoral supervisor, Prof Dr Barbara Hoffmann, who passionately, ingeniously and proficiently shared her insights and understanding of environmental epidemiology and scientific publication practices. With her unique sense of when more and when less attention to detail is vital for the quality of a research process, she taught me about quality assurance in research beyond the scope of my thesis or the research field and thereby transmitted her conviction and experience on the potential of science in guiding evidence-based policy.

I also would like to extend my sincere gratitude to my co-supervisor, Prof Dr Oliver Kuss, who pointed out and patiently explained the statistical pitfalls that time series studies in environmental epidemiology can face. His input allowed me to view the statistical tools typically used for air pollution time series studies from a broader perspective.

Statistical coding advice, particularly with the seemingly endless sand traps of running changing combinations of R® packages on Windows and Macintosh machines, was granted by my colleague and mathematician, Lina Glaubitz. She was approachable when endless calculations failed due to single characters, and she taught me how to approach issues in R® coding systematically and with a smile.

Through their involvement in publications, adjacent projects and daily office time, numerous persons facilitated the advancement of my topical understanding and enriched the past three years professionally and personally. I would first like to highlight the members of the environmental epidemiology working group: Meltem Baydak, Anna Buschka, Frauke Hennig, Haeran Jeong, Sarah Lucht, Simone Ohlwein, Vitaliys Rodins, Vanessa Soppa, and Pascale Thoelke; before expressing my thanks to the experts at IUTA, namely Heinz Kaminski and Christopf Asbach; at UBA, namely Bryan Hellack; at IT.NRW, namely Dana Leenders and Felix Moritz; my various colleagues in the BEAR-Project, that also focuses on UFP-related health effects; as well as my colleagues in projects on urban health, including the effect of green spaces on PM exposure.

Finally, a doctoral thesis seemingly inevitably involves some hardship and long hours. I have treasured every warm word and hot coffee, but most appreciated the positive energy and the mental battery recharges through good moments. Thank you to my wonderful partner, Vera.